12-2022

Water availability as a cross-scale driver of microbial functions and free viral abundance in soil

Aubrey K. Fine
University of Tennessee, Knoxville, afine3@vols.utk.edu

To the Graduate Council:

I am submitting herewith a dissertation written by Aubrey K. Fine entitled "Water availability as a cross-scale driver of microbial functions and free viral abundance in soil." I have examined the final electronic copy of this dissertation for form and content and recommend that it be accepted in partial fulfillment of the requirements for the degree of Doctor of Philosophy, with a major in Plant, Soil and Environmental Sciences.

Sean M. Schaeffer, Major Professor

We have read this dissertation and recommend its acceptance:

Mark Radosevich, Jie Zhuang, Melanie Mayes

Accepted for the Council:

Dixie L. Thompson

Vice Provost and Dean of the Graduate School

(Original signatures are on file with official student records.)

WATER AVAILABILITY AS A CROSS-SCALE DRIVER OF MICROBIAL FUNCTIONS AND FREE VIRAL ABUNDANCE IN SOIL

A Dissertation Presented for the
Doctor of Philosophy
Degree
The University of Tennessee, Knoxville

Aubrey K. Fine
December 2022

ACKNOWLEDGEMENTS

I express my sincere gratitude to Dr. Sean Schaeffer, my major advisor, for being a dedicated and supportive mentor. Dr. Schaeffer has always been committed to my development as a scientist and encouraged me to pursue my own research interests.
I also express my appreciation to members of my doctoral committee, Dr. Mark Radosevich, Dr. Jie Zhuang, and Dr. Melanie Mayes, who played an integral role in the completion of this work. I also thank Dr. Essington who provided valuable guidance on research not included in this dissertation.

I give thanks to members of the Department of Biosystems Engineering and Soil Science for helping me feel at home at UT. I give special thanks to Dr. Julie Carrier, Scott Tucker, Andrew Sherfy, and the administrative team of BESS. I also express my gratitude to my fellow lab mates, especially Marie English, Dr. Lidong Li, Lydia Turpin, Karalee Corbeil, Megan Davis, and Dr. Julie Konkel.

Finally, I thank my parents, Mark and Eve, for their love and support, as well as my siblings, Julia, Alex, Kenyon, and Keaton and step-parents Loreen and Robert.

ABSTRACT

Viral infection is widespread in natural microbial communities, with extensive study in aquatic ecosystems demonstrating direct influence on host physiology, functional activity, and mortality. While similar dynamics are assumed to occur across ecosystems, soils are distinct microbial habitats where soil physiochemical structure and water availability constrain resource availability. These unique environmental conditions have been widely demonstrated to affect microbial distribution, diversity, and functional activity in bulk soil, while their influence on virus-microbe interactions and free viral abundance remains limited. To address this knowledge gap, this research had three broad aims: i) to investigate variability in microbial responses to drying-rewetting cycles at the scale of aggregate size fractions, ii) to explore potential for aggregate-scale variability in free viral abundance and net virus production rates over time, and iii) to study the influence of dynamic soil drying and rewetting processes on microbial stress responses relative to free viral abundance. Three multifactorial incubation experiments were conducted testing treatment effects of soil aggregate size (Large Macro, Small Macro, and Micro), induction of viral lysis using Mitomycin C (MMC), drying-rewetting processes (i.e., drought length, rewetting frequency), and time. Microbial activity was monitored by repeated sampling of respiration rates with destructive sampling was performed for analysis of dissolved organic carbon, inorganic nitrogen, aggregate stability, activities of hydrolytic extracellular microbial enzymes, and viral particles and bacterial cell abundances. Results from multivariate statistical analysis indicate

overarching control of time and water availability on microbial activities, as well as viral abundance and net production rates, across aggregates and in response to induction of viral lysis. In bulk soil, free viral abundance was negatively affected by soil drying and sharply decreased with drying beyond 20% gravimetric water content. Rewetting of dry soil was associated with a burst of microbial activity along with a spike in lytic viral reproduction that increased viral abundance up to 40-fold within 24 h. Together, these findings illustrate the dynamic nature of the responses of soil microbial and viral processes to soil-specific environmental factors at lesser studied spatial and temporal scales.

TABLE OF CONTENTS

LIST OF TABLES

LIST OF FIGURES

CHAPTER ONE
INTRODUCTION

1.1 Background Information

On a global scale, soils store an estimated 1417 Pg of carbon (C), greater than that of atmosphere and land vegetation pools combined (Scharlemann et al., 2014; Hiederer and Kochy, 2011). The majority (67%) of soil C is associated with the soil organic matter (SOM) pool (Scharlemann et al., 2014), which is broadly defined to include all living organisms and non-living organic residues at varying stage of decomposition present in a soil. While living soil microbes occupy a small proportion of total SOM, their activity directly mediates critical biogeochemical processes of terrestrial ecosystems associated with OM decomposition, nutrient transformations, and C stabilization.

In terrestrial and aquatic ecosystems alike, it is currently estimated that up to 40-90% of microbes can be classified as lysogens (i.e., bacterial cells that have at least one prophage (i.e., viral, or phage, genome) integrated into their chromosome) (Howard-Varona et al., 2017; Marsh and Wellington, 1994). Data from culture studies and marine ecosystems were first used to develop understanding of virus-microbe interactions in the environment, with the preliminary goal to explain consistent observations of high viral abundances in the oceans (Fuhrman, 1999; Proctor and Fuhrman, 1990; Bergh et al., 1989). For example, phage-mediated lysis of bacterial hosts is responsible for an estimated 20-60% of daily bacterial morality in oceanic surface waters (Suttle, 2005; Fuhrman and Noble, 1995). Viral lysis functions as a

direct control on microbial populations, having downstream effects on microbial community structure and energy transfer to higher trophic levels (Wommack and Colwell, 2000). While data from a limited number of studies in soils suggest that viruses are equally if not more abundant on a volumetric basis than in water samples, current knowledge viral ecology in soils remains limited (Williamson et al., 2017).

Soils are distinct from aquatic systems with the added influence of a three-dimensional, physically structured, and chemically reactive matrix. Soil physicochemical structure influences distribution of soil water, which is a key physiological driver of microbial metabolism. Within the soil physicochemical structure water also functions as a transport medium that controls spatiotemporal contact between microbes, enzymes, and dissolved substrates. While interactions between soil structure and water function as an inherently coupled control on microbial activity, it is unknown how soil physical structure and wetting influence virus production and survival. This is a fundamental barrier to the incorporation of viral processes and virus-microbe dynamics into soil biogeochemical process models.

In an effort to explore this important knowledge gap, the goal for this dissertation research is to improve mechanistic understanding of how soil structure and wetting affect microbial processes and virus-microbe interactions across time. Four extended incubation experiments are proposed that will combine measurement of common biogeochemical properties (e.g., C, N, P pools, extracellular enzymes, microbial biomass, aggregate stability) with bacterial cell and viral particle enumeration by epifluorescence microscopy. Multivariate statistical analyses will be performed to

investigate temporal trends across and within aggregate fractions within each dataset. The proposed studies will represent the first effort to place viral ecology within the context of soil physical structure and wetting using direct observations of microbial processes and viral abundance, which will ultimately lay a foundation for understanding how viruses affect biogeochemical cycling in terrestrial ecosystems.

Current models of microbial decomposition processes in soil

Whereas biochemical complexity or recalcitrance of substrate has traditionally been viewed as a principal control of soil organic matter (OM) decomposition, the past decade has seen the development of new models of soil C cycling and stabilization processes that focus on the role of abiotic 'ecosystem' properties (precipitation, temperature, biotic communities) as controls on microbial accessibility to OM (Lehman and Kleber, 2015; Cotrufo et al., 2011; Schmidt et al., 2011). This shift in focus has increased interest in understanding how interactions between multiple environmental drivers influence key microbial processes across spatiotemporal scales (Schmidt et al., 2011).

Organic residues must be biochemically degraded from complex organic polymers into simple substrates before assimilation through microbial cell walls. Extracellular enzymes mediate the transformation of particulate OM (POM) into dissolved OM (DOM). Microbes produce and release extracellular enzymes to balance nutrient and energy supply with demand (Burns et al., 2013; Schimel and Schaeffer, 2012). Decomposition of complex OM inputs requires the combined activities of many different types of enzymes, ultimately achieved by the microbial community rather

than a single microbe (Burns et al., 2013). Enzymatic decomposition requires contact between enzyme and substrate, with mineralization of liberated monomers dependent upon diffusion back to active cells. Interactions with the soil physicochemical matrix can promote the persistence of otherwise decomposable OM in soils via spatiotemporal isolation (e.g., physical occlusion) and/or chemical association (e.g., sorption/desorption) with reactive clay minerals and/or SOM (Bailey et al., 2019; Lehman and Kleber, 2015; Schmidt et al., 2011; von Lutzow et al, 2006). Leading evidence suggests that long-lived, stable pools of SOC are dominated by microbially processed OM, linking microbial activity to long-term C stabilization in soil (Liang et al., 2019; Liang et al., 2017; Miltner et al., 2012; Cotrufo et al., 2011).

Viral ecology: knowns and unknowns

Viruses are unique biological, yet non-living, entities that have a range of effects on microbial ecology in aquatic ecosystems. Two generally recognized reproductive strategies have evolved in viruses, which each has its own consequences for microbial hosts. Lysogeny is a baseline, non-productive state where the prophage replicates as the host proliferates without production of viral progeny (Howard-Varona et al., 2017; Wommack and Colwell, 2000). Virulent lytic infection is induced from a lysogenic state in response to poorly understood factors including host cell damage and stressful environmental conditions (Wommack and Colwell, 2000). During lytic reproduction, host cell metabolism is rerouted towards the production of viral progeny and lytic enzymes that lyses the host cell. Lysis releases active phages in addition to nutrient-rich cytoplasmic components (e.g., nucleic acids, enzymes, dissolved and free amino

acids) and complex cell wall material (e.g., lipid bilayers, large proteins, peptidoglycan) (Middelboe and Jørgensen, 2006; Wilhelm and Suttle, 1999). Readily available lysis products can be rapidly recycled within the pool of microbial biomass, whereas more complex cell wall materials degrade more slowly over time aided by extracellular enzymes (Wommack and Colwell, 2000; Wilhelm and Suttle, 1999). Biogeochemical effects of lysis are represented in models of marine C cycles as the viral shunt, a distinct component of the microbial C pump describing internal cycling of C and nutrients among viruses, hosts, and dissolved OM (DOM) pools (Weitz and Wilhelm, 2012; Jiao et al., 2010; Wilhelm and Suttle, 1999; Fuhrman, 1999). Through the viral shunt, viral lysis functions as top-down (predatory) control on microbial populations as well as a bottom-up control on substrate availability for newly growing microbes. The viral shunt diverts C away from higher trophic levels, instead promoting production of microbially processed C and retention of C in dissolved form (Jiao et al., 2010; Fuhrman, 1999).

Study of viral ecology in aquatic ecosystems has traditionally included measurement of virus and bacteria abundances, calculation of Virus-to-Bacteria Ratio (VBR) (i.e., number of viruses per bacteria), and assay of Inducible Fraction (IF) (i.e., the proportion of the total bacterial population harboring an experimentally inducible prophage) (Weinbauer, 2004; Paul and Jiang, 2001). Since the early 2000s, single timepoint measurement of the same properties in a limited number of studies report virus abundance in bulk soil ranging from 10^3-10^9 virus particles per g soil dry weight, VBR as high as 8200, and IF ranging from 4-85% (Liang et al., 2020; Ghosh et al.,

2008; Williamson et al., 2007). Across studies, current data suggest i) the existence of weak positive correlations between soil virus abundance and bacteria abundance, soil type, and soil water content (Williamson, 2011; Kimura et al., 2008; Williamson et al., 2005) and ii) a lack of correlation between IF and bulk soil properties (pH, water content, percent organic matter (OM), and particle size distribution) except possibly soil depth (Liang et al., 2020; Williamson et al., 2007). While the presence of free viruses and lysogens in soil ecosystems has been documented in recent decades, knowledge of the underlying mechanisms controlling the distribution, abundance, and lytic activities of viruses in soil remain unknown.

Soil as a physically structured microbial habitat

The size and arrangement of soil solids and pore spaces is defined as soil physical structure, for which the aggregate is a fundamental unit (Oades, 1984). Aggregates form when organic and inorganic soil components mix and become physiochemically stabilized into a roughly spherical structure. In the currently accepted model, soil aggregate structure develops as a hierarchy where large macroaggregates are composed of many smaller microaggregates and primary particles (<53 μm) stabilized by microbial residues and inorganic cementing agents (Totsche et al., 2018; Six et al., 2004; Tisdall and Oades, 1982). Aggregation of soil solids creates a complex network of soil pore spaces, with a wider distribution of pore sizes (i.e., micro- plus macro-pores) associated with larger aggregates. Reflecting these differences in physicochemical character, two principal aggregate size fractions are generally recognized: i) microaggregates (53-250 μm diameter) and ii) macroaggregates (250-

2000 µm diameter), with macroaggregates commonly divided further into large (1000-2000 µm) and small (250-1000 µm) (Totsche et al., 2018; Six et al., 2004).

The physicochemical properties of aggregate fractions represent differing biogeochemical habitats. While larger aggregates have a greater proportion of newly deposited, labile plant derived particulate substrate relative to microaggregates, most microbes are thought to reside in micropores that are more physically stable, retentive of water, and exclusive towards higher predators (Totsche et al., 2018; Six et al., 2004; Angers and Giroux, 1996; Elliot, 1986). This comes at a tradeoff of lower substrate availability, as OM in the microaggregate fraction features increased chemical complexity and greater predominance of organo-mineral associated OM (Totsche et al., 2018; Six et al., 2004; Six et al., 2000). These differences in substrate quality and accessibility have been shown to impact OM mineralization and turnover rates, which are generally faster in larger aggregates (Gupta and Germida, 1988; 2015).

At the pore scale, microbial biogeography is driven by physical transport processes combined with ecological interactions. Aggregates provide spatial protection of OM by reducing access of enzymes and microorganisms to substrate, slowing diffusion of enzymes and substrate into intra-aggregate spaces, and limiting the supply of oxygen for aerobic respiration within aggregates (von Lutzow et al., 2006). Intra-aggregate spaces can serve as key anaerobic microsites in bulk soil where anerobic processes dominate despite the presence of oxygen (Keiluweit et al., 2017). Observed higher bacterial abundance and diversity in micro- vs. macro-aggregates reflects these factors along with additional physical protection afforded to microaggregate-associated

bacteria against predation (Upton et al., 2019; Trivedi et al., 2015; Zhang et al., 2013; Ranjard et al., 2000). For example, bacterivores (e.g., protozoa, nematodes) are physically excluded by size from micropores with pore neck sizes less than 6 µm (Wright et al., 1995). Distinct microbial communities have been observed in aggregate microhabitats when comparing whole macro- and microaggregates (Trivedi et al., 2015; Smith et al., 2014; Davinic et al., 2012; Väisänen et al., 2005) and microaggregate surfaces and interiors (Mummey and Stahl, 2004; Ranjard et al., 2000). Such findings support the idea that soil aggregates function as distinct microhabitats with increased ecological niche space relative to unaggregated soil.

Soil water availability as a control on microbial activity

Microbes depend upon the availability of water to complete biochemical reactions, but also for transport processes that influence the spatial distribution of organisms, extracellular enzymes, and solutes in soil (Schimel, 2018; Manzoni et al., 2012a). While often expressed on a gravimetric or volumetric basis (e.g., g water g soil^{-1}), expression of soil water as a potential describes the strength of force by which the soil holds water relative to gravity. For example, fully saturated soil has a water potential of 0 MPa that becomes increasingly negative as the soil progressively dries. Water potential accounts for within soil heterogeneity in water distribution related to texture and structure, better describing water availability to microbes at the pore scale where they reside (Moyano et al., 2013; Manzoni et al., 2012a). Microbial processes in soil are affected by the absolute value of soil water potential (i.e., how wet a soil is at a

given time) as well as the rate and magnitude of changes in water potential (e.g., upon rewetting of dry soil) (Kieft et al., 1987).

At maximal soil dryness (i.e., highly negative matric potential), microbial respiration and mineralization processes practically cease (Manzoni and Katul, 2014; Moyano et al., 2013; Moyano et al., 2012; Hueso et al., 2012). This is generally attributed to the combined effects of resource limitation and dehydration stress (Manzoni and Katul, 2014; Manzoni et al., 2014; Schimel et al., 2007). Current evidence suggests that accessibility limits microbial activity before soil becomes dry enough to cause physiological stress arising from cell dehydration (estimated below a water potential of -0.6 MPa; Herron et al., 2009; Stark and Firestone, 1994) and death under extreme conditions (estimated below a water potential of -15 MPa; Manzoni and Katul, 2014). Soil microbial community responses to drought stress remain a subject of active investigation, with increasing evidence suggesting influence of adaptation strategies such as dormancy, altered C allocation (e.g., towards production of cell wall mucilage, phospholipids, and extracellular polymeric substances), osmolyte accumulation, and/or mass cell death (Warren, 2020; Preece et al., 2019; Schimel, 2018; Manzoni et al., 2014; Meisner et al., 2013; Kakumanu et al., 2012). Effects of drought on microbial biomass C (MBC) are unclear, as some studies report negative effects (Liang et al., 2021; Hueso et al., 2012; Baldrian et al., 2010) while others observed neutral or positive influence (Singh et al. 2021; Schindlbacher et al., 2012). These differences could be related to methodology as well as a shift towards fungal dominance and/or changes in active rather than total MBC (Singh et al., 2021; Liang et

al., 2021; Bastida et al., 2016; Barnard et al., 2013). Drought can also impact expression of traits within populations and the relative abundance of microbial taxa; for example, Actinobacteria have been shown to be more tolerant to soil dryness (Barnard et al., 2013).

Extended soil dryness limits microbial activity including both C and N mineralization processes. Unfavorable conditions for microbial growth could downregulate extracellular enzyme production, resulting in a net decline in potential activities of soil enzymes over time (Singh et al., 2021; Alster et al., 2013; Steinweg et al., 2013; Hueso et al., 2012; Geissler et al., 2011). Depressed microbial growth, along with the continued degradative activity of extracellular enzymes, leads to a net accumulation of dissolved soil OC (Tiwari et al., 2022; Deng et al., 2021; Singh et al., 2021; Schaeffer et al., 2017; Sowerby et al., 2010).

In contrast to dry soils, where substrate accessibility due to hydrologic discontinuity limits microbial activity, slow gas diffusion and low oxygen availability are the predominant constraints experienced by soil microbes under saturated conditions (Moyano et al., 2013). Over time, anaerobic conditions can prompt a shift in microbial community structure and a decrease in the rate and efficiency of OM decomposition (Zheng et al., 2019; Manzoni et al., 2012b; Šantrůčková et al., 2004). At the community level, microbial activity is greatest at intermediate soil water contents with a balance between water- and air-filled pore spaces (Moyano et al., 2013; Franzluebbers et al., 1999).

Fluctuations in soil moisture content are common at the pore scale of soil microbial habitats, with perhaps the most well studied flux being rewetting of dry soil. Rewetting of dry soil is associated with a characteristic rapid burst of C and N mineralization, most often observed in field and laboratory experiments as a spike of CO_2 production, known as the 'Birch' effect (Birch, 1958). A large proportion of soil CO_2 and nitrous oxide export is associated the Birch effect, and despite substantial research the source of substrate fueling this pulse of microbial activity remains unclear (Rousk and Brankgari, 2022; Barnard et al., 2020; Ruser et al., 2006). Current hypotheses of underlying mechanisms for the Birch effect include a combination of physicochemical (e.g., aggregate slaking, OM desorption) and microbial responses (Barnard et al., 2020; Schimel, 2018; Navarro-Garcia et al., 2011). For example, microbial mortality and subsequent release of accumulated intracellular osmolytes have long been suggested to fuel the pulse of microbial growth upon rewetting (Kieft et al., 1987). Respiration pulses upon rewetting of soil have been observed to decrease with increasing drought intensity (Li et al., 2018), increasing soil moisture (Shi and Marschner, 2018), increasing number and frequency of drying-rewetting cycles (Meisner et al., 2017; Baumann and Marschner, 2013), and increasing SOM content and coarse texture (Canarini et al., 2017; Harrison-Kirk et al., 2013). Legacy effects arising from land use and prior drought history have also been demonstrated to influence the magnitude of the CO_2 pulse upon rewetting (Patel et al., 2020; Schimel, 2018; Evans and Wallenstein, 2012).

1.2 Research questions, hypotheses, and approach

Research questions

The following overarching research questions will be addressed by this dissertation:

1. Do responses of microbial C allocation processes to rewetting vary across aggregate size fractions?
2. Do soil viral abundance and virus-microbe interactions vary across aggregate size fractions?
3. How does length of soil drought influence microbial C allocation processes and virus-microbe interactions upon rewetting?

Hypotheses and rationale

Hypothesis 1. Sensitivity of microbial responses to rewetting will be positively related to aggregate size but only at low frequency of rewetting. Macroaggregates have greater structural sensitivity to physical disturbance relative to microaggregates. Slaking of dry macroaggregates upon rewetting will release aggregate-occluded OM for microbial decomposition. The extent of physical slaking will be positively related to aggregate size, but only at low-to-intermediate frequency of rewetting. Microaggregates have greater physical stability and higher water potential, so the microbial habitat will be less affected by rewetting-drying treatments relative to macroaggregates.

Hypothesis 2. Larger aggregates will have higher microbial activity and viral abundances relative to microaggregates. Differences in substrate quality and quantity across aggregate fractions will affect microbial growth and C allocation processes. Larger aggregates have greater OM availability to support greater microbial activity and higher microbial density, which will then increase rates of lytic viral production. Free viruses in macroaggregates will be subject to organic-organic sorption reactions, whereas microaggregates will include additional virus-mineral associations. Viral abundances measured at single timepoints represent the balance of production and destruction processes; virus particle interactions with soil components can promote virus persistence (e.g., decreased destruction). Microaggregates will tend to favor viral particle stabilization vs. production processes, decreasing net viral abundance over time.

Hypothesis 3. Microbial activity, viral abundance, and net lytic production rates will be positively correlated with length of soil drought. Low levels of microbial activity and viral lysis under dry conditions will decrease viral abundance over time. Longer drought will increase the proportion of the microbial community experiencing drought stress, which will increase microbial activity along with net lytic viral production upon rewetting. Limits on spatiotemporal contact for enzyme-substrate-microbe and virus-host systems in dry soil will limit microbial activity and viral infection processes. Rewetting will reestablish spatiotemporal contact as water potential becomes less negative, redistributing dissolved substrates and viral particles out of fine pores that exclude larger microbial hosts.

Research approach

The primary research objective is to investigate how interactions between soil aggregate size and wetting influence microbial C allocation processes and virus-microbe dynamics over time. These important but lesser known controls on soil microbial activity and C cycling in soils will be studied using a series of controlled, fully factorial incubation experiments. Soils will be collected from select research sites in eastern Tennessee, with the goal of investigating *within* soil mechanisms controlling microbial activity rather than drawing comparisons *across* soils or, for example, related to landscape scale management. Furthermore, it is likely that observed influences of soil moisture dynamics are dependent on matrix physical composition (e.g., microaggregates existing within the unfractionated soil matrix might not behave the same when incubated independently as a physically isolated fraction).

The proposed studies will measure treatment effects related to drying-rewetting, soil aggregate size fraction, and/or increased viral lysis. Viral lysis will be induced by direct application of Mitomycin C, a widely used experimental induction agent (Otsuji et al., 1959), to bulk soil and aggregate fractions. This research will use a combination of analytical techniques including measurement of common soil biogeochemical properties (i.e., respiration, microbial biomass C, total and dissolved organic C, inorganic N, extracellular enzyme activities, permanganate- and peroxide-oxidizable C), physical stability of aggregate size fractions, and epifluorescence microscopy for enumeration of bacterial and viral particles. Datasets for each incubation will be

analyzed for statistical significance of treatment effects using Analysis of Variance (ANOVA) and multivariate trends using Principal Components Analysis (PCA).

1.3 Significance and expected outcomes

This research advances knowledge of how soil physicochemical properties interact with dynamic wetting processes to control microbial functions in soil. Findings from these studies will contribute to understanding of fundamental responses of terrestrial ecosystems to changing precipitation regimes associated with climate change. Such work has potential to improve computational models of microbially-mediated processes across soils while contributing to the evolving conceptual views of soil organic matter formation and persistence.

Despite growing evidence of the great abundance and diversity of viruses in soils, the underlying soil-specific mechanisms affecting viral production and residence time remain unexplored. This dissertation research is a preliminary step towards the incorporation of viral ecology into current models of soil decomposition processes, as proposed conceptually in Figure 1.1. Viruses are overlooked as potential controllers of microbial activity and C cycling in soils, such that the unique interactions between soil physicochemical structure, wetting, and virus-microbe dynamics remain unaddressed. The goal of the proposed experiments is to improve mechanistic understanding of how soil aggregate structure and wetting influence microbial processes and to shed light on the unique ecological controls of virus-microbe interactions in soil.

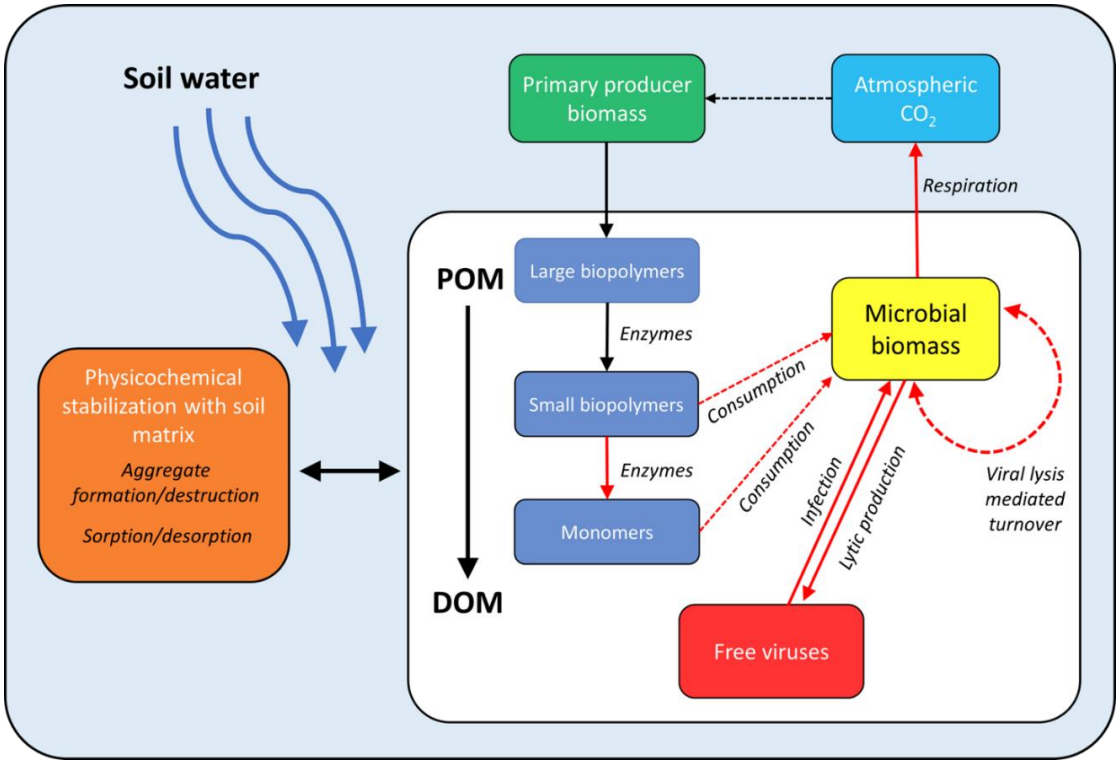

Figure 1.1 Conceptual diagram displaying updated soil decomposition model to reflect the proposed role of viruses in microbial decomposition processes.

Dashed arrows refer to biotic consumption processes, and red arrows highlight the pathways that would be stimulated by viral lysis. Plant residues are increasingly decomposed from particulate OM (POM) into dissolved OM (DOM), largely by the action of extracellular microbial enzymes. Small biopolymers (< 600 Da) and monomers are assimilated by the microbial biomass, producing CO_2. Free viruses exist as a component of the DOM pool where they infect susceptible microbial hosts. While viral lysis causes host mortality, it also increases local substrate availability that can fuel growth of new microbial biomass. Spatiotemporal contact is necessary for both enzymatic OM decomposition (i.e., between microbes, substrates, and enzymes) and viral infection (i.e., between virus and host) processes, but can be hindered by OM (including viruses) stabilization with the soil matrix (e.g., via aggregate occlusion, mineral sorption). Soil water, as intercepted by physical soil matrix, functions as an overarching control on microbial physiology, dissolution reactions, and transport processes that drive physicochemical OM (de)stabilization processes. Diagram is revised from the Soil Continuum Model of Lehmann and Kleber (2015).

References

Alster, C. J., German, D. P., Lu, Y., & Allison, S. D. (2013). Microbial enzymatic responses to drought and to nitrogen addition in a southern California grassland. *Soil Biol. Biochem.* 64, 68-79.

Angers, D. A. & Giroux, M. (1996). Recently Deposited Organic Matter in Soil Water-Stable Aggregates. *Soil Sci. Soc. Am. J.* 60, 1547-1551.

Bailey, V. L., Hicks Pries, C., & Latjtha, K. (2019). What do we know about soil carbon

Baldrian, P., Merhautová, V., Petránková, M., Cajthaml, T., & Šnajdr, J. (2010). Distribution of microbial biomass and activity of extracellular enzymes in a hardwood forest soil reflect soil moisture content. *Appl. Soil Ecol. 46,* 177-182.

Barnard, R. L., Osborne, C. A., & Firestone, M. K. (2013). Responses of soil bacterial and fungal communities to extreme desiccation and rewetting. *ISME J. 7,* 2229-2241.

Barnard, R. L., Blazewicz, S. J., & Firestone, M. K. (2020). Rewetting of soil: revisiting the origin of soil CO_2 emissions. *Soil Biol. Biochem.* 147, 107819.

Bastida, F. et al. (2017). Differential sensitivity of total and active soil microbial communities to drought and forest management. *Glob. Chang. Biol.* 23, 4185-4203.

Baumann, K., & Marschner, P. (2013). Effects of salinity on microbial tolerance to drying and rewetting. *Biogeochem.*112, 71-80.

Bergh, O., Borsheim, K. Y., Brakbak, G., & Heldal, M. (1989). High abundance of viruses found in aquatic environments. *Nature* 340, 467-468.

Birch, H. F. The effect of soil drying on humus decomposition and nitrogen availability. *Plant Soil* 10, 9-31 (1958).

Burns, R. G., et al. (2013). Soil enzymes in a changing environment: current knowledge and future directions. *Soil Biol. Biochem.* 58, 216-234.

Canarini, A., Kiær, L. P., & Dijkstra, F. A. (2017). Soil carbon loss regulated by drought intensity and available substrate: A meta-analysis. *Soil Biol. Biochem.* 112, 90-99.

Cotrufo, M. F., Wallenstein, M. D., Boot, C. M., Denef, K., & Paul, E. (2013). The Microbial Efficiency-Matrix Stabilization (MEMS) framework integrates plant litter decomposition with soil organic matter stabilization: do labile plant inputs form stable soil organic matter? *Global Change Biol.* 19, 988-995.

Davinic, M., et al. (2012). Pyrosequencing and mid-infrared spectroscopy reveal distinct aggregate stratification of soil bacterial communities and organic matter composition. *Soil Biol. Biochem.* 46, 63-72.

Deng, L., et al. (2021). Drought effects on soil carbon and nitrogen dynamics in global natural ecosystems. *Earth-Science Rev.* 214, 103501.

Elliot, E. T. (1986). Aggregate structure and carbon, nitrogen, and phosphorus in native and cultivated soils. *Soil Sci. Soc. Am. J.* 50, 627-633.

Evans, S. E., & Wallenstein, M. D. (2012). Soil microbial community response to drying and rewetting stress: does historical precipitation regime matter? *Biogeochem.* 109, 101-116.

Franzluebbers, A. J. (1999). Microbial activity in response to water-filled pore space of variably eroded southern Piedmont soils. *Appl. Soil Ecol.* 11, 91-101.

Fuhrman, J. A. (1999). Marine viruses and their biogeochemical and ecological effects. *Nature* 399, 541.

Fuhrman, J. A. & Noble, R. T. (1995). Viruses and protists cause similar bacterial mortality in coastal seawater. *Limnol. Oceanogr.* 40, 1236-1242.

Geisseler, D., Horwath, W. R., & Scow, K. M. Soil moisture and plant residue addition interact in their effect on extracellular enzyme activity. *Pedobiologia* 54, 71-78.

Ghosh, D., et al. (2008). Prevalence of Lysogeny among Soil Bacteria and Presence of 16S rRNA and trzN Genes in Viral-Community DNA. *Appl. Environ. Microbiol.* 74, 495-502.

Gupta, V. V. S. R. & Germida, J. J. (2015). Soil aggregation: Influence on microbial biomass and implications for biological processes. *Soil Biol. Biochem.* 80, A3-A9.

Gupta, V. V. S. R. & Germida, J. J. (1988). Distribution of microbial biomass and activity in different soil aggregates classes as affected by cultivation. *Soil Biol. Biochem.* 20, 777-786.

Harrison-Kirk, T., Beare, M. H., Meenken, E. D., & Condron, L. M. (2013). Soil organic matter and texture affect responses to dry/wet cycles: Effects on carbon dioxide and nitrous oxide emissions. *Soil Biol. Biochem.* 57, 43-55.

, P. M., Stark, J. M., Holt, C., Hooker, T., & Cardon, Z. G. Microbial growth efficiencies across a soil moisture gradient assessed using 13C-acetic acid vapor and 15N-ammonia gas. *Soil Biol. Biochem.* 41, 1262–69 (2009).

Hiederer, R. & Kochy, M. (2011). Global Soil Organic Carbon Estimates and the Harmonized World Soil Database. EUR 252225 EN. Publications Office of the EU, Luxembourg.

Howard-Varona, C., Hargreaves, K. R., Abedon, S. T., & Sullivan, M. B. (2017). Lysogeny in nature: mechanisms, impacts, and ecology of temperate phages. *ISME J.* 11, 1511-1520.

Hueso, S., García, C., & Hernández, T. (2012). Severe drought conditions modify the microbial community structure, size and activity in amended and unamended soils. *Soil Biol. Biochem.* 50, 167-173.

Jiao, N., et al. (2010). Microbial production of recalcitrant dissolved organic matter: long-term carbon storage in the global ocean. *Nat. Rev. Microbiol.* 8, 593-599.

Kaiser, M., Kleber, M., & Berhe, A. A. (2015). How air-drying and rewetting modify soil organic matter characteristics: an assessment to improve data interpretation and inference. *Soil Biol. Biochem.* 80, 324-340.

Kakumanu, M. L., Cantrell, C. L., & Williams, M. A. (2013). Microbial community response to varying magnitudes of desiccation in soil: A test of the osmolyte accumulation hypothesis. *Soil Biol. Biochem.* 57, 644-653.

Keiluweit, M., Wanzek, T., Kleber, M., Nico, P., & Fendorf, S. (2017). Anaerobic microsites have an unaccounted for role in soil carbon stabilization. *Nature Communications* 8, 1771.

Kieft, T. L., Soroker, E., & Firestone, M. K. (1987). Microbial biomass response to a rapid increase in water potential when dry soil is wetted. *Soil Biol. Biochem.* 19, 119-126.

Kimura, M., Jia, Z.-J., Nakayama, N., & Asakawa, S. (2008). Ecology of viruses in soils: Past, present, and future perspectives. *J. Soil Sci. Plant Nutr.* 54, 1-32.

Lehmann, J. & Kleber, M. (2015). The contentious nature of soil organic matter. *Nature* 528, 60-68.

Li, J. T., Wang, J. J., Zeng, D. H., Zhao, S. Y., Huang, W. L., Sun, X. K., & Hu, Y. L. (2018). The influence of drought intensity on soil respiration during and after multiple drying-rewetting cycles. *Soil Biol. Biochem.* 127, 82-89.

Liang, C., Ding, Y., Yue, Y., Zhang, X. Y., Song, M. H., Gao, J. Q., & Yu, F. H. (2021). Litter affects CO_2 emission from Alpine wetland soils experiencing drying-rewetting cycles with different intensities and frequencies. *Catena* 198, 105025.

Liang, C., Amelung, W., Lehmann, J., & Kästner, M. (2019). Quantitative assessment of microbial necromass contribution to soil organic matter. *Glob. Change Biol.* 25, 3578-3590.

Liang, C., Schimel, J. P., & Jastrow, J. D. (2017). The importance of anabolism in microbial control over soil carbon storage. *Nature Microbiol.* 2, 17105.

Liang, X., et al. (2020). Lysogenic reproductive strategies of viral communities vary with soil depth and are correlated with bacterial diversity. *Soil Biol. Biochem.* 144, 107767.

Manzoni, S. & Katul, G. (2014). Invariant soil water potential at zero microbial respiration explained by hydrological discontinuity in dry soils. *Geophys. Res. Lett.* 41, 7151-7158.

Manzoni, S., Schaeffer, S. M., Katul, G., Porporato, A., & Schimel, J. P. (2014). A theoretical analysis of microbial ecophysiological and diffusion limitations to carbon cycling in drying soils. *Soil Biol. Biochem.* 73, 69–83.

Manzoni, S., Schimel, J. P., & Porporato, A. (2012a). Responses of soil microbial communities to water stress: results from a meta-analysis. *Ecology* 93, 930-938.

Manzoni, S., Taylor, P., Richter, A., Porporato, A., & Agren, G. (2012b). Environmental and stoichiometric controls on microbial carbon-use efficiency in soils. *New Phytol.* 196, 79-91.

Marsh, P. & Wellington, E. M. H. (1994). Phage-host interactions in soil. *FEMS Microbiol. Ecol.* 15, 99-108.

Meisner, A., Leizeaga, A., Rousk, J., & Bååth, E. (2017). Partial drying accelerates bacterial growth recovery to rewetting. *Soil Biol. Biochem.* 112, 269-276.

Middelboe, M. & Jørgensen, J. O. G. (2006). Viral lysis of bacteria: an important source of dissolved amino acids and cell wall compounds. *J. Mar. Biol. Ass. U.K.* 86, 605-612.

Miltner, A., Bombach, P., Schmidt-Brücken, B., & Kästner, M. (2012). SOM genesis: microbial biomass as a significant source. *Biogeochem*. 111, 41-55.

Moyano, F. E., Manzoni, S., & Chenu, C. (2013). Responses of soil heterotrophic respiration to moisture availability: An exploration of processes and models. *Soil Biol. Biochem.* 59, 72-85.

Moyano, F. E., et al. (2012). The moisture response of soil heterotrophic respiration: interaction with soil properties. *Biogeosci.* 9, 1173-1182.

Mummey, D. L. & Stahl, P.D. (2004). Analysis of soil whole- and inner-microaggregate bacterial communities. *Microb. Ecol.* 48, 41-50.

Navarro-Garcia, F., Casermeiro, M. A., & Schimel, J. P. (2012). When structure means conservation: Effect of aggregate structure in controlling microbial responses to rewetting events. *Soil Biol. Biochem.* 44, 1-8.

Oades, J. M. (1984). Soil organic matter and structural stability: mechanisms and implications for management. *Plant Soil* 76, 319-337.

Otsuji, N., Sekiguchi, M., Iijima, T., & Takagi, Y. (1959). Induction of Phage Formation in the Lysogenic Escherichia coli K-12 by Mitomycin C. *Nature* 184, 1079-1080.

Patel, K. F., et al. (2020). Soil carbon dynamics during drying vs. rewetting: Importance of antecedent moisture conditions. *Soil Biol. Biochem.* 156, 108165.

Paul, J. H. & Jiang, S. C. (2001). Lysogeny and transduction. In: *Methods in Microbiology* (Paul, J., Ed.), vol. 30, 105-125. Academic Press, San Diego CA.

Preece, C. Verbruggen, E., Liu, L., Weedon, J. T., & Penuelas, J. (2019). Effects of past and current drought on the composition and diversity of soil microbial communities. *Soil Biol. Biochem.* 131, 28-39.

Procotor, L. M. & Fuhrman, J. A. (1990). Viral mortality of marine bacteria and cyanobacteria. *Nature* 343, 60-62.

Ranjard, L., Poly, F., Combrisson, J., Richaume, A., Gourbiere, F., Thioulouse, J., & Nazaret, S. (2000). Heterogeneous cell density and genetic structure of bacterial pools associated with various soil microenvironments as determined by enumeration and DNA fingerprinting approach (RISA). *Microb. Ecol.* 39, 263-272.

Rousk, J., & C Brangarí, A. (2022). Do the respiration pulses induced by drying–rewetting matter for the soil–atmosphere carbon balance? *Glob. Chang. Biol.* 28, 3486-3488.

Ruser, R., Flessa, H., Russow, R., Schmidt, G., Buegger, F., & Munch, J. C. (2006). Emission of N2O, N2 and CO2 from soil fertilized with nitrate: effect of compaction, soil moisture and rewetting. *Soil Biol. Biochem.* 38, 263-274.

Šantrůčková, H., Picek, T., Tykva, R., Simek, M., & Pavlu, B. (2004). Short-term partitioning of 14C-glucose in the soil microbial pool under varied aeration status. *Biol. Fert. Soils* 40, 386-392.

Schaeffer, S. M., Homyak, P. M., Boot, C. M., Roux-Michollet, D., & Schimel, J. P. (2017). Soil carbon and nitrogen dynamics throughout the summer drought in a California annual grassland. *Soil Biol. Biochem.* 115, 54-62.

Scharlemann J. P. W., Tanner E. V. J., Hiederer, R., & Kapos, V. (2014). Global soil carbon: understanding and managing the largest terrestrial carbon pool. *Carbon Management* 5, 81-91.

Schimel, J. P. (2018). Life in Dry Soils: Effects of Drought on Soil Microbial Communities and Processes. *Annu. Rev. Ecol. Evol. S.* 49, 409-432.

Schimel, J., Balser, T. C., & Wallenstein, M. (2007). Microbial stress-response physiology and its implications for ecosystem function. *Ecology* 88, 1386-1394.

Schimel, J. P. & Schaeffer, S. M. Microbial control over carbon cycling in soil. *Front. Microbiol.* 3, 348 (2012).

Schindlbacher, A., Wunderlich, S., Borken, W., Kitzler, B., Zechmeister-Boltenstern, S., & Jandl, R. (2012). Soil respiration under climate change: prolonged summer drought offsets soil warming effects. *Glob. Chang. Biol.* 18, 2270-2279.

Schmidt, M. W., et al. (2011). Persistence of soil organic matter as an ecosystem property. *Nature* 478, 49-56.

Shi, A., & Marschner, P. (2014). Drying and rewetting frequency influences cumulative respiration and its distribution over time in two soils with contrasting management. *Soil Biol. Biochem.* 72, 172-179.

Singh, S., Mayes, M. A., Shekoofa, A., Kivlin, S. N., Bansal, S., & Jagadamma, S. (2021). Soil organic carbon cycling in response to simulated soil moisture variation under field conditions. *Sci. Rep.* 11, 1-13.

Six, J., Bossuyt, H., Degryze, S., & Denef, K. (2004). A history of research on the link between (micro)aggregates, soil biota, and soil organic matter dynamics. *Soil Till. Res.* 79, 7-31.

Six, J., Elliot, E. T., & Paustian, K. (2000). Soil macroaggregate turnover and microaggregate formation: a mechanism for C sequestration under no-tillage agriculture. *Soil Biol. Biochem.* 32, 2099-2103.

Smith, A. P., Marin-Spiotta, E., de Graaff, M. A., & Balser, T. C. (2014). Microbial community structure varies across soil organic matter aggregate pools during tropical land cover change. *Soil Biol. Biochem.* 77, 292-303.

Sowerby, A., Emmett, B. A., Williams, D., Beier, C., & Evans, C. D. (2010). The response of dissolved organic carbon (DOC) and the ecosystem carbon balance to experimental drought in a temperate shrubland. *Euro. J. Soil Sci.* 61, 697-709.

Suttle, C. A. (2005). Viruses in the sea. *Nature* 437, 356-361.

Stark, J. M. & Firestone, M. K. (1995). Mechanisms for soil moisture effects on activity of nitrifying bacteria. *Appl. Environ. Microbiol.* 61, 218-221.

Steinweg, J. M., Dukes, J. S., Paul, E. A., & Wallenstein, M. D. (2013). Microbial responses to multi-factor climate change: effects on soil enzymes. *Front. Microbiol.* 4, 146.

Tisdall, J. M. & Oades, J. M. (1982). Organic matter and water-stable aggregates in soils. *J. Soil Sci.* 62, 141-163.

Tiwari, T., Sponseller, R. A., & Laudon, H. (2022). The emerging role of drought as a regulator of dissolved organic carbon in boreal landscapes. *Nat. Comm.* 13, 1-11.

Trivedi, P., et al. (2015). Soil aggregate size mediates the impacts of cropping regimes on soil carbon and microbial communities. *Soil Biol. Biochem.* 91, 169-181.

Totsche, K. U., et al. (2018). Microaggregates in soils. *J. Plant Nut. Soil Sci.* 181, 104-136.

Upton, R.N., Bach, E.M., & Hofmockel, K.S. (2019). Spatio-temporal microbial community dynamics within soil aggregates. *Soil Biol. Biochem.*132, 58-68.

Väisänen, R. K., Roberts, M. S., Garland, J. L., Frey, S. D., & Dawson, L. A. (2005). Physiological and molecular characterization of microbial communities associated with different water-stable aggregate size classes. *Soil Biol. Biochem.* 37, 2007-2016.

Veach, A. M., & Zeglin, L. H. (2020). Historical drought affects microbial population dynamics and activity during soil drying and re-wet. *Microb. Ecol.* 79, 662-674.

von Lutzow, M., Kogel-Knabner, I., Ekschmitt, K., Matzner, E., Guggenberger, G., Marschner, B., & Flessa, H. (2006). Stabilization of organic matter in temperate soils: mechanisms and their relevance under different soil conditions—a review. *Euro. J. Soil Sci.* 57, 426-445.

Warren, C. R. (2020). Pools and fluxes of osmolytes in moist soil and dry soil that has been re-wet. *Soil Biol. Biochem.* 150, 108012.

Weitz, J. S. & Wilhelm, S. W. (2012). Ocean viruses and their effects on microbial communities and biogeochemical cycles. *F1000 Biol. Rep.* 4, 17.

Weinbauer, M. G. (2004). Ecology of prokaryotic viruses. *FEMS Microbiol. Rev.* 28, 127-181.

Wilhelm, S. W. & Suttle, C. A. (1999). Viruses and Nutrient Cycles in the Sea. *Biosci.* 49, 781-788.

Williamson, K. E. (2011). Soil Phage Ecology: Abundance, Distribution, and Interactions with Bacterial Hosts. In: *Biocommunication in Soil Microorganisms. Soil Biology* (Witzany, G., Ed.), vol. 23. Springer, Berlin, Heidelberg.

Williamson, K. E., Fuhrmann, J. J., Wommack, K. E. & Radosevich, M. (2017). Viruses in Soil Ecosystems: An Unknown Quantity Within an Unexplored Territory. *Annu. Rev. Virol.* 4, 201-219.

Williamson, K. E., Radosevich, M., Smith, D. W., & Wommack, K. E. (2007). Incidence of lysogeny within temperate and extreme soil environments. *Environ. Microbiol.* 9, 2563-2574.

Williamson, K. E., Radosevich, M., & Wommack, K.E. (2005). Abundance and Diversity of

Wommack, K. E. & Colwell, R. R. (2000). Virioplankton: Viruses in Aquatic Ecosystems. *Microbiol. Mol. Biol. R.* 64, 69-114.

Wright, D. A., Killham, K., Glover, A., & Prosser, J. L. (1995). Role of pore size location in determining bacterial activity during predation by protozoa in soil. *Appl. Env. Microbiol.* 61, 3537-3543.

Zhang, S., Li, Q., Lu, Y., Zhang, X., & Liang, W. (2013). Contributions of soil biota to C sequestration varies with aggregate fractions under different tillage systems. *Soil Biol. Biochem.*62, 147-156.

Zheng, Q., et al. (2019). Growth explains microbial carbon use efficiency across soils differing in land use and geology. *Soil Biol. Biochem.*128, 45-65.

CHAPTER TWO

SOIL AGGREGATE SIZE INFLUENCES MICROBIAL FUNCTIONAL ACTIVITY UPON REWETTING AND IS DEPENDENT UPON DROUGHT INTENSITY

A version of this chapter will be originally submitted to *Soil Science Society of America Journal* by Aubrey K. Fine and Sean M. Schaeffer*.

Department of Biosystems Engineering and Soil Science, University of Tennessee, Knoxville, TN 37996, United States.

*Corresponding author: sschaef5@utk.edu

Acknowledgements: This study was partially supported by the National science Foundation (NSF) Grant # EAR-1331906 for the Intensively Managed Landscape Critical Zone Observatory, a multi-institutional collaborative effort. Financial assistance was also provided by the Institute for a Secure and Sustainable Environment at the University of Tennessee. Laboratory assistance was appreciated from M. Davis, M. English, L. Turpin, and X. Xu.

Abstract

The effects of drought on soil physical, biological, and chemical properties remain unclear, but have important implications for soil carbon (C) storage. In this study, we investigated how soil aggregate size mediates the microbial transformation of soil C and nitrogen (N) pools in response to varying intensity of drought. Agricultural soil from eastern Tennessee USA was dry sieved into three aggregate fractions (large macro-, small macro-, and micro-aggregates) that were subsequently incubated for 42 d. Aggregates were re-wetted to 50% water holding capacity at varying frequency, such that dry days in between wetting events also varied; after each moisture pulse, 24 h respiration was measured. Post-incubation, aggregate fractions were subsampled for wet aggregate stability, dissolved organic C (DOC), permanganate oxidizable C (POXC), inorganic N pools, and activities of seven major microbial hydrolytic extracellular enzymes. Significant effects ($p < .05$) for re-wetting frequency and aggregate size were observed for aggregate stability, with large macroaggregates having the lowest stability. Effects of number of dry days between re-wetting events were consistent across aggregate fractions, with wetting every five days producing a peak in cumulative respiration greater than a daily-wetted control. DOC decreased with one wetting event, while the opposite was observed for POXC; no correlation was observed between these two measures of labile C. Extractable nitrate and net nitrification and N mineralization increased as wetting frequency increased, with the magnitude of increase proportional to aggregate size. Most enzyme activities decreased with increasing wetting and were always lowest in the microaggregate

fraction. Our data indicate that slaking of macroaggregates had been maximized by treatment application, such that no differences in post-wetting respiration (day 42) were observed among aggregate fractions. Low drought intensity (i.e., high frequency of wetting) resulted in the highest microbial net C and N transformations and an increase in POXC relative to longer-term drought treatments. These findings suggest a decreased ability of soils to accumulate stable, microbially processed C under intensive drought regardless of initial aggregate size distribution. Furthermore, it is demonstrated that soils from the southeastern USA, although not traditionally considered especially prone to drought, are susceptible to deleterious effects on soil microbes associated with prolonged declines in soil water availability.

2.1 Introduction

Climate change is projected to increase the frequency and magnitude of extreme weather events including flooding and drought across the globe (Frank et al., 2015; Trenberth, 2011). Shifts in climate patterns have the potential to alter key terrestrial ecosystem functions ranging from net primary production to microbial decomposition. Soil microorganisms mediate the biochemical transformation of plant residues into stable forms of microbially processed soil organic matter (SOM), representing a major mechanism of soil carbon (C) accumulation. Microbial processes in soil directly rely on available water to meet physiological requirements, but also to physically access organic residues within the soil physicochemical matrix. Ecosystem scale shifts in precipitation patterns have the potential to alter microscale habitat characteristics

within the soil pore network, with unknown consequences for microbial growth and SOM formation.

Soil microbes exist in a three-dimensional matrix that is a dynamic mixture of solid, liquid, and gas phases. Soil texture (i.e., distribution of sand, silt, clay) and physical structure (e.g., aggregation), with the resulting network of soil pores, largely control the distribution of microbes and water within the soil over time and in response to wetting events (Kravchenko et al., 2015; Ruamps et al., 2011). Intermediate soil water contents generally provide an ideal balance between oxygen and water availability that supports efficient aerobic microbial activity and hydraulic connectivity among soil pores (Moyano et al., 2013). When the soil dries, matric potential decreases as water becomes increasingly unavailable and concentrated in micropores (Yan et al., 2016; Borken and Matzner, 2008). Concentration of water in discreet patches as films on soil particles minimizes diffusive transport of microbes, extracellular enzymes, and substrates, ultimately imposing a stress on living organisms that increases with time (Moyano et al., 2013; Manzoni et al., 2012a). Evidence suggests that microbes differ in their tolerance to drought stress (Manzoni et al., 2012a), but the functional response of whole soil microbial communities to varying intensity (i.e., length) of drought across ecosystem types remains unclear (Boot et al., 2013).

In agroecosystems, soil aggregation has been identified as a key process that can increase soil C storage over intermediate-to-long terms (Six et al., 2000). Soil aggregates occur in a dynamic hierarchy, with larger aggregates being composed of

smaller sized aggregates bound together by organic residues (Six et al., 2004; Tisdall and Oades, 1982). Soil aggregates differ in their mode of formation and stability in the soil depending on size, where larger aggregates are generally considered to be the result of more recent microbial (especially fungal) processes and are less physically stable (i.e., more susceptible to slaking and faster turnover) (Six and Paustian, 2014; Denef et al., 2001). There remain large knowledge gaps in the interactive effects of soil aggregation and climate on microbial processes. For example, it is unknown how microbial drought stress affects production of biomass and extracellular products such as enzymes and polysaccharides that contribute to macroaggregate formation. While studies into effects of drought have justifiably focused on the most drought-prone ecosystems (e.g., deserts, Mediterranean climates), it is increasingly clear that climate change will alter precipitation patterns in agriculturally important regions across the globe including the southeastern United States that also experience soil water stress.

This study was conducted to investigate how microbial C and N cycling processes within aggregate size fractions are affected by varying intensity of drought in a silt loam agricultural soil of eastern Tennessee, USA. Specifically, we sought to address how varying wetting frequency affects wet stability of aggregate fractions and the release of aggregate-occluded OM upon re-wetting. We broadly hypothesized that microbial processes would be sensitive to wetting treatments and that these effects would scale positively with aggregate size.

2.2 Materials and Methods

Soil collection and processing

Soils were collected in May 2018 from the East Tennessee Research and Education Center, Plant Sciences Farm owned by the University of Tennessee. Soils of this site are classified as Fine, Mixed, Semiactive, Thermic Typic Hapludults that formed in a clayey residuum weathered from shale parent material (Soil Survey Staff, 2019). Soil cores (2.5 cm diameter) were randomly collected (0-10 cm depth) and composited to a total mass of 2 kg (approximately 40 individual cores). Soil was transported back to the laboratory and laid out to air dry the same day. Once dried to a constant weight (approximately 0.01 g water g dry soil^{-1}), soil was sieved using a series of stacked soil sieves to isolate three fractions for experimentation: large macroaggregates (1000-2000 µm; Large Macro), small macroaggregates (250-1000 µm; Small Macro), and microaggregates (53-250 µm; Micro) (Six et al., 2000). Aggregate fractions were initially analyzed for soil pH (1 part soil-to-2 parts deionized water), 33 mM potassium sulfate (K_2SO_4) extractable dissolved OC (DOC) and microbial biomass C (MBC), and water holding capacity (WHC). For MBC, the chloroform slurry method was used (paired extractions in 33 mM K_2SO_4 (10 g soil in 40 mL), with one being treated with ethanol-free chloroform to lyse microbial cells. Increase in DOC resulting from chloroform addition was used to calculated MBC (Gregorich et al., 1990; Vance et al., 1987). Water holding capacity (WHC) was determined by saturating aggregates (~10 cm^3) inside a filter funnel with deionized water and determining water retained by soil after drainage from gravity after 6 h.

Incubation of aggregate fractions

Aggregate fractions were weighed (40 g) into pint-sized glass jars with n=4 replicates per treatment combination (3 aggregate fractions * 6 wetting frequency treatments * 4 replicates = 72 jars). Three LM samples (one each for F0, F1, and F2 treatments) were lost over the incubation period, providing a total count of n = 69 jars. During re-wetting events, aggregate fractions were wetted with deionized water using a spray bottle until reaching 50% of measured WHC by mass (0.49 g water g dry soil^{-1} for Large Macro, 0.44 g water g dry soil^{-1} for Small Macro, and 0.33 g water g dry soil^{-1} for Micro). Immediately following wetting, jars were sealed with a screw cap lid fitted with a rubber septum for headspace gas sampling. At time t = 0, headspace CO_2 concentration was measured using an infrared gas analyzer (IRGA) (LI-850, Licor Inc., Lincoln, NE USA). Sealed jars were incubated for 24 h, at which time headspace CO_2 was again measured to assess CO_2 production rates. Headspace production of CO_2 was calculated using the ideal gas law. After measuring t = 24 h CO_2, jars were opened to the atmosphere and left to dry under ambient incubator conditions (i.e., jars were only sealed during 24 h respiration incubation to allow for dry-down between wetting events). All samples (except for no wetting (F0) controls) were subjected to a first wetting event (day 1; InitialResp) as well as a final re-wetting event (day 42; FinalResp), with varying frequency of rewetting performed depending on assigned rewetting treatment (Table 2.1 and Figure 2.1; all Tables and Figures for Chapter 2 are available in Appendix A). All incubations were carried out inside an incubator at 25 °C.

Post-incubation soil analyses

After the final respiration measurement (day 42), samples were left open and allowed to air dry inside the incubator. After one week, soils were gently mixed using a spatula and then sub-sampled for wet aggregate stability (WAS), extracellular enzyme activity assays, and soil C and inorganic N and P pools. Wet aggregate stability (WAS) was measured by spreading aggregates (5-10 g) on a wet sieve, allowing aggregates to draw up water from the sieve for 30 seconds, then lowering the sieve into a tub filled with 5 cm deionized water. The sieve was raised to right below the water surface, and the submersion process was repeated sixty times over two minutes (Elliot, 1986). Stability of large macroaggregates (1000-2000 µm) was determined using a 250 µm sieve, and for small macro- and micro-aggregates a 53 µm sieve was used. With a target sieve size for stability measurement that is 25% of the low end of the aggregate size range, microaggregates would have ideally been sieved past a 13 µm sieve which was not available. The water stable fraction retained on the sieve after dunking was rinsed into an aluminum pan then dried overnight (80 °C) before determining dry mass. To correct for sand content, the water-stable fraction was subjected to dispersion using five percent sodium hexametaphosphate treatment followed by sieving past 53 µm to isolate sand particles (Six et al., 2000). The mass of oven-dried sand was subtracted from total water stable fraction dry mass then multiplied by 100% to determine sand-corrected WAS (Kemper and Rosenau, 1986). The size range of sand particles overlaps with the size range used to classify soil aggregates, so percent aggregate-associated sand (i.e., proportion of total sample mass

attributed to the sand-sized fraction retained on 53 µm sieve post-chemical dispersion) was also calculated.

Incubated soil (5.0 g) was extracted using 20 mL of 33 mM K_2SO_4. Extracts were filtered through glass microfiber filters with 1.0 µm pore size (Whatman GF/B) and frozen at 4 °C until analysis. Extractable dissolved OC (DOC) was quantified by reacting extracts with a potassium persulfate reagent (Doyle et al., 2004) to oxidize soil organic C to gaseous CO_2. A series of potassium hydrogen phthalate standards was included in each analysis to use for calculation of persulfate-oxidized organic C. Samples and standards were reacted overnight (80 °C) in sealed glass vials equipped with rubber septa for headspace gas sampling, which was conducted after samples had cooled to room temperature using an IRGA.

Salt extracts were carried through three colorimetric assays to measure extractable nitrate (NO_3^-), ammonium (NH_4^+), and phosphate (PO_4^{3-}) concentrations. Nitrate was determined using a vanadium (III) chloride reagent (Doane and Horwath, 2003). Ammonium was quantified using the Berthelot reaction (Rhine et al., 1998). Inorganic phosphate was measured using the Malachite Green assay (D'Angelo et al., 2001). All N and P assays were conducted using colorimetric protocols modified for a 96-well microplate reader (Synergy H1 Hybrid Reader, Biotek Inc., Winooski, VT USA).

The method of Weil et al. (2003) was used to extract and quantify POXC for aggregate fractions. Briefly, 2.5 g was reacted with 20 mL 0.02 M potassium permanganate ($KMnO_4$) + 0.1 M calcium chloride solution with shaking at 120 rpm for 2 minutes. After settling, extracts were diluted x100 then measured for absorbance

at 550 nm wavelength using a microplate spectrophotometer. Standards of known concentration $KMnO_4$ were included with each plate and used to determine moles of KMnO4 oxidized upon reaction with soil OC. Assuming 9000 mg C oxidized per mole $KMnO_4$ (Weil et al., 2003), the amount of POXC was corrected for soil water content and reported in µg POXC g dry $soil^{-1}$.

Maximum potential activities for seven major C, N, and P hydrolytic enzymes were assayed using fluorometric methods (Saiya-Cork et al., 2002; Bell et al., 2013) (Table 2.2). Air-dried soils (2.75 g) were pre-incubated for 24 h after wetting to 50% WHC (25 °C). After 24 h, samples were immediately extracted with 91 mL 50 mM sodium acetate buffer (pH 6.3, matching mean soil pH) using high-speed blending. Variability in soil matrix effects was accounted for with standard additions of fluorescent labels-MUC (7-amino-4-methylcoumarin) and MUB (4-methylumbelliferone) made to each soil slurry. Soil slurries were incubated with MUC and MUB standards and labeled substrates (200 µl of 200 µM solution) at 25 °C in the dark for 3 hours. Fluorescence was measured using a microplate reader with 365 nm excitation wavelength and 450 nm emission wavelength set at optimal gain. Enzyme activity was calculated in nmol g dry $soil^{-1}$ h^{-1}, with higher activities indicating a greater amount of fluorescently labeled substrate that was degraded under the ideal conditions of incubation. Enzyme stoichiometric ratios were calculated by summing the individual EE activities for C (AG, BG, XYL, CB), N (NAG, LAP), and P (PHOS) degrading enzymes and calculating activity ratios for C:N, C:P, and N:P (Sinsabaugh and Follstad Shah, 2012).

Statistical analyses

This experiment was set up with a factorial treatment arrangement. Two-way analysis of variance (ANOVA) was conducted using both factors and Wetting * Aggregate interaction as fixed effects. Final respiration (FinalResp; day 42) was compared with initial respiration (InitialResp; day 1) by including time as a repeated measure sub-plot factor in the ANOVA model. A separate one-way ANOVA was conducted using respiration data collected across rewetting events 1 through 9 and within each aggregate fraction with the goal of identifying significant changes in mean CO_2 production rates between successive rewetting events. For all ANOVAs, significant effects were identified with a 95% confidence level ($p < .05$), then computed using least squares means and separated using Tukey's least significant difference (LSD). Linear relationships between all pairs of variables were evaluated by calculating Pearson product-moment correlation coefficients. Principal component analysis (PCA) was conducted on the correlation matrix to examine multivariate relationships ($n = 69$). All statistical analyses were conducted in SAS 9.4 (Cary, NC USA).

2.3 Results

Heterotrophic respiration

Respiration (i.e., CO_2 production) rates measured post-wetting to 50 % WHC were i) highest in Large Macro aggregates for both InitialResp and FinalResp and ii) positively related to aggregate size (Large Macro > Small Macro > Micro; $p < .05$).

(Table 2.3 and Figure 2.2). Initial (t = 0) microbial biomass C (MBC) of aggregate fractions were 0.84 ± 0.07 mg MBC g dry soil^{-1} for Large Macro, 0.26 ± 0.03 mg MBC g dry soil^{-1} for Small Macro, and 0.45 ± 0.04 mg MBC g dry soil^{-1} for Micro. MBC was only measured at t = 0). Based on measured respiration rates of the first re-wetting pulse (InitialResp), Small Macro had the largest amount of CO_2 produced per unit MBC. The ratio of FinalResp to InitialResp increased as length of drought increased (or as wetting frequency decreased) and was inversely related to aggregate size (Figure 2.2). By the last re-wetting pulse (FinalResp), there were no differences among aggregate fractions in respiration rates ($p < .0001$).

Aggregate C, N, and P pools

Across aggregate fractions, mean DOC was significantly affected by both rewetting frequency and aggregate treatments (Table 2.4 and Figure 2.3a). Lack of two-way interaction indicates consistent effects of rewetting frequency across aggregates, with Large Macro having significantly more DOC on average than both Small Macro and Micro ($p = 0.0006$) for all rewetting treatments. One rewetting event significantly decreased DOC ($p < .0001$). POXC was significantly affected by rewetting frequency ($p < .0001$) but not aggregate size (Table 2.4). The high frequency of rewetting treatments (F4, F8, F32) had higher POXC than F0 and all low frequency rewetting treatments (F1, F2) (Figure 2.3b).

Nitrate, ammonium, and phosphate were all significantly affected by Aggregate and Wetting Frequency treatments ($p < .05$) but with significant two-way Aggregate * Rewetting Frequency interactions ($p < .01$) (Table 2.4). Total extractable inorganic N

increased as wetting frequency increased, with NH_4 greater than NO_3 at low-to-mid frequency of rewetting (Figure 2.3c, d). The highest NH_4 concentration was observed for F1 across aggregates (2.47 ± 0.03 µg NH_4-N g dry soil^{-1}). Nitrate increased as Wetting Frequency increased ($p < .0001$), with maximal values for F8 (32.1 ± 0.76 µg NO_4-N g dry soil^{-1}) and F32 (34.98 ± 0.76 µg NO_4-N g dry soil^{-1}). Nitrate was the predominant form of extractable inorganic N for these samples, a trend which is indicative of increasing relative net nitrification as incubation proceeded. Across rewetting treatments, phosphate significantly increased with decreasing aggregate size ($p = 0.0002$; Large Macro < Small Macro < Micro) and was greatest with F0 (no rewetted control) (0.058 ± 0.003 µg PO_4-P g dry soil^{-1}) (Figure 2.4e).

Wet aggregate stability

Wet aggregate stability increased as aggregate size decreased ($p < .0001$) (15.5 ± 0.4 % for Large Macro, 31.0 ± 0.4 % for Small Macro, and 32.4 ± 0.4 % for Micro) (Table 2.4 and Figure 2.3f). Significant effects of rewetting frequency were only observed for Large Macro ($p = 0.0162$) (Table 2.4). A loss of macroaggregate structure was visibly apparent as re-wetting frequency increased, especially for large macroaggregates (Figure 2.4). Aggregate-associated sand content significantly increased as aggregate size decreased. Large Macro had less than 50% aggregate-associated sand content relative to Small Macro and Micro which were similar (60-70% by weight of stable aggregates) (Table 2.5).

Extracellular enzyme activities and stoichiometric ratios

Enzyme activities that were significantly ($p < .05$) affected by Freq and Agg treatments with meaningful two-way interaction include: AG, LAP, and NAG; without interaction, BG, PHOS, and XYL were significantly affected by both Freq and Agg while CB was only affected by Freq (Table 2.6). Rewetting effect on activities of AG, CB, and XYL was significant ($p < .05$) only in Small Macro and Micro aggregates which both decreased in activity as rewetting frequency increased (Figure 2.5). Of the four C-degrading enzymes assayed, BG had greater activity than the other three (AG, CB, and XYL) combined (Figure 2.5Figure 2.5). Activities of LAP were drastically lowered with one wetting event (F1) for all aggregate fractions, with the lowest activity observed in Micro (Figure 2.6a). Activities of NAG reached a maximum after one-to-two wetting events (F1 for Large Macro, F1 and F2 for Small Macro, F2 for Micro) (Figure 2.7b). With high frequency of wetting, activities of NAG decreased across aggregate fractions. Activities of PHOS were highest with F0 (not rewetted Control; 27.6 nmole g dry soil^{-1} h^{-1}) and lowest with F32 (24.7 ± 0.6 nmole g dry soil^{-1} h^{-1}). Across all rewetting frequency treatments, Small Macro and Micro had just over twice the PHOS activity of Large Macro.

Calculated enzyme stoichiometric ratios for C:N indicated effects of wetting as well as aggregate size but with a significant two-way interaction (Table 2.7). Relative to F0 control, soils that received re-wetting treatments all had significantly higher extracellular enzyme C:N ratios (Figure 2.7a). This ratio was similar between Large and Small Macro aggregates (excluding F0, which was lower in Small Macro), both of

which were lower than C:N ratio calculated for Micro (EE C:N = 1.1 ± 0.03). Large Macro had the greatest enzyme C:P ratio, and there was a slight decrease in C:P with increasing frequency of wetting observed in all aggregate fractions (mean EE C:P for F0 was 0.64 ± 0.01 and for F32 was 0.37 ± 0.01 (Figure 2.7b). Stoichiometry of enzyme N:P had opposite trends as C:N, with F0 having a greater N:P (1.3 ± 0.02) that decreased with increasing wetting frequency (F8 and F32 had EE N:P of 0.46 ± 0.02 (Figure 2.7c).

Multivariate statistical relationships

InitialResp had significant ($p < .05$) moderate positive correlation with NO_3, NH_4, phosphatase activity (PHOS), and enzyme C:N ratio (in addition to FinalResp); moderate negative correlations were observed with DOC, PO_4, WAS, and all enzyme activities except CB, NAG, and PHOS (Tables 2.8 and 2.9). FinalResp had high positive correlation with NH_4 ($r = 0.88$) and N-acetyl glucosamine activity (NAG) ($r = 0.75$) and moderate negative correlation with POXC ($r = -0.58$) and NO_3 ($r = -0.50$). POXC was negatively correlated with NH_4 ($r = -0.62$) and NAG ($r = -0.45$) and positively correlated with NO_3 ($r = 0.54$).

Nitrate (NO_3) had moderate positive correlation with PHOS ($r = 0.43$) and negative correlation with NH_4, PO_4, WAS, and all enzyme activities (Tables 2.8 and 2.9). Ammonium showed less correlation with other variables than NO_3 but was highly correlated with NAG activity ($r = 0.73$). DOC had high positive correlation with LAP ($r = 0.71$). Moderate-to-high positive correlation was observed among pairs of enzyme activities that excluded PHOS, with the highest correlations between AG and LAP ($r =$

0.75), AG and XYL (r = 0.73), and BG and CB (r = 0.69). Activity of PHOS had low negative correlation with PO_4 (r = -0.28).

Four principal components (PCs) accounted for 82.3 % of the total variance in the dataset and fulfilled criteria outlined by Jolliffe (2002) of having eigenvalues greater than one and a cumulative fraction of total variance of at least 70 % (Table 2.10). PC1 explained 34.5 % of the variance, with relatively high positive loadings for NH_4, Wet Aggregate Stability, and activities of C- and P- degrading enzymes (AG, BG, CB, PHOS, and XYL); high negative loadings were found for InitialResp and POXC. PC2 had a variance contribution of 25.8 % (cumulative for first two PCs of 60.3 %), with the highest loadings associated with FinalResp, NO_3, and LAP (positive loadings) and DOC (negative loading). For PC3 (13.3 % variability), loading scores show primary influence of PO_4 and for PC4 (8.7 % of variability) of NAG activity.

The PCA loading plot of PCs 1 and 2 (Figure 2.8a) displays distribution of variables across all four quadrants consistent with findings from the correlation analysis. Score plots with observations coded by Aggregate size (Figure 2.8b) and Rewetting Frequency (Figure 2.8c) shows the following trends: i) a separate cluster for F1 Microaggregates sand F2 Large Macroaggregates was formed apart from other samples pointing towards influence of WAS, DOC, PO_4, and activities of AG and LAP, ii) Large Macroaggregates tend to cluster together with high scores for PC1, whereas Small Macro and Micro are similarly distributed in PC space, and iii) excluding F0, clustering by Rewetting Frequency was observed representing a shift from positive to negative PC1 and PC2 values.

2.4 Discussion

Shifts in climate patterns have important implications not only for water quality but also for soil health and C storage. Changes in precipitation frequency with flooding or drought, for example, result in fundamental alterations to the habitat of soil microorganisms. Extended dry conditions in soil impart direct physiological stress on microbial communities while also limiting diffusion and transport of assimilable substrates to microbial cells (Schimel, 2018; Manzoni et al., 2014).

In this study, we measured soil microbial processes and wet aggregate stability in response to varying frequency of soil rewetting. Inherent in this experimental design, wetting treatments increased in frequency as the number of dry (i.e., drought) days between wetting events decreased. Furthermore, aggregates subsampled at the end of incubation formed a gradient of moisture contents, with the F0 and F1 treatments representing the longest-term (42 d) drought (i.e., greatest number of days since wetting) and the driest conditions (i.e., most negative water potential). The driest aggregates had moisture contents below the reported threshold for mineral soils of -13.8 MPa where microbial physiology (e.g., efficiency and growth) is negatively impacted (Schimel, 2018; Manzoni and Katul, 2014; Manzoni et al., 2012a). Aggregates receiving greater frequency of wetting (F2-F32) did not dry down to this extreme between rewetting events, representing a decrease in drought stress on microbes (Schimel, 2018; Meisner et al., 2017). Assuming there was adequate water available for microbes in these treatments, substrate limitations associated with spatiotemporal accessibility would have been the major constraint on microbial

activity and growth (Schimel, 2018; Manzoni et al., 2012a; Stark and Firestone, 1995). Soil wet aggregate stability data indicate that large macroaggregates were most responsive to effects of soil re-wetting. Stability of this fraction was low (11-18%), which reflects the low SOC of these soils that likely limited macro-aggregation. Wet stability of Small Macro and Microaggregates were similarly unaffected by wetting treatments, as it has been shown that aggregate structure is more stable as size decreases (Totsche et al., 2018; Trivedi et al., 2015; Denef et al., 2001).

The microbial burst of CO_2 post-wetting of dry soil (i.e., the Birch effect; Birch, 1958) showed significant ($p < .05$) initial differences among aggregate fractions with greater initial respiration rates associated with larger aggregates. With a lack of new C inputs during incubation, 24 h respiration rates decreased with each subsequent re-wetting pulse, and differences in respiration rates among aggregate fractions were negligible after a single wetting event. While physical slaking would increase microbial accessibility to previously aggregate-occluded substrate (e.g., as particulate organic matter (POM)), especially in the larger, POM-rich macroaggregates (Six et al., 2000), the lack of DOC accumulation and consistent decrease in microbial activity with incubation suggests increased substrate made available by slaking was quickly consumed by the actively growing microbial community (likely during the first wetting event) (Denef et al., 2001a; Denef et al., 2001b).

Permanganate oxidizable C (POXC) has been proposed as a standard soil health indicator based on data of sensitivity to sustainable land management in agricultural systems (Fine et al., 2017; Hurisso et al., 2016; Culman et al., 2013; Culman et al.,

2012; Plaza-Bonilla et al., 2014). This pool of C is thought to have a faster turnover time than the total SOC pool, but detailed studies on temporal responses of POXC using laboratory incubations have not been conducted to our knowledge. In this study, we observed changes in POXC on a 42-day timescale as the result of soil rewetting treatments. Low frequency wetting appears to decrease POXC relative to no-wetting control, but with high wetting frequency treatments an increase in POXC relative to F0 (no wet control) was observed. While the precise chemical composition of the POXC pool remains unclear, in the absence of new C inputs the observed increase is likely attributable to an increase in microbial-residue C from biomass turnover. This idea is consistent with findings of Romero et al. (2018) who used electrospray ionization Fourier transform ion cyclotron resonance mass spectrometry (ESI FT-ICR MS) to show that the $KMnO_4$-oxidation resistant fraction had a strongly reduced chemical character (O/C ratio less than 0.4) and higher condensed aromaticity and hydrogen saturation relative to unoxidized samples. POXC showed no effect of aggregate size, whereas DOC was lower in smaller aggregates. The lack of any correlative relationship between POXC and extractable DOC ($r = 0.11$, $p = 0.48$) suggests that the two measurements target different C pools; however, several authors have reported significant positive correlations between POXC and total soil organic C (Culman et al., 2012; Weil et al., 2003).

Soil inorganic N dynamics indicate that an increase in C mineralization with increasing frequency of re-wetting was accompanied by an increase in net N mineralization in the macroaggregate fraction (Large Macro and Small Macro).

Measured inorganic N pools were more sensitive to soil aggregate size than organic C pools, with the microaggregate fraction driving most of this sensitivity. Observed trends of low inorganic N in microaggregates could be related to an increase in soil organic N and a decrease in C:N ratio with decreasing aggregate size (Totsche et al., 2018; Nie et al., 2014; Six et al., 2004). Observations of nitrogen-degrading enzymes may support this idea because activities of both N-degrading enzymes (NAG, LAP) decreased with decreasing aggregate size. This could reflect a shift in soil organic N character among aggregate size classes with an increase in microbially processed and/or recalcitrant N with decreasing aggregate size (Totsche et al., 2018).

Extracellular enzyme activity assays measure maximum potential activity when substrate limitations and constraints on physical accessibility between enzyme and substrates are removed. Activities also represent the net balance between microbial production and consumption (Burns et al., 2014; Allison et al., 2011). With a lack of new substrate inputs to the system over the course of 42-day incubation, we expect a gradual decrease in activity and metabolic efficiency as microbes are increasingly C and nutrient limited (Manzoni et al., 2014). Extracellular enzyme production rates, therefore, would have been minimal (i.e., produced at low constitutive levels) (Burns et al., 2014; Manzoni et al., 2012b; Schimel and Schaeffer, 2012) and it is possible that N-rich enzymes themselves served as microbial substrate under these conditions (Geisseler et al., 2010). While we did not observe long-lasting effects (e.g., via increased respiration) of intra-aggregate released C (e.g., POM) made available upon

slaking during rewetting, this does not rule out short-term dynamics not captured by our experimental design.

Enzyme activities were greater in large and/or small macroaggregate fractions but were generally of the same order of magnitude as activities measured in the microaggregate fractions (even for the F0, no wet control). Other authors have reported the opposite trends, where decreasing aggregate size is associated with increasing enzyme activities, especially for C-degrading enzymes (Awad et al., 2018; Trivedi et al., 2015; Nie et al., 2014; Bailey et al., 2012; Dorodnikov et al., 2009; Allison and Jastrow, 2006; Fansler et al., 2005). Such disparities could be related to differing methodologies used to isolate aggregates (Bach and Hofmockel, 2014), but also variability in sampling season (Hargreaves and Hofmockel, 2014) and soil properties such as texture, mineralogy, available C contents, and microbial community structure (Bailey et al., 2013; Lagomarsino et al., 2012; Allison, 2006). Immobilization of enzymes by sorption to mineral particles and colloids may, in particular, lead to a high potential activity measurement when realized *in situ* activity is actually low (Allison and Jastrown, 2006). Increased frequency of rewetting (i.e., less time between rewetting events) decreased all EE activities besides PHOS, possibly reflecting alterations in OM-mineral associations related to changes in hydration of organic mineral coatings or localized ionic strength upon repeated rewetting (Kleber, 2007).

Interpretation of extracellular enzyme activities and stoichiometric ratios is complex, but some interesting trends were observed in this study. With the exception of higher enzyme C:N ratio in the microaggregate fraction, stoichiometric ratios and

effects of rewetting treatments were consistent across aggregate fractions. This is in contrast to data reported by the only other study to calculate extracellular enzyme stoichiometric ratios on aggregate fractions, where aggregate size effects for enzyme C:N and C:P were observed (Nie et al., 2014). The higher enzyme C:N ratio in the microaggregate fraction of our study is curious, especially because the no rewetting (42 d drought) control is not similarly elevated. If we assume a decrease in enzyme ratio occurs with increasing limitation of the element in the denominator relative to that in the numerator, findings from our PCA scores suggest i) decreased N limitation (perhaps replaced by C limitation as incubation proceeded) in the microaggregate fraction relative to large and small macroaggregates and ii) a decrease in N limitation with increased rewetting for all aggregate fractions. In contrast to stoichiometric ratio for extracellular enzyme C:N, ratios of enzyme C:P and N:P both decreased with increasing rewetting frequency. These results suggest that P limitation increased upon just one rewetting event and increased with high frequency rewetting. PHOS tended to increase with increasing frequency of rewetting in all aggregate fractions, which may represent an increase in production rates aimed at acquiring organic P made increasingly available with high frequency rewetting (Turner and Haygarth, 2001).

There were dramatic shifts in soil C and N pools with one rewetting event (i.e., F0 vs. F1). DOC was nearly 50% greater in the F0 control, where we also observed a low availability of inorganic N (both nitrate and ammonium). It has been suggested that DOC, which we quantified by performing a dilute salt extraction, accumulates in dry soils because of low levels of microbial demand (e.g., via increased dormancy or death

and/or decreases in activity) (Sheik et al., 2011; Schimel et al., 2007). Upon a single rewetting event (F1), available water would temporarily (i.e., until dry-down) increase diffusive transport of microbial cells, enzymes, and substrates, leading to a burst of microbial activity observed as a pulse of CO_2 production. At low rewetting frequency, when hydrological connectivity among soil pores is still transient, we expect soil microbes to experience N limitation that leaves them primarily dependent on SOM mineralization of organic N (Schimel and Bennett, 2004). At intermediate rewetting frequency (F4, F8), N limitation in microsites would decrease further due to enhanced diffusion; as a result, mineralization of SOM and nitrification are both expected to proceed, likely by separate microbial populations (Schimel and Bennett, 2004).

As rewetting frequency increased, we measured positive net nitrification (i.e., nitrate production) and net N mineralization (i.e., sum of nitrate and ammonium production) largely driven by the accumulation of nitrate. Similar increases of dissolved inorganic N with dry/rewet cycles have been associated with increases in DOC and DON of leachates (Gordon et al., 2008) and water extracts (Miller et al., 2005). While several pathways could be responsible for the observed increases in nitrate (e.g., increasing nitrification, decreasing denitrification) (Schimel and Bennett, 2004), other authors have reported declines in nitrification potential associated with increased rewetting that points towards mineralization of soil organic N as the primary transformation process (Miller et al., 2005). While we did not observe much response of dilute salt-extractable phosphate to experimental treatments, rewetting of dry soil has been associated with increased release of resin-extractable P (Butterly et al., 2009)

and water-soluble organic P (Turner and Haygarth, 2001). Within a larger ecosystem perspective, increases in dissolved C, N, and P with increasing frequency of rewetting could decrease soil storage of bioactive elements and increase export associated with runoff and leaching.

Most properties measured in this study are commonly used as measures of soil health, most commonly including wet aggregate stability, respiration, POXC, and enzyme activities (Fine et al., 2017; Andrews et al., 2004; Arshad and Martin, 2002). It is generally assumed that higher measured values for these properties correspond to increased soil health for assessment purposes (Fine et al., 2017; Andrews et al., 2004). During this soil incubation, POXC responded positively to increasing rewetting frequency. This was especially evident in larger aggregates which generally have higher microbial biomass, suggestive of a largely microbially-derived POXC pool. The opposite trends were observed for wet aggregate stability, respiration, and extracellular enzyme activities which all decreased with successive rewetting events. Lower measured values for these properties have been experimentally associated with a decline in agricultural soil functions at the field scale (Veum et al., 2014; Stott et al., 2009; Moebius et al, 2007). Extended drought conditions may, therefore, increase measured soil health properties in the short term, but long-term effects associated with soil C and nutrient stability across ecosystems remain unclear.

2.5 Conclusions

Ecosystems across the globe will experience future cross-scale shifts in temperature and precipitation patterns. Much of the previous work investigating

effects of drought and rewetting frequency in soil have been conducted in those systems that have been identified as especially susceptible such as Mediterranean and arid environments. In this study, we evaluated how soil wetting dynamics interact with soil aggregate size fractions to control soil microbial processes (respiration, extracellular enzyme activities) and soil C, N, and P availability in low organic matter content agricultural soil from eastern Tennessee. Using multivariate analysis, we observed shifts toward i) increasing net nitrification, extractable nitrate, and POXC with increasing rewetting frequency and ii) increasing wet aggregate stability and extracellular enzyme stoichiometric C:N ratio with decreasing aggregate size. Our findings indicate that high frequency rewetting increases heterotrophic respiration (i.e., CO_2 production) that scales with aggregate size, while promoting C and N transformations that result in changed SOM character over time. Evidence suggests that these changes are affected by shifts in microbial extracellular enzyme dynamics (e.g., production and degradation) in response to spatiotemporal availability of substrates driven by soil moisture. Such microscale interactions contribute to the ability of soil to accumulate SOM, which has larger-scale impacts on the ability of soils across the world to provide critical ecosystem services under a changing climate.

References

Allison, S. D. (2005). Cheaters, diffusion and nutrients constrain decomposition by microbial enzymes in spatially structured environments. *Ecol. Lett.* 8, 626-635.

Allison, S. D. (2006). Soil mineral and humic acids alter enzyme stability: implications for ecosystem processes. *Biogeochem*. 81, 361-373.

Allison, S. D. & Jastrow, J. D. (2006). Activities of extracellular enzymes in physically isolated fractions of restored grassland soils. *Soil Biol. Biochem.* 38, 3245-3256.

Allison, S. D., Lu, L., Kent, A. G., & Martiny, A. C. (2014). Extracellular enzyme production and cheating in *Pseudomonas fluorescens* depend on diffusion rates. *Front. Microbiol.* 5, 169.

Alster, C. J., German, D. P., Lu, Y., & Allison, S.D. (2013). Microbial enzymatic responses to drought and to nitrogen addition in a southern California grassland *Soil Biol. Biochem.* 64, 68-79.

Andrews, S.S., Karlen, D.L., & Cambardella, C. A. (2004). The Soil Management Assessment Framework: A Quantitative Soil Quality Evaluation Method. *Soil Sci. Soc. Am. J.* 68, 1945-1962.

Arshad, M. A. & Martin, S. (2002). Identifying critical limits for soil quality indicators in agro-ecosystems. *Agric. Ecosyst. Environ.* 88, 153-160.

Bell, C. W., Fricks, B. E., Rocca, J. D., Steinweg, J. M., McMahon, S. K., & Wallenstein, M. D. (2013). High-throughput Fluorometric Measurement of Potential Soil Extracellular Enzyme Activities. *J. Visualized Exp.* 81, e50961.

Birch, H. (1958). The effect of soil drying on humus decomposition and nitrogen availability. *Plant Soil* 10, 9-31.

Boot, C. M., Schaeffer, S. M., & Schimel, J. P. (2013). Static osmolyte concentrations in microbial biomass during seasonal drought in a California grassland. *Soil Biol. Biochem.* 57: 356-361.

Burns, R. G., et al. (2013). Soil enzymes in a changing environment: Current knowledge and future directions. *Soil Biol. Biochem.* 58: 216-234.

Cotrufo, M. F., Wallenstein, M. D., Boot, C. M., Denef, K., & Paul, E. (2013). The Microbial Efficiency-Matrix Stabilization (MEMS) framework integrates plant litter decomposition with soil organic matter stabilization: do labile plant inputs form stable soil organic matter? *Global Change Biol.* 19, 988-995.

Culman, S. W., et al. (2012). Permanganate Oxidizable Carbon Reflects a Processed Soil Fraction that is Sensitive to Management. *Soil Sci. Soc. Am. J.* 76, 494-504.

D'Angelo, E., Crutchfield, J., & Vandiviere, M. (2001). Rapid, Sensitive, Microscale Determination of Phosphate in Water and Soil. *J. Environ. Qual.* 30, 2206-2209.

DeForest, J. L., Smemo, K. A., Burke, D. J., Elliott, H. L., & Becker, J. C. (2012). Soil microbial responses to elevated phosphorus and pH in acidic temperate deciduous forests. *Biogeochem*. 109, 189-202.

Denef, K., et al. (2001a). Influence of dry-wet cycles on the interrelationship between aggregate, particulate organic matter, and microbial community dynamics. *Soil Biol. Biochem.* 33, 1599-1611.

Denef, K., Six, S., Paustian, K., & Merckx, R. (2001b). Importance of macroaggregate dynamics in controlling soil carbon stabilization: short-term effects of physical disturbance induced by dry-wet cycles. *Soil Biol. Biochem.* 33, 2145-2153.

Doane, T.A. & Horwath, W.R. (2003). Spectrophotometric Determination of Nitrate with a Single Reagent. Analytical Letters 36: 2713-2722.

Doran, J. W. (2002). Soil health and global sustainability: translating science into practice. *Agric. Ecosyst. Environ.* 88, 119-127.

Doyle, A., Weintraub, M. N., & Schimel, J. P. (2004). Persulfate Digestion and Simultaneous Colorimetric Analysis of Carbon and Nitrogen in Soil Extracts. *Soil Sci. Soc. Am. J.* 68, 669-676.

Elliot, E. T. (1986). Aggregate structure and carbon, nitrogen, and phosphorus in native and cultivated soils. *Soil Sci. Soc. Am. J.* 50, 627-633.

Fine, A. K., Schmidt, M. P., Martínez, C. E. (2018). Nitrogen-rich compounds constitute an increasing proportion of organic matter with depth in Oi-Oe-Oa-A horizons of temperate forests. *Geoderma* 323, 1-12.

Fine, A. K., van Es, H. M., & Schindelbeck, R. R. (2017). Statistics, Scoring Functions, and Regional Analysis of a Comprehensive Soil Health Database. *Soil Sci. Soc. Am. J.* 81, 589-601.

Frank, D., et al. (2015). Effects of climate extremes on the terrestrial carbon cycle: concepts, processes and potential future impacts. *Global Change Biol.* 21, 2861-2880.

Gregorich, E. G., Wen, G., Voroney, R. P., & Kachanoski, R. G. (1990). Calibration of a rapid direct chloroform extraction method for measuring soil microbial biomass C. *Soil Biol. Biochem.* 22, 1009-1011.

Jolliffe, I. T. (2002). *Principal component analysis.* Spring, London, United Kingdom.

Kallenbach, C. M., Frey, S. D., & Grandy, A. S. (2016). Direct evidence for microbial-derived soil organic matter formation and its ecophysiological controls. *Nat. Comm.* 7, 13630.

Kemper, W. D. & Rosenau, R. C. (1986). Aggregate Stability and Size Distribution. Chapter 17 in: *Methods of Soil Analysis, Part 1*. Physical and Mineralogical Methods—Agronomy Monograph no. 9 (2nd ed). American Society of Agronomy-Soil Science Society of America, Madison, WI USA.

Kravchenko, A. N., Negassa, W. K., Guber, A. K., Rivers, M. L. (2015). Protection of soil carbon within macro-aggregates depends on intra-aggregate pore characteristics. *Nat. Sci. Rep.* 5, 16261.

Lal, R. (2015). Sequestering carbon and increasing productivity by conservation agriculture. *J. Soil Water Conserv.* 70, 55A-62A.

Lehman, R. M., et al. (2015). Understanding and Enhancing Soil Biological Health: The Solution for Reversing Soil Degradation. *Sustainability* 7, 988-1027.

Liao, J. D., Boutton, T. W., & Jastrow, J. D. (2006). Storage and dynamics of carbon and nitrogen in soil physical fractions following woody plant invasion of grassland. *Soil Biol. Biochem.* 38, 3184-3196.

Manzoni, S. & Katul, G. (2014). Invariant soil water potential at zero microbial respiration explained by hydrological discontinuity in dry soils. *Geophys. Res. Lett.* 41, 7151-7158,

Manzoni, S., Schimel, J. P., & Porporato, A. (2012a). Responses of soil microbial communities to water stress: results from a meta-analysis. *Ecol*. 93, 930-938.

Manzoni, S., Taylor, P., Richter, A., Porporato, A., & Ågren, G. I. (2012b). Environmental and stoichiometric controls on microbial carbon-use efficiency in soils. *New Phytol.* 196, 79-91.

Matson, P. A., Parton, W. J., Power, A. G., & Swift, M. J. (1997). Agricultural Intensification and Ecosystem Properties. *Science* 277, 504-509.

McBratney, A., Field, D. J., & Koch, A. (2013). The dimensions of soil security. *Geoderma* 213, 203-213.

Miltner, A., Bombach, P., Schmidt-Brücken, B., & Kästner, M. (2012). SOM genesis: microbial biomass as a significant source. *Biogeochem*. 111, 41-55.

Moebius, B. N., van Es, H. M., Schindelbeck, R. R., Idowu, O. J., Clune, D. J., & Thies, J. E. (2007). Evaluation of Laboratory-Measured Soil Properties as Indicators of Soil Physical Quality. *Soil Sci.* 172, 895-912.

Moyano, F. E., Manzoni, S., & Chenu, C. (2013). Responses of soil heterotrophic respiration to moisture availability: An exploration of processes and models *Soil Biol. Biochem.* 59, 72-85.

Nie, M., Pendall, E., Bell, C., & Wallenstein, M. D. (2014). Soil aggregate size distribution mediates microbial climate change feedbacks. *Soil Biol. Biochem.* 68, 357-365.

Olander, L. P. & Vitousek, P. M. (2000). Regulation of soil phosphatase and chitinase activity by N and P availability. *Biogeochem.* 49, 175-190.

Paustian, K., Six, J., Elliott, E. T., & Hunt, H. W. (1999). Management options for reducing CO2 emissions from agriculturl soils. *Biogeochem*. 48, 147-163.

Rhine, E. D., Sims, G. K., Mulvaney, R. L., & Pratt, E. J. (1998). Improving the Berthelot Reaction for Determining Ammonium in Soil Extracts and Water. *Soil Sci. Soc. Am. J.* 62, 473-480.

Ruamps, L. S., Nunan, N., & Chenu, C. (2011). Microbial biogeography at the soil pore scale. *Soil Biol. Biochem.* 43, 280-286.

Saiya-Cork, K. R., Sinsabaugh, R. L., & Zak, D. F. (2002). The effects of long term nitrogen deposition on extracellular enzyme activity in an Acer saccharum forest soil. *Soil Biol. Biochem.* 34, 1309-1315.

Salazar-Villegas, A., Blagodatskaya, E., & Dukes, J. S. (2016). Changes in the Size of the Active Microbial Pool Explain Short-Term Soil Respiratory Responses to Temperature and Moisture. *Front. Microbiol.* 7,524.

Schimel, J. P., Balser, T. C., & Wallenstein, M. D. (2007). Microbial stress-response physiology and its implications for ecosystem function. *Ecol.* 88, 1386-1394.

Schimel, J. P. & Bennett, J. (2004). Nitrogen Mineralization: Challenges of a Changing Paradigm. *Ecol*. 85, 591-602.

Schimel, J. P. & Schaeffer, S. M. (2012). Microbial control over carbon cycling in soil. *Front. Microbiol.* 3, 348: 1-11.

Schimel, J. P. & Weintraub, M. N. (2003). The implications of exoenzyme activity on microbial carbon and nitrogen limitations in soil: a theoretical model. *Soil Biol. Biochem.* 35, 549-563.

Sheik, C. S., Beasley, W. H., Elshahed, M. S., Zhou, X., Luo, Y., & Kryumholz, L. R. (2011). Effect of warming and drought on grassland microbial communities. *ISME J.* 5, 1692-1700.

Sinsabaugh, R. L. & Follstad Shah, J. J. (2012). Ecoenzymatic Stoichiometry and Ecological Theory. *Annu. Rev. Ecol. Evol. Syst.* 43, 313-343.

Six, J., Elliott, E. T. & Paustian, K. (2000). Soil macroaggregate turnover and microaggregate formation: a mechanism for C sequestration under no-tillage agriculture. *Soil Biol. Biochem.* 32, 2099-2103.

Six, J. & Paustian, K. (2014). Aggregate-associated soil organic matter as an ecosystem property and a measurement tool. *Soil Biol. Biochem.* 68, A4-A9.

Soil Survey Staff, Natural Resources Conservation Service, United States Department of Agriculture (2019). Web Soil survey. Available online. Accessed November 1, 2019.

Stott, D. E., Andrews, S. S., Liebig, M. A., Wienhold, B. J., & Karlen, D. L. (2009). Evaluation of B-Glucosidase Activity as a Soil Quality Indicator for the Soil Management Assessment Framework. *Soil Sci. Soc. Am. J.* 74, 107-119.

Tisdall, J. M. & Oades, J. M. (1982). Organic matter and water-stable aggregates in soils. *J. Soil Sci.* 62, 141-163.

Trenberth, K. E. (2011). Changes in precipitation with climate change. *Clim. Res.* 47, 123-138.

Totsche, K. U., et al. (2018). Microaggregates in soils. *J. Plant Nutr. Soil Sci.* 181, 104-136.

Trivedi, P., et al. (2015). Soil aggregate size mediates the impacts of cropping regimes on soil carbon and microbial communities. *Soil Biol. Biochem.* 91, 169-181.

Vance, E. D., Brookes, P. C., & Jenkison, D. S. (1987). An Extraction Method for Measuring Soil Microbial Biomass C. *Soil Biol. Biochem.* 19, 703-707.

Weil, R. R., Islam, K. R., Stine, M. A., Gruver, J. B., Samson-Liebig, S. E. (2003). Estimating active carbon for soil quality assessment: A simplified method for laboratory and field use. *Am. J. Altern. Agric.* 18, 3-17.

Yan, Z., Liu, C., Todd-Brown, K. E., Liu, Y., Bond-Lamberty, B., and Bailey, V. L. (2016). Pore-scale investigation on the response of heterotrophic respiration to moisture conditions in heterogeneous soils. *Biogeochem*. 131, 121-134.

Appendix A

Table 2.1. Schedule of aggregate rewetting events.

Rewetting schedule indicating the day of incubation when the 24 h post-rewetting respiration incubation was initiated (t = 0). Six rewetting treatments and three aggregate fractions were tested in a factorial treatment arrangement (n = 4 replications).

Rewetting Frequency (F) Treatment	# Rewetting Events	# Days Dry	Incubation Day								
			1	6	11	16	21	26	31	36	41
F0	0	42									
F1	1	39	X								X
F2	2	19	X				X				X
F4	4	9	X		X		X		X		X
F8	8	5	X	X	X	X	X	X	X	X	X
F32*	32	1	X	X	X	X	X	X	X	X	X

*F32 samples were rewetted to 50% of measured water holding capacity daily but were only sampled for 24 h respiration every five days along with F8 samples.

Table 2.2. Extracellular enzymes assayed for maximum potential activities on aggregate fractions.

Table includes enzyme abbreviation, enzyme commission (EC) number, and the fluorescently labeled substrate used for the assay. Fluorescent labels of substrates are 4-methylumbelliferyl (MUB) and 4-methylcoumarin (MUC). Broad degradation target for enzymes are as follows: sugars (AG, BG), cellulose (CB), protein (LAP), chitin/amino sugar polymer (NAG), organic phosphorous (PHOS), and hemicellulose (XYL).

Enzyme	EC	Substrate
α-Glucosidase (AG)	3.2.1.20	4-MUB-α-D-Glucopyranoside
β-Glucosidase (BG)	3.2.1.21	4-MUB-β-D-Glucopyranoside
β-D-Cellubiosidase (CB)	3.2.1.91	4-MUB-β-D-Cellobioside
Leucine Aminopeptidase (LAP)	3.2.11.1	L-Leucine-MUC Hydrochloride
N-Acetyl-β-D-Glucosaminidase (NAG)	3.2.1.30	4-MUB-N-Acetyl-β-D-Glucosaminide
Acid Phosphatase (PHOS)	3.1.3.2	4-MUB Phosphate
β-Xylosidase (XYL)	3.2.1.37	4-MUB-β-D-Xylopyranoside

Table 2.3. Results of two-way Analysis of Variance (ANOVA) for initial respiration rate (InitialResp), final respiration rate (FinalResp), and ratio of final to initial respiration rates (RespRatio).

Fixed effects of Rewetting Frequency (Freq) and Aggregate size fraction (Agg) were included in the ANOVA model along with two-way interaction. Num DF is Numerator Degrees of Freedom and Denominator Degrees of Freedom = 45. Significant *p* values ($p < .05$) are indicated by bold text with an '*' for $p < .0001$.

Source	**Num DF**	InitialResp		FinalResp		RespRatio	
		F	***p***	**F**	***p***	**F**	***p***
Freq	4	7.8	*****	1825.9	*****	2257.8	*****
Agg	2	513.4	*****	195.6	*****	26.8	*****
Freq*Agg	8	4.3	**3E-04**	44.2	*****	9.8	*****

Table 2.4. Results of two-way Analysis of Variance (ANOVA) for dissolved organic c, permanganate oxidizable C, nitrate, ammonium, phosphate, and wet aggregate stability.

Fixed effects of Rewetting Frequency (Freq) and Aggregate size fraction (Agg) were included in the ANOVA model along with two-way interaction. Num DF is Numerator Degrees of Freedom and Denominator Degrees of Freedom = 54. Significant *p* values ($p < .05$) are indicated by bold text with an '*' for $p < .0001$.

Source	**Num**	DOC		POXC		NO_3		NH_4	
	DF	**F**	***p***	**F**	***p***	**F**	***p***	**F**	***p***
Freq	5	39.6	*****	15.6	*****	342.9	*****	342.6	*****
Agg	2	8.4	**0.001**	0.9	0.410	10.8	**0.000**	22.9	*****
Freq * Agg	10	1.2	0.328	1.6	0.143	3.7	**0.001**	6.6	*****

Abbreviations: dissolved organic carbon (DOC), permanganate oxidizable carbon (POXC), nitrate (NO_3), ammonium (NH_4), phosphate (PO_4), and wet aggregate stability (WAS).

Table 2.4 continued

Source	Num DF	PO_4		WAS	
		F	***p***	**F**	***p***
Freq	5	2.7	**0.030**	3.1	**0.016**
Agg	2	10.3	**0.000**	556.3	*****
Freq * Agg	10	2.6	**0.012**	2.2	**0.032**

Table 2.5. Wet aggregate stability (WAS) with chemical dispersion (WAS_d), without chemical dispersion (i.e., including sand-sized particles; WAS_s), and intra-aggregate sand content of each aggregate fraction.

WAS_d is only reported in this table, and otherwise is only indicated by WAS (no subscript) in the text. Standard error of $n = 4$ replications per treatment combination is indicated in parentheses.

Aggregate	Wetting	WAS_d (%)	WAS_s (%)	Sand (%)
Large Macro	F0	16.9 (0.8)	30.8 (0.6)	34.2 (0.2)
	F1	18.0 (0.8)	32.2 (0.4)	30.8 (1.6)
	F2	14.9 (2.0)	30.3 (0.4)	32.6 (0.8)
	F4	15.5 (0.6)	30.9 (0.8)	32.3 (1.1)
	F8	15.9 (1.3)	30.6 (0.3)	32.2 (0.9)
	F32	11.3 (0.9)	30.3 (1.8)	32.4 (0.2)
Small Macro	F0	45.4 (1.7)	93.8 (0.5)	92.1 (0.5)
	F1	47.9 (1.9)	94.9 (0.9)	91.2 (1.1)
	F2	40.2 (4.4)	94.3 (0.4)	91.2 (1.1)
	F4	41.8 (1.2)	95.2 (0.4)	91.9 (1.1)
	F8	41.5 (2.9)	96.0 (0.6)	89.5 (2.1)
	F32	31.1 (1.6)	92.6 (0.4)	88.2 (5.7)
Micro	F0	28.4 (0.8)	62.1 (0.9)	65.7 (0.2)
	F1	29.9 (1.2)	62.6 (1.0)	67.3 (0.8)
	F2	25.2 (2.3)	64.0 (0.6)	67.3 (0.8)
	F4	26.3 (0.6)	64.3 (1.0)	67.6 (1.3)
	F8	25.5 (1.7)	65.4 (0.4)	67.7 (0.9)
	F32	20.5 (0.7)	62.6 (2.8)	68.3 (0.8)

Table 2.6. Results of two-way Analysis of Variance (ANOVA) for extracellular enzyme activities.

Fixed effects of Rewetting Frequency (Freq) and Aggregate size fraction (Agg) were included in the ANOVA model along with two-way interaction. Num DF is Numerator Degrees of Freedom and Denominator Degrees of Freedom = 54. Significant *p* values ($p < .05$) are indicated by bold text with an '*' for $p < .0001$.

Source	**Num**	AG		BG		CB		LAP	
	DF	**F**	***p***	**F**	***p***	**F**	***p***	**F**	***p***
Freq	5	35.1	*****	15.7	*****	5.2	**0.000**	139.4	*****
Agg	2	3.2	**0.05**	4.5	**0.02**	2.6	0.086	96.2	*****
Freq * Agg	10	6.7	*****	0.6	0.84	2.2	**0.033**	4.6	*****

Abbreviations: α-Glucosidase (AG), β-Glucosidase (BG), β-D-Cellubiosidase (CB), Leucine Aminopeptidase (LAP), N-Acetyl- β-Glucosaminidase (NAG), Acid Phosphatase (PHOS), and β-Xylosidase (XYL).

Table 2.6 continued

Source	Num	NAG		PHOS		XYL	
	DF	**F**	***p***	**F**	***p***	**F**	***p***
Freq	5	23.5	*****	6.1	**0.000**	21.9	*****
Agg	2	7.5	**0**	9.0	**0.000**	20.3	*****
Freq * Agg	10	3.5	**0**	0.5	0.900	1.7	0.098

Table 2.7. Results of two-way Analysis of Variance (ANOVA) for extracellular enzyme C:N, C:P, and N:P stoichiometric ratios.

Fixed effects of Rewetting Frequency (Freq) and Aggregate size fraction (Agg) were included in the ANOVA model along with two-way interaction. Num DF is Numerator Degrees of Freedom and Denominator Degrees of Freedom = 54. Significant *p* values ($p < .05$) are indicated by bold text with an '*' for $p < .0001$.

Source	**Num DF**	EE C:N		EE C:P		EE N:P	
		F	***p***	**F**	***p***	**F**	***p***
Freq	5	15.0	*****	50.6	*****	198.3	*****
Agg	2	48.5	*****	5.2	**0.009**	70.6	*****
Freq * Agg	10	3.9	**5E-04**	1.5	0.173	6.7	*****

Table 2.8. Matrix of correlation coefficients (*r*) used for the Principal Components Analysis (PCA) (*n* = 60).

Statistically significant ($p < .05$) correlations are indicated by bold text; significance at $p < .1$ is indicated by an '*'and NS is not statistically significant at $p < .1$. All probability levels are provided in Table 2.9.

.

	InitialResp	FinalResp	DOC	POXC	NO_3	NH_4	PO_4	WAS
FinalResp	**0.39**							
DOC	**-0.56**	NS						
POXC	NS	**-0.58**	NS					
NO_3	**0.52**	**-0.5**	-0.22*	**0.54**				
NH_4	**0.33**	**0.88**	**-0.31**	**-0.62**	**-0.62**			
PO_4	**-0.7**	**-0.26**	**0.33**	NS	**-0.44**	NS		
WAS	**-0.61**	NS	NS	NS	**-0.36**	NS	**0.5**	
AG	**-0.66**	NS	**0.57**	NS	**-0.52**	NS	**0.56**	NS
BG	**-0.39**	NS	**0.26**	**-0.26**	**-0.6**	**0.31**	**0.38**	NS
CB	NS	NS	NS	NS	**-0.29**	NS	**0.31**	NS
LAP	**-0.7**	**-0.26**	**0.71**	NS	**-0.35**	**-0.3**	**0.46**	NS
NAG	NS	**0.75**	NS	**-0.45**	**-0.59**	**0.73**	NS	NS
PHOS	**0.43**	NS	**-0.35**	NS	**0.43**	NS	**-0.28**	NS
XYL	-0.22*	**0.26**	**0.35**	-0.22*	-0.56	**0.37**	0.23*	-0.22*

Abbreviations: α-Glucosidase (AG), ammonium (NH_4), β-Glucosidase (BG), β-D-Cellubiosidase (CB), dissolved organic carbon (DOC), Leucine Aminopeptidase (LAP), N-Acetyl-β-Glucosaminidase (NAG), nitrate (NO_3), Acid Phosphatase (PHOS), phosphate (PO_4), permanganate oxidizable carbon (POXC), and β-Xylosidase (XYL).

Table 2.8 continued

	AG	BG	CB	LAP	NAG	PHOS
FinalResp						
DOC						
POXC						
NO_3						
NH_4						
PO_4						
WAS						
AG						
BG	**0.56**					
CB	**0.56**	**0.69**				
LAP	**0.75**	**0.45**	**0.34**			
NAG	NS	**0.49**	**0.4**	NS		
PHOS	-0.22*	NS	NS	NS	NS	
XYL	**0.73**	**0.57**	**0.61**	**0.39**	**0.49**	NS

Table 2.9. Probability (*p*) values for correlation coefficients calculated between variable pairs.

Bold text indicates significance at $p < .05$ with a '°' added to designate $p < .1$ and an '*' to indicate $p < .0001$.

	InitialResp	FinalResp	DOC	POXC	NO_3	NH_4	PO_4	WAS
FinalResp	**0.002**							
DOC	*	0.127						
POXC	0.975	*	0.399					
NO_3	*	*	0.087°	*				
NH_4	**0.011**	*	**0.015**	*	*			
PO_4	*	**0.043**	**0.011**	0.663	**0.001**	0.335		
WAS	*	0.321	0.670	0.139	**0.004**	0.478	*	
AG	*	0.196	*	0.533	*	0.699	*	0.544
BG	**0.002**	0.140	**0.046**	**0.045**	*	**0.016**	**0.003**	0.131
CB	0.204	0.506	0.139	0.417	**0.023**	0.215	**0.016**	0.663
LAP	*	**0.043**	*	0.591	**0.006**	**0.021**	**0.000**	0.401
NAG	0.310	*	0.832	**0.000**	*	*	0.555	0.160
PHOS	**0.001**	0.285	**0.006**	0.117	**0.001**	0.589	**0.030**	0.109
XYL	0.089°	**0.044**	**0.006**	0.089°	*	**0.003**	0.078°	0.091°

Abbreviations: α-Glucosidase (AG), ammonium (NH_4), β-Glucosidase (BG), β-D-Cellubiosidase (CB), dissolved organic carbon (DOC), Leucine Aminopeptidase (LAP), N-Acetyl-β-Glucosaminidase (NAG), nitrate (NO_3), Acid Phosphatase (PHOS), phosphate (PO_4), permanganate oxidizable carbon (POXC), and β-Xylosidase (XYL).

Table 2.9 continued

	AG	BG	CB	LAP	NAG	PHOS
FinalResp						
DOC						
POXC						
NO_3						
NH_4						
PO_4						
WAS						
AG						
BG	*					
CB	*	*				
LAP	*	**0.000**	**0.008**			
NAG	0.155	*	**0.001**	0.536		
PHOS	0.085°	0.445	0.138	0.155	0.931	
XYL	*	*	*	**0.002**	*	0.616

Table 2.10. Eigenanalysis for Principal Components (PCs) 1, 2, 3, and 4 calculated from the correlation matrix used for the Principal Components analysis (PCA).

InitialResp is respiration rate from first rewetting event and FinalResp is respiration rate from the ninth/final rewetting event. Additional PCs had eigenvalues less than one. Variables contributing to each PC based on magnitude of loading scores are indicated by bold text. CumPercent is Cumulative Percent of variance explained with successive addition of each PC.

Eigenanalysis	**PC1**	**PC2**	**PC3**	**PC4**
Eigenvalue	5.18	3.87	2.00	1.30
Percent	34.5	25.8	13.3	8.7
Cum Percent	34.5	60.3	73.6	82.3
Loading scores	**PC1**	**PC2**	**PC3**	**PC4**
InitialResp	**-0.683**	0.605	0.331	-0.037
FinalResp	0.183	**0.903**	-0.155	-0.174
DOC	-0.354	**-0.581**	0.398	-0.032
POXC	**-0.826**	-0.331	0.364	0.029
NO_3	0.270	**0.911**	-0.151	0.005
NH_4	**0.620**	-0.421	-0.273	0.268
PO_4	0.262	-0.273	**-0.712**	0.493
WAS	**0.847**	-0.288	0.235	-0.074
AG	**0.774**	0.154	0.215	0.380
BG	**0.612**	0.113	0.516	0.360
CB	**0.691**	-0.480	0.189	-0.181
LAP	0.482	**0.730**	0.147	-0.082
NAG	-0.326	0.108	0.584	**0.599**
PHOS	**0.737**	0.234	0.412	-0.125
XYL	**0.756**	-0.020	0.441	-0.124

Abbreviations: α-Glucosidase (AG), ammonium (NH_4), β-Glucosidase (BG), β-D-Cellubiosidase (CB), dissolved organic carbon (DOC), Leucine Aminopeptidase (LAP), N-Acetyl-β-Glucosaminidase (NAG), nitrate (NO_3), Acid Phosphatase (PHOS), phosphate (PO_4), permanganate oxidizable carbon (POXC), and β-Xylosidase (XYL).

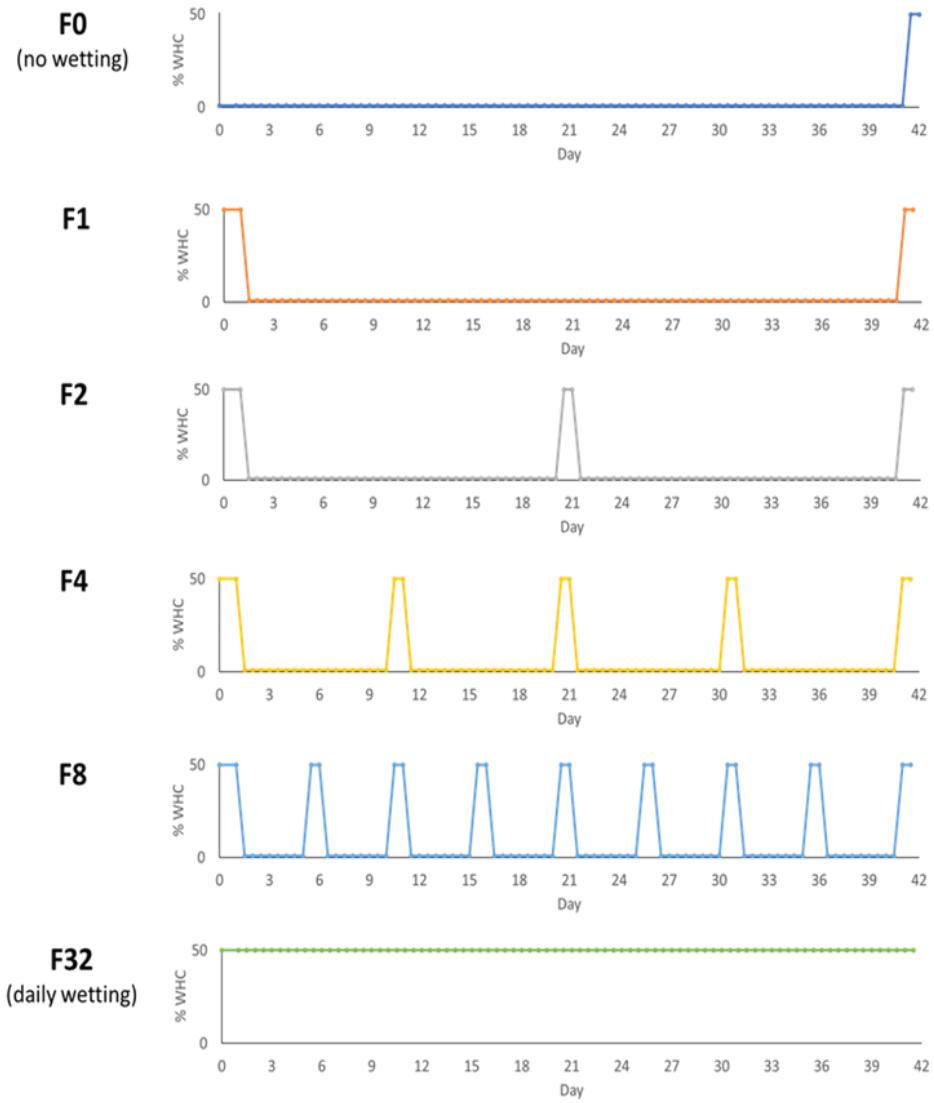

Figure 2.1. Record of soil gravimetric water content during incubation across aggregate fractions for Rewetting Frequency (F) treatments.

Aggregates were rewetted to 50% water holding capacity. F0 is dry (not-rewetted) control and F32 is constant moisture control.

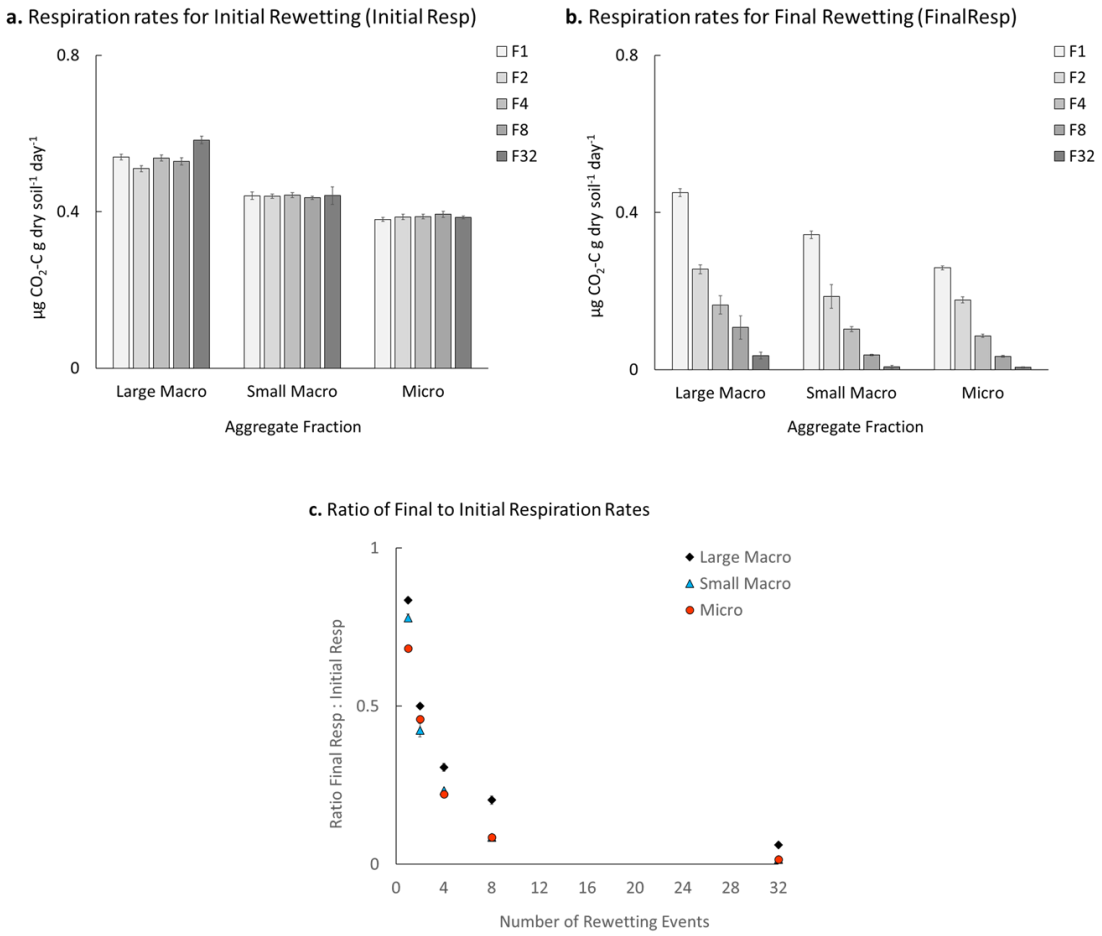

Figure 2.2. Mean heterotrophic respiration (i.e., CO_2 production) measured over 24 h immediately following wetting of soil aggregate fractions for the initial wetting event (InitialResp) (a) and the final rewetting event (FinalResp) (b), and Ratio of FinalResp (day 42) to InitialResp (day 1) (c) by Aggregate size fraction and Rewetting Frequency (F) treatments.

Error bars represent standard error of n = 4 replications per treatment combination.

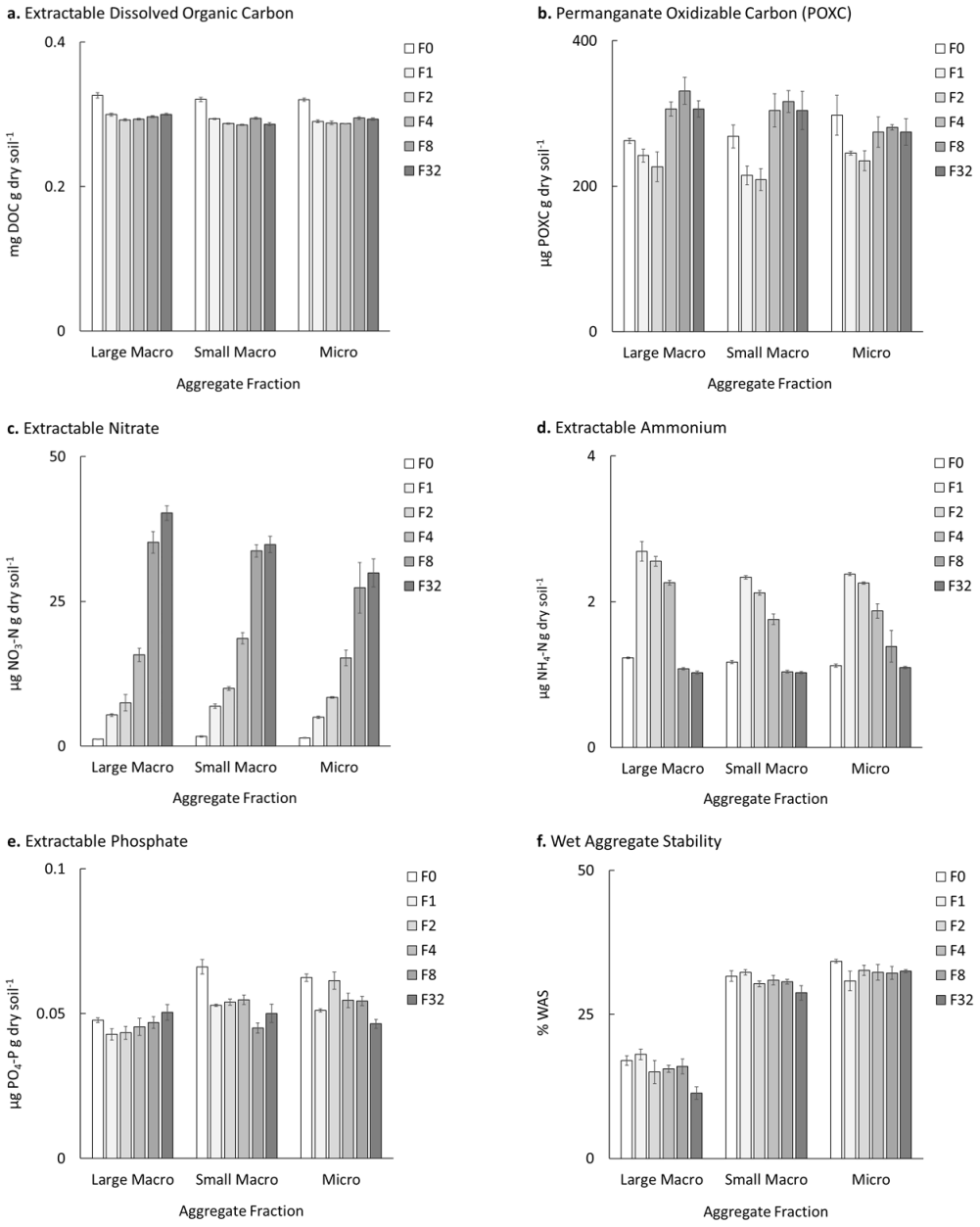

Figure 2.3. Mean extractable dissolved organic carbon (DOC) (a), permanganate oxidizable carbon (POXC) (b), nitrate (NO_3) (c), ammonium (NH_4) (d), phosphate (PO_4) (e), and wet aggregate stability (WAS) (f) by aggregate size fraction and rewetting Frequency (F).

All properties were measured after 42 d incubation. Error bars represent the standard error of *n* = 4 replications per treatment combination.

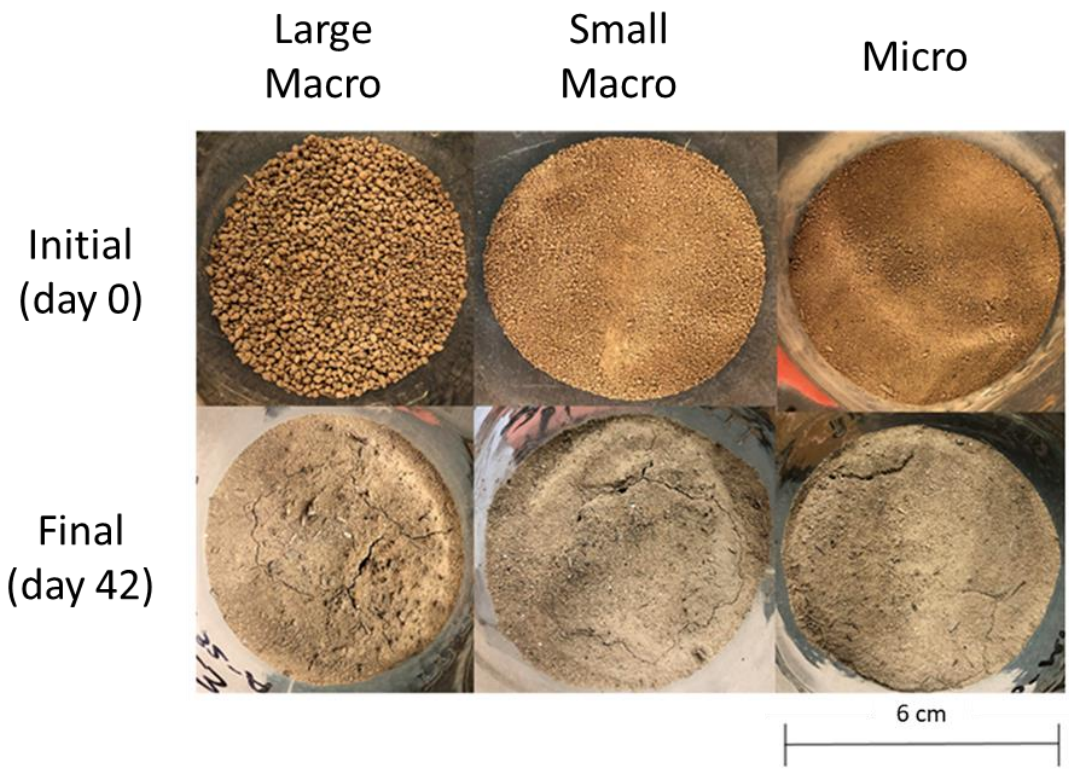

Figure 2.4. Images of aggregate fractions from time *t* = 0 d (start of incubation) and *t* = 42 d (end of incubation after receiving rewetting treatments).

Samples pictured are F32 (daily rewetting treatment, highest frequency rewetting). A loss of macroaggregate structure is observed by the end of 43 d incubation).

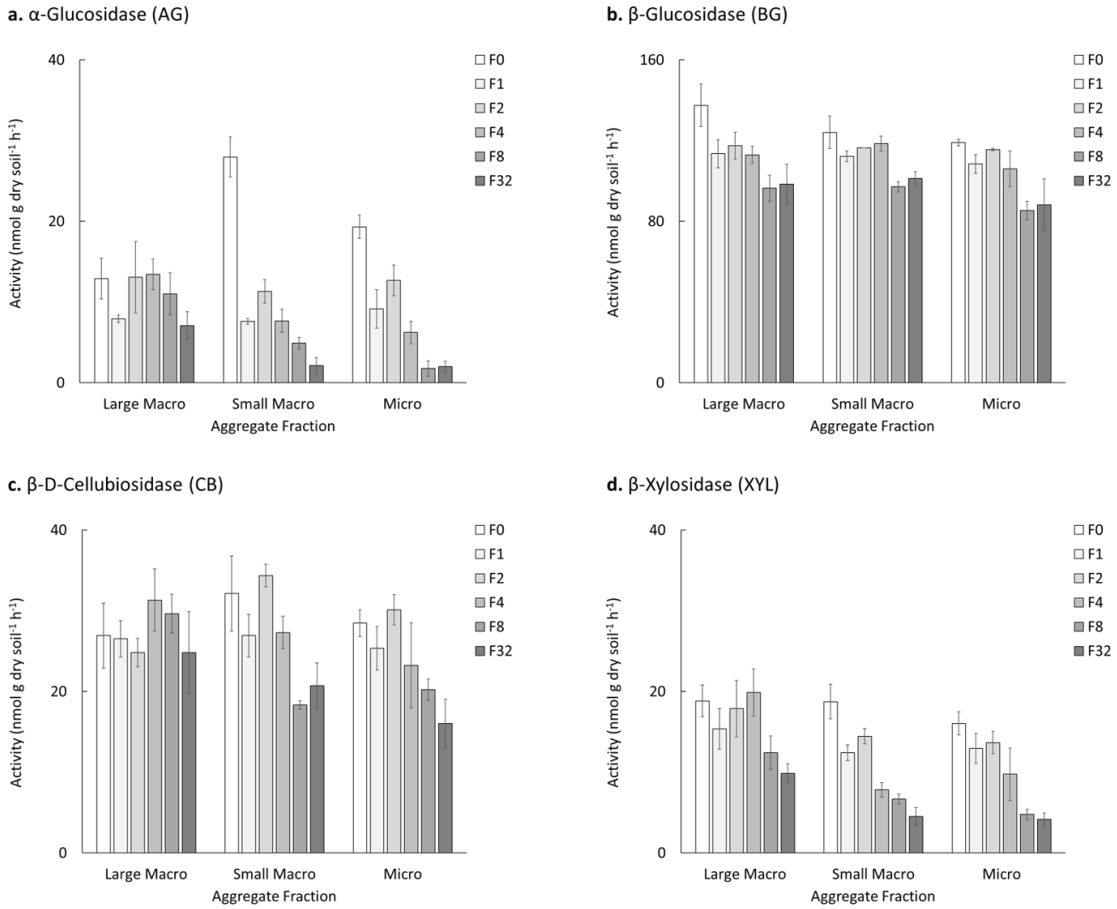

Figure 2.5. Activities of C-degrading extracellular enzymes measured on aggregate fractions post-incubation: AG (a), BG (b), CB (c), and XYL (d).

Note differences in scale among panels. Errors bars represent standard error of $n = 4$ replications per treatment combination.

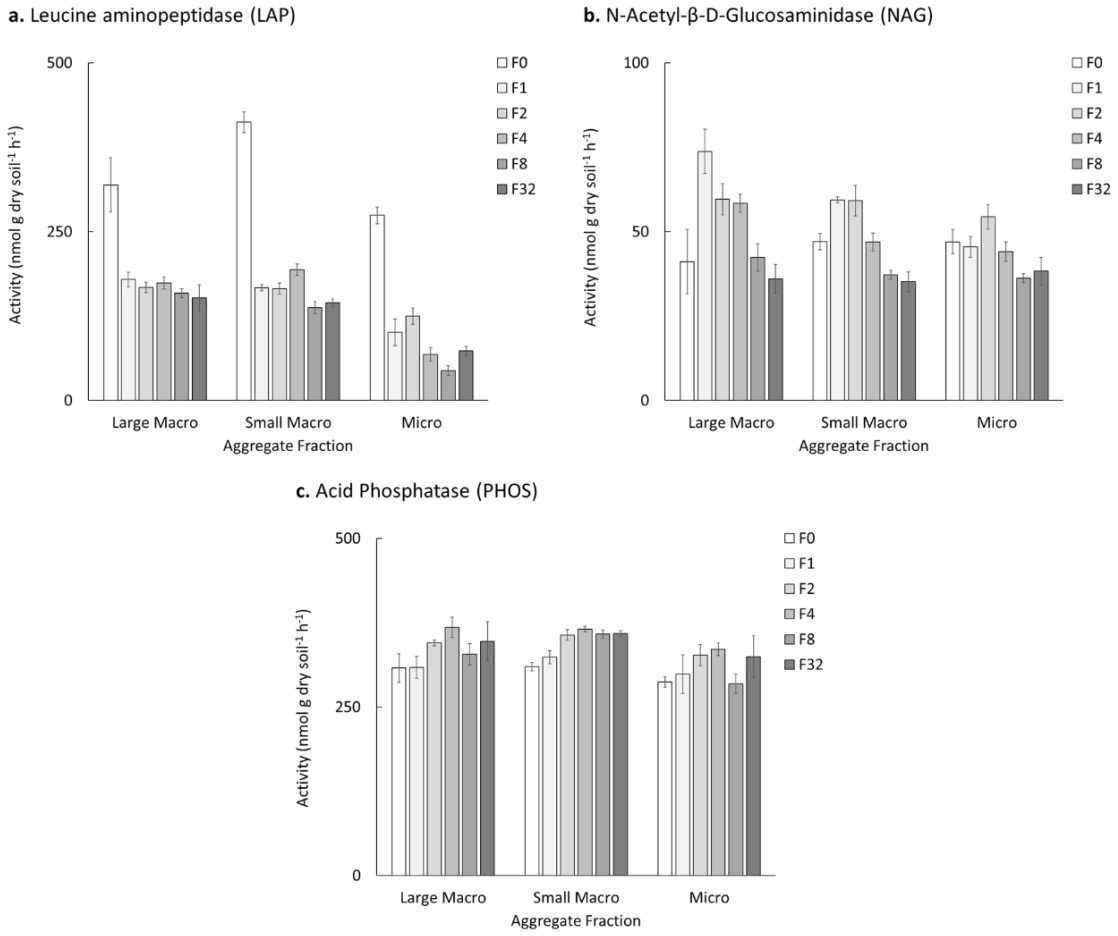

Figure 2.6. Activities of N- and P-degrading extracellular enzymes measured on aggregate fractions post-incubation: LAP (a), NAG (b), and PHOS (c).

Note differences in scale among panels. Errors bars represent standard error of $n = 4$ replications per treatment combination.

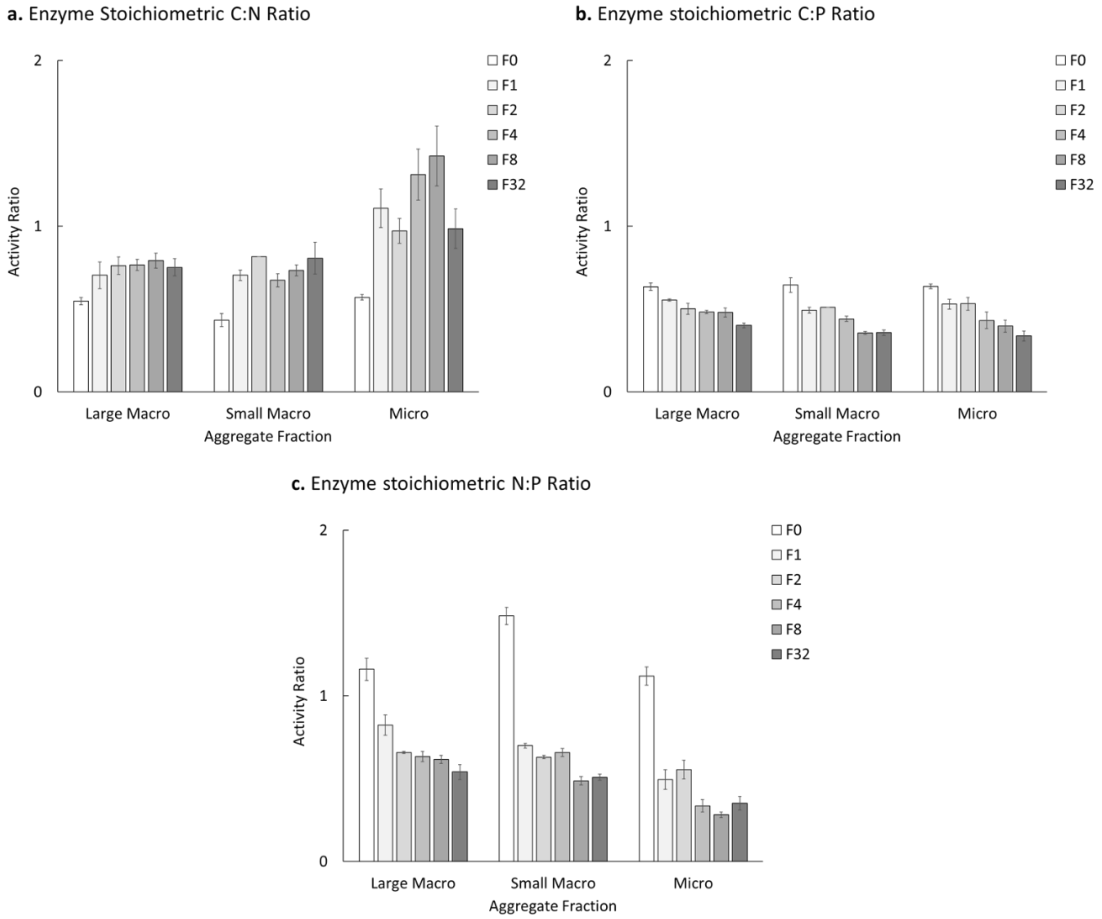

Figure 2.7. Stoichiometric ratios calculated from extracellular enzyme activities for C:N (a), C:P (b), and N:P (c).

Ratios were calculated by summing activities as follows: C-degrading enzymes are AG, BG, CB, XYL, N-degrading enzymes are LAP and NAG, and P-degrading enzyme is PHOS. Errors bars represent standard error of $n = 4$ replications per treatment combination.

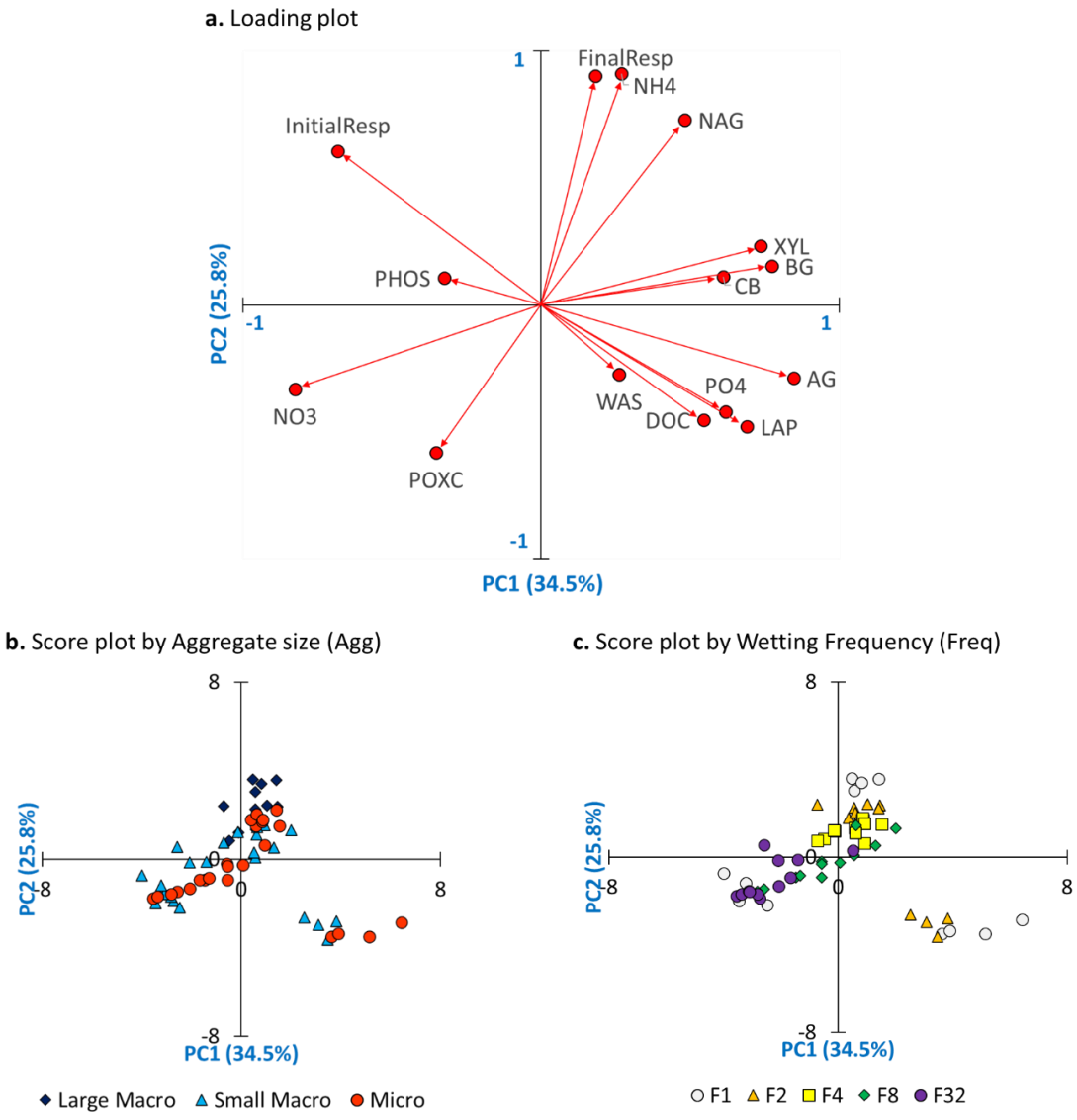

Figure 2.8. Loading plot (a) and Score plot with individual observations marked by Aggregate size (a) and Rewetting Frequency (b) treatments from the Principal Components Analysis (*n* = 60).

Principal Component (PC) 1 is along the x-axis and PC2 is along the y-axi

CHAPTER THREE

RESPONSES OF SOIL MICROBIAL CARBON ALLOCATION PATTERNS TO INDUCTION OF VIRAL LYSIS IN AGGREGATE SIZE FRACTIONS

A version of this chapter will be originally submitted to Soil Biology and Biochemistry by Aubrey K. Fine, Mark Radosevich, and Sean M. Schaeffer*.

Department of Biosystems Engineering and Soil Science, University of Tennessee, Knoxville, TN 37996, United States.

*Corresponding author: sschaef5@utk.edu

Acknowledgements: This research was supported by the United States Department of Agriculture National Institute of Food and Agriculture (Award 2018-67019-27792). We thank Dr. L. Schneider at University of Tennessee for statistical consulting on this project, as well as K. Corbeil, M. Davis, X. Liang, and R. McDearis for laboratory assistance. We thank anonymous reviewers for their input on the manuscript.

Abstract

Viral lysis exerts control on microbial mortality and dissolved organic matter production in oceans. Virus-microbe dynamics have rarely been experimentally observed in soils, which contrast aquatic systems with their complex aggregated physical structure. Soil aggregates have been operationally classified into size fractions reflecting differences in physicochemical and biological character. In this incubation study, Mitomycin C (MMC) was directly applied to induce lysis in three aggregate size fractions (large macro-, small macro-, and micro-) under slurry conditions. Treatment with MMC shifted microbial mortality, substrate availability, and viral production, the effects of which were studied over time relative to non-induced control using a fully factorial experimental design. Destructive sampling was performed on days 0, 3, 7, 14, and 28 for common soil biogeochemical measurements of microbial activity and dissolved organic C and inorganic N combined with viral particle and bacterial cell abundances determined using epifluorescence microscopy. Using multiple statistical approaches, data indicate the potential for aggregate-scale variability in virus-microbe interactions that were strongly dependent on time. After an initial six day stress response, viral lysis induction was associated with a hot spot of increased microbial activity relative to control. Mid-incubation was characterized by active microbial growth, increased enzyme activities, and high viral predation pressure. By day 28, altered microbial carbon allocation patterns were observed along with net negative viral production, interpreted to reflect a shift towards lysogenic viral reproduction. These findings point toward the

dynamic nature of virus-microbe interactions in soil beyond the scale of single timepoint measurement of bulk soil.

3.1 Introduction

Microorganisms mediate key biogeochemical transformations that influence the export and net accumulation of organic carbon (C) and essential nutrients in terrestrial and aquatic ecosystems. It is currently estimated that up to 40-90% of microbes in the environment can be classified as lysogens (Howard-Varona et al., 2017; Marsh and Wellington, 1994), which are bacterial cells that have at least one prophage (i.e., viral, or phage, genome) integrated into their chromosome. In oceanic surface waters, phage-mediated lysis of bacterial hosts is responsible for an estimated 20-60% of daily bacterial morality (Suttle, 2005; Fuhrman and Noble, 1995). While data from a limited number of studies in soils suggest that viruses are equally if not more abundant on a volumetric basis than in water samples, current consideration of their ecological role in terrestrial ecosystems remains principally based on knowledge from aquatic systems rather than observations of these dynamics in soils (Williamson et al., 2017; Wommack and Colwell, 2000).

Temperate phages reproduce using one of two generally recognized strategies: lysogeny and lysis. Lysogeny is a baseline, non-productive yet mutualistic relationship where the prophage proliferates as the host reproduces without production of viral progeny (Chen et al., 2021; Tuttle and Buchan, 2020; Howard-Varona et al., 2017; Wommack and Colwell, 2000). During lytic reproduction, which is induced from a lysogenic state, host cell metabolism is rerouted towards the production of viral progeny

and lytic enzymes that results in lysis of the host cell. Lysis releases active phages in addition to nutrient-rich cytoplasmic components (e.g., nucleic acids, enzymes, dissolved and free amino acids) and complex cell wall material (e.g., lipid bilayers, large proteins, peptidoglycan) (Middelboe and Jørgensen, 2006; Wilhelm and Suttle, 1999). Readily available lysis products can be recycled within the pool of microbial biomass, whereas more complex cell wall materials degrade more slowly over time aided by extracellular enzymes (Wommack and Colwell, 2000; Wilhelm and Suttle, 1999). Biogeochemical effects of lysis are represented in models of marine C cycles as the viral shunt, a distinct component of the microbial C pump describing internal cycling of C and nutrients among viruses, hosts, and dissolved OM (DOM) pools (Weitz and Wilhelm, 2012; Jiao et al., 2010; Wilhelm and Suttle, 1999; Fuhrman, 1999). The viral shunt diverts C and bioactive elements (e.g., phosphorus, nitrogen, iron) away from higher trophic levels, instead promoting production of microbially processed OM and retention of C in dissolved form (Jiao et al., 2010; Fuhrman, 1999).

Study of aquatic viral ecology has traditionally included measurement of viral particle and bacterial cell abundances, calculation of Virus-to-Bacteria Ratio (VBR) (i.e., number of viruses per bacteria), and assay of Inducible Fraction (IF) (i.e., the proportion of the total bacterial population harboring an experimentally inducible prophage) (Weinbauer, 2004; Paul and Jiang, 2001). Controls on the lytic-lysogenic switch in aquatic systems have traditionally been ascribed to nutrient availability, host density, and host growth rate; specifically, eutrophic waters with high host density and growth rates have been hypothesized to promote high rates of lytic viral production whereas oligotrophic

conditions favor lysogeny (Paul and Jiang, 2001; Wommack and Colwell, 2000; Thingstad and Lignell, 1997). Growing observations of high levels of lysogeny under conditions of high host density, growth rate, and nutrient availability, however, have led to the development of an alternative hypothesis that proposes lysogeny as a beneficial survival strategy for both virus and host under favorable conditions (Chen et al., 2021; Lara et al., 2017; Knowles et al., 2016; Ortmann et al., 2002). The interactive controls on the lytic-lysogenic switch remain a subject of active investigation, with several controlled microcosm and modeling studies suggesting a role of energy and nutrient availability (Pourtois et al., 2020; Chen et al., 2019; Pradeep Ram and Sime-Ngando 2008, 2010; Weinbauer et al., 2003; Thingstad and Lignell, 1997).

Since the early 2000s, single timepoint studies of viral ecology in bulk soil report viral abundances ranging from 10^3-10^9 virus particles per g soil dry weight, VBR as high as 8200, and IF ranging from 4-85% (Liang et al., 2020; Ghosh et al., 2008; Williamson et al., 2007). The ranges of these values are generally consistent with those reported on a volumetric basis for aquatic systems (Srinivasiah et al., 2008; Reavy et al., 2014). Across studies of soils, current data suggest i) the existence of weak positive correlations between bulk soil viral abundance and bacterial abundance, soil type, and soil water content (Williamson, 2011; Kimura et al., 2008; Williamson et al., 2005) and ii) a lack of correlation between IF and bulk soil properties (pH, water content, percent organic matter (OM), and particle size distribution) except possibly soil depth (Liang et al., 2020; Williamson et al., 2007). While the presence of free viruses and lysogens in soil ecosystems has been documented in recent decades, knowledge of the underlying

mechanisms controlling the distribution, abundance, and lytic activities of viruses in soil remain limited.

Soils are distinct from aquatic systems because of the added influence of a heterogeneous, physically structured and chemically reactive matrix. Soil structure is developed through the process of aggregation, for which the microaggregate (53-250 µm diameter) is the fundamental unit (Totsche et al., 2018; Six et al., 2004; Tisdall and Oades, 1982). Enmeshment of many microaggregates with particulate OM, fungal hyphae, and microbial residues leads to formation of macroaggregates (250-2000 µm diameter) (Six et al., 2004). Aggregate size fractions have been operationally defined based on distinct characteristics observed across soil types. As aggregate size decreases, C:Nitrogen (C:N) and C:Phosphorus ratios generally decrease, with larger aggregates having a higher C:N ratio but a greater proportion of newly deposited, labile plant-derived OM. (Totsche et al., 2018; Six et al., 2004; Angers and Giroux, 1996; Elliott, 1986; Tisdall and Oades, 1982). These differences in substrate quality have been shown to impact OM mineralization and turnover rates, which are generally faster in larger aggregates. (Gupta and Germida, 2015; Gupta and Germida, 1988).

While physicochemical constraints imposed on microbial activity (e.g., slow oxygen diffusion, low substrate availability) by soil aggregates could also affect rates of viral production and turnover, these influences have yet to be explored in soils. To address this knowledge gap, our goal for this study was to examine how differing microbial habitats provided by aggregate fractions affect virus-microbe-DOM interactions. In this effort, we consider larger macroaggregates to represent a more favorable, nutrient-rich habitat for

the microbial community relative to more oligotrophic microaggregates. Over a four week incubation, we examined effects of induced viral lysis in three aggregate size fractions (large and small macro-, micro- aggregates) with destructive sampling for five biogeochemical pools included in the viral shunt: respired carbon dioxide (CO_2), viral abundance, bacterial abundance, extracellular enzyme activities, and dissolved OC. We hypothesized that i) induced viral lysis will increase respiration, viral and bacterial abundances, enzyme activities, and DOC relative to non-induced control, ii) these effects will be observed on an extended 28 d timescale, and iii) large macroaggregates will have a greater positive response to induction of lysis than microaggregates.

3.2 Materials and Methods

Soil collection and aggregate isolation

Bulk surface soil (0-20 cm; A horizon) was collected in August 2019 from an upland forest site located at the East Tennessee Research and Education Center in Knoxville, Tennessee U. S. A. Soils are classified as Fine, mixed, semiactive, thermic Typic Paleudults with a silt loam texture (10 % sand, 75-80 % silt, 10-15 % clay). Soils were formed in clayey residuum weathered from shale/interbedded sandstone and shale. Slope of the site was measured at 9% with southeast aspect of 160. Soil pH (10 g soil: 20 mL) was 3.9 in water and 4.0 in 0.01 M calcium chloride. Loss on ignition (24 h at 400 °C) was measured on triplicate samples and calculated as 6.0 ± 0.1 % organic matter. Soil color was determined on moist soil as 10 YR 4/3. Water holding capacity (WHC) was estimated at 0.64 g water per g dry soil by saturating sieved soil (~10 cm^3) inside a filter

funnel with deionized water and determining mass of water retained by the soil after drainage for 6 h.

Soil was transported back to the laboratory where it was broken up by hand and laid out for two weeks to thoroughly air dry. Dry sieving was used to physically fractionate bulk soil into three aggregate fractions (Nimmo and Perkins, 2002): Large Macroaggregates (Large Macro), 1000-2000 µm; Small Macroaggregates (Small Macro), 250-1000 µm; and Microaggregates (Micro), 53-250 µm. Dry soil was first passed through 2000 µm and was then sieved through a series of three stacked sieves (1000, 250, and 53 µm) that was shaken for three minutes before collecting aggregate fractions. Aggregates were passed through the lower size limit sieve a second time before weighing aggregates into incubation jars.

Experimental design

Manipulation of lytic activity and virus production in aggregate slurries was achieved by direct addition of Mitomycin C (MMC), an antibiotic extensively demonstrated to induce viral lysis of infected microbial cells when applied at a non-lethal exposure level (Paul and Jiang, 2001; Otsuji et al., 1959). Mitomycin C treatment was applied at the start of the experiment to manipulate viral abundance and substrate availability relative to control by triggering induction of viral lysis. An induction response is expected from a subset of MMC-inducible populations, rather than the whole microbial community. Extended temporal impacts of MMC-induced viral lysis on microbial processes were studied using a full factorial experimental design testing main effects of aggregate size (Agg; a = 3), +/- MMC induction treatment (MMC; m = 2), and time (t; t = 5). Each

treatment combination included four replications (total n = 120 plus no soil blanks). Isolated aggregate fractions (30.0 g) were mixed with 100 mL of either sterile deionized water (control) or 3 ppm MMC, with immediate sampling performed for time zero measurement. Dosage of Mitomycin C was determined after preliminary experimentation, which demonstrated ~30% sorption of MMC to soil solids (unpublished data, A. Fine).

Incubations were conducted on soil slurries rather than unsaturated aggregates, providing three key benefits: i) standardization of soil water potential at zero across aggregate fractions, ii) minimization of constraints on accessibility between microbes-enzymes-substrates and viruses-hosts, and iii) improved distribution of dissolved MMC within the aggregate pore network to maximize exposure. While slurry conditions are different than typical soil conditions, this experiment was viewed as a necessary step of investigation given the lack of current knowledge about complex interactions among virus-host systems, physicochemical processes, and wetting in soils. Samples were incubated at 25 °C in the dark in sealed incubation jars equipped with rubber septa. Headspace CO_2 was sampled every 1-2 days throughout the 28 day incubation using an infrared gas analyzer (IRGA) (LI-COR Biosciences, NE U. S. A.). Cumulative respiration (CumResp) was calculated as the increase of CO_2-C produced with each successive sampling event and respiration rate (RespRate) is the total CO_2-C produced divided by the elapsed time. Viral and bacterial abundances, extractable dissolved OC (DOC), and activities of extracellular hydrolytic enzymes were destructively sampled on days 0, 3, 7, 14, and 28 as described below.

Laboratory analyses

Virus and Bacteria extraction and enumeration

Sterile potassium phosphate buffer was added to incubated soil slurry to achieve a final concentration of 1% (pH 7.0). Buffered slurries were blended for one minute using a high speed commercial blender. Virus extract was obtained by centrifuging blended soil slurry at 10,000 x*g* (4 °C, 20 minutes) and filtering the supernatant using a Millex-GV 0.22 µm pore size syringe filter (EMD Millipore, MA U. S. A.) (Williamson et al., 2003). Bacterial cells were extracted from soil slurry using a 60% Nycodenz® density gradient (Accurate Chemical and Scientific Co., NY U. S. A.) (2 mL + 9 mL slurry) (Williamson et al., 2007). Bacterial extracts were diluted 20% with glycerol to decrease freezing stress. All extracts were immediately frozen in liquid nitrogen and stored at -80 °C until analysis.

Thawed virus and bacteria extracts were treated with DNase I enzyme (RNA-free; Fisher Bioreagents) for 20 minutes to remove free DNA (Williamson et al., 2003). Virus extracts were vacuum filtered through 0.02 µm pore size Whatman® Anodisc filters (Cytiva Life Sciences, Buckinghamshire, U. K.), retaining the fraction greater than 20 nm and defining viral particles as having diameter of 20-200 nm (Williamson et al., 20003; Patel et al., 2003). Bacteria extracts were vacuum filtered through 0.22 µm pore size Whatman® Nuclepore™ Track-Etched Polycarbonate Membrane filters (Cytiva Life Sciences, Buckinghamshire, U. K.). Viral particles and bacteria retained on their respective filters were directly stained for 20 minutes in the dark using 500 µL of 2x

SYBR™ Gold Nucleic Acid Gel Stain (Molecular Probes-Invitrogen, OR U. S. A.). Filters were mounted using anti-fade reagent (Patel et al., 2007).

Stained viruses and bacteria were counted using a Nikon Eclipse E600 Epifluorescence Microscope (EFM) with a fluorescein isothiocyanate excitation (467-498 nm) and emission (513-556 nm) filter set at 1000x magnification. Ten randomly selected fields of view were digitally photographed using a Retiga™ Ex-I CCD camera (Qimaging, BC Canada). After user image normalization, fluorescent particles were counted using IP Laboratory software (BD Biosciences, CA U. S. A.). The mean count from all ten fields was used to calculate abundance per g dry soil using equation (1) (Patel et al., 2007), where RSF is the microscope grid-reticle scaling factor (59,000 for this setup) and volume of extract filtered ranged from 0.15-0.30 mL. Virus-to-Bacteria Ratio (VBR) was calculated as mean viral abundance divided by mean bacterial abundance. Net production rates of viral particles and bacterial cells were estimated using equation (2) where the change in abundance (A) is divided by the total elapsed time (t2-t1) (Malits and Weinbauer, 2009). Net production rates, representing net change in abundance over between successive sampling events, were estimated using equation (2) where change in abundance (A) is divided by total elapsed time (t2-t1).

$$\boldsymbol{Abundance} = \frac{\boldsymbol{Mean\ count * RSF}}{\boldsymbol{Volume\ extract\ filtered\ (mL)}} * \frac{\boldsymbol{100\ mL\ extractant}}{\boldsymbol{35.0\ g * (1 - \frac{g\ water}{g\ soil})}} \qquad (1)$$

$$\boldsymbol{Net\ Production\ Rate} = \frac{\boldsymbol{A2 - A1}}{\boldsymbol{(t2 - t1)}} \qquad \textbf{(2)}$$

Dissolved Organic Carbon and Inorganic Nitrogen

Aliquots of soil slurry were filtered through glass microfiber filters 1.0 size (Whatman GF/B, 1.0 µm pores) and frozen at 4 °C until analysis. Extracts were adjusted to 1% potassium sulfate to facilitate clay flocculation. Dissolved OC was quantified by reacting extracts with a potassium persulfate reagent overnight (80 °C) in sealed glass vials equipped with rubber septa for headspace gas analysis using an Infrared Gas Analyzer (IRGA, LI820, LiCor Inc., Lincoln, NE USA) (Doyle et al., 2004). A series of potassium hydrogen phthalate calibration standards was included for calculation of persulfate-oxidized OC in samples. Soil extracts were carried through colorimetric assays to quantify concentrations of extractable nitrate (NO_3^-, Doane and Horwath, 2003) and ammonium (NH_4^+; Rhine et al., 1998) using a 96-well microplate reader (Synergy H1 Hybrid Reader, Biotek Inc., Winooski, VT U. S. A.).

Extracellular Enzyme Activities

Maximum potential activities for seven major C, N, and P hydrolytic enzymes were assayed using fluorometric methods (Burns et al., 2013; Saiya-Cork et al., 2002). The following enzymes were assayed: α-Glucosidase (AG), β-Glucosidase (BG), β-D-Cellubiosidase (CB), leucine aminopeptidase (LAP), N-acetyl-β-Glucosaminidase (NAG), acid phosphatase (PHOS), and β-Xylosidase (XYL) (Table 3.1; all tables for Chapter 3 are available in Appendix B). A subsample of incubated soil slurry was adjusted to 50 mM sodium acetate buffer (pH 5.0) for control of pH during incubation with enzyme substrates. Variability in soil matrix effects was accounted for with standard additions of fluorescent MUC (7-amino-4-methylcoumarin) and MUB (4-

methylumbelliferone) made to each soil slurry. Soil slurries were incubated with standards and labeled substrates (200 µl of 200 µM solution) at 25 °C in the dark for 3 hours. Fluorescence (365 nm excitation, 450 nm emission) was measured using a microplate reader under optimal gain settings. Enzyme activity was calculated in nmol g dry soil^{-1} h^{-1}, with higher activities indicating a greater amount of fluorescently labeled substrate degraded under ideal conditions of incubation.

Statistical analyses

Data were analyzed as a three-factorial completely randomized design using a mixed model Analysis of Variance (ANOVA) with aggregate fraction (Agg), Mitomycin C induction treatment (MMC), and sampling day (Day) as fixed effects with all two- and three-way interactions. The ANOVA model for CumResp and RespRate included an additional repeated measures and a random replicate (Agg * MMC) effect using values calculated at timepoints corresponding to destructive sampling events (0, 3, 7, 14, and 28 days). Least squares (LS) means were separated using Tukey's least significant difference test with statistical significance indicated at the 95% ($p < .05$) confidence level. All data were confirmed to meet ANOVA assumptions after Virus, Bacteria, and NH_4 were log10 transformed (reported in back-transformed format). All ANOVA calculations were performed using the GLIMMIX procedure in SAS v. 9.4 (SAS Institute, Inc., NC U. S. A.).

The high frequency respiration data was used to provide additional temporal resolution of microbial activity between destructive sampling events. For each aggregate,

these data were control-normalized by dividing the mean of MMC-induced samples by the mean of control (non-induced) samples with propagation of error. One-way ANOVA was used on the control-normalized data with Day as a fixed effect (total $n = 19$) with the main goal being to focus on MMC-associated changes in daily CO_2 production rates over time. Tukey's Least Significant Difference (LSD) test was used for comparison of means.

A Principal Component Analysis (PCA) was conducted using JMP® Pro v. 15.0.0 (SAS Institute, Inc., NC U. S. A.) to investigate multivariate trends and clustering among variables. Analysis was performed on the correlation matrix from a subset of data including all samples ($n = 120$) but excluding respiration data that was only available for days 3, 7, 14, and 28. Virus, Bacteria, and NH_4 were log10 transformed prior to standardization for PCA, which included subtraction of the mean and division by the standard deviation.

3.3 Results

Laboratory analyses

Heterotrophic respiration

Cumulative respiration (CumResp) and daily respiration rates (RespRate) were significantly affected by all three main treatments ($p < .0001$) with two- and three-way interactions (Table 3.2). In all samples, total CO_2 production significant increased with each destructive sampling event (days 0, 3, 7, 14, and 28) (Figure 3.1a and 3.3; all figures for Chapter 3 are available in Appendix B). Across sampling days, i) CumResp was greatest in Small Macro and Micro aggregates (2.2 +/- 0.01 µg and 2.1 +/- 0.01 µg CO_2-C

g dry soil^{-1}, respectively) and lowest in Large Macro (1.8 +/- 0.01 µg CO_2-C g dry soil^{-1}) regardless of MMC treatment and ii) MMC treatment decreased mean CumResp relative to control until day 28 for Small Macro and Micro (Figure 3.1b and 3.3). RespRate was lowest across aggregates on day 3 (0.15 +/- 0.002 µg CO_2-C g dry soil^{-1} day^{-1}), then increased to a maximum on day 14 and 28 for all aggregate and MMC treatments (0.31 +/- 0.002 µg CO_2-C g dry soil^{-1} day^{-1}) (Figure 3.2).

Total CO_2 production and calculated daily production rates both had a negative response to MMC treatment (MMC < control by 20-30 %) for the first six days after MMC application on day 0 (Figures 3.2 and 3.4). From days 6-7, there was spike in CO_2 production rates with MMC treatment observed across aggregates (2.8, 1.4, and 1.8 times control for Large Macro, Small Macro, and Micro, respectively). MMC-induced microaggregates had additional significant ($p < .0001$) peaks in control-normalized respiration rates on days 7-8 and 15-16 (both 1.5 times control) that were absent in Large and Small Macro (Tables 3.3, 3.4, 3.5, and 3.6). From days 7-14, MMC treatment trended towards a slight increase in respiration rates for all aggregates relative to non-induced control. After day 14, MMC treatment decreased total CO_2 production for the duration of the experiment in Large Macro (MMC < control) but not in Small Macro (MMC = control) and Micro (MMC > control) aggregates.

Viral and Bacterial Abundances

Mean viral particle abundance (Virus) was significantly affected by day ($p < .0001$) and aggregate fraction ($p = 0.01$), both of which showed significant interactions with MMC treatment (Table 3.7). Across aggregate and MMC treatments, Virus was lowest

on day 0 ($3.4 \times 10^7 \pm 2.6 \times 10^6$ viral particles g dry soil^{-1}) and highest on day 14 ($1.7 \times 10^9 \pm 1.3 \times 10^8$ viral particles g dry soil^{-1}, representing a 50-fold increase from day 0 levels) (Figure 3.5a). Net viral particle production rates were positive through day 14, and highest across Agg and MMC treatments from days 0-3 (ranging from 12-to-19 x 10^7 viral particles day^{-1}. From days 14 to 28, there was a net decrease in Virus (i.e., negative production) by ~80% was observed across MMC treatments and aggregate fractions on day 28. Virus tended to scale negatively with aggregate size, with Micro having significantly greater Virus than Large Macro and Small Macro aggregates across all sampling days and MMC treatments. Relative to control, MMC treatment had a positive effect (MMC > control) on Virus in Large Macro on days 7, 14, and 28, in Small Macro on days 14 and 28, and in Micro on day 28.

Mean bacterial abundance (Bacteria) was significantly affected by MMC treatment and sampling day ($p < .0001$) (Table 3.7).. Significant ($p < .05$) two-way interactions were observed between Agg * Day and MMC * Day, indicative of inconsistent trends in response to MMC treatment by day and aggregate size. Bacteria significantly increased by sampling day across Agg and MMC treatments, with MMC treatment initially decreasing Bacteria relative to control by 24% ($2.03 \times 10^7 \pm 1.5 \times 10^6$ cells g dry soil^{-1} for control, $1.55 \times 10^7 \pm 1.1 \times 10^6$ cells g dry soil^{-1} for MMC) (Figure 3.5b). Across aggregates, maximum net virus production rates were observed from days 0-3 in MMC-treated samples (mean of 24 x 10^6 cells g dry soil^{-1} day^{-1}) and from days 7-14 in non-induced control (means of 23, 50, and 30 x 10^6 cells g dry soil^{-1} day^{-1} for Large Macro, Small Macro, and Micro aggregates, respectively). At the end of incubation (day 28),

Bacteria was 25-30 times greater than day 0 with MMC resulting in a net decrease relative to control by 38%. Differences among aggregate fractions became more pronounced as incubation progressed, with Small Macro ≥ Micro > Large Macro at day 28.

Virus-Bacteria Ratio (VBR) was significantly affected by MMC and Day with three-way Agg * MMC * Day interaction ($p < .05$) (Table 3.7). Across aggregate fractions, mean VBR was initially low on day 0 (1.8 ± 0.5 for control and 2.4 ± 0.5 for MMC), increased to a maximum over days 3-14, then decreased to a minimum value by day 28 (Figure 3.5c). The greatest VBR observed was in Small Macro on day 14 (11.0 ± 0.9). MMC treatment increased VBR as incubation proceeded, with MMC significantly increasing VBR relative to control on days 14 and 28 for all aggregate sizes.

Dissolved Organic Carbon and Inorganic Nitrogen

DOC varied significantly with aggregate size, MMC induction treatment, and day ($p < .05$) (Table 3.7 and Figure 3.6a). Two-way interactions were significant for Agg * Day and MMC * Day indicating response to MMC treatment varied by aggregate and day. Effects of Agg were significant only on days 0 and 3 (greatest in Small Macro) and of MMC treatment on day 3 (control < MMC). On day 7, MMC-treated Micro aggregates had elevated DOC relative other treatment combinations (0.21 ± 0.003 mg DOC g dry soil^{-1}). No significant effects of Agg and MMC treatment were observed for DOC on days 14 and 28 when all samples converged at a mean of 0.19 ± 0.001 mg DOC g dry soil^{-1}.

The inorganic N pool was dominated by ammonium with small contribution from nitrate (less than 0.5 µg NO_3-N g dry soil^{-1}) throughout the experiment. Ammonium was significantly affected by aggregate size and day with significant Agg * Day and MMC * Day interactions ($p < .05$; Table 3.7). Across aggregate and MMC treatments, NH_4 significantly increased with each sampling day. Insignificant effect of MMC treatment was observed across aggregates until Day 28 in the Micro aggregate fraction (57.1 ± 5.0 µg NH_4-N g dry soil^{-1} for control and 72.7 ± 6.3 µg NH_4-N g dry soil^{-1} for MMC) (Figure 3.6b). Large Macro tended to have lower mean NH_4 regardless of MMC or Day.

Extracellular Enzyme Activities

All enzymes were significantly affected by Day and two-way Agg * MMC interaction ($p < .05$) indicating varying response to MMC treatment with aggregate size (Table 3.8). Of the seven enzymes assayed, PHOS had the highest activity followed by BG then NAG (Figures 3.7 and 3.8). Activities of AG, CB, LAP, and XYL less than 10 nmol g dry soil^{-1} h^{-1}. The effect of sampling day was significant ($p < .05$) without interactions for AG, BG, CB, and LAP. Except for PHOS, which peaked in activity at day 3, Activities of all enzymes except PHOS increased from day 0 through day 14 and showed minimum activities on days 0 and 28. For PHOS, MMC-treated aggregates had peak activity on days 7-14 while control (non-induced) aggregates had peak activity on day 3.

Relative to control, MMC treatment tended to decrease enzyme activities in Large Macro and increase activities in Small Macro and Micro aggregates (except LAP). Microaggregates showed a spike in activities of LAP (day 3) and NAG (day 14) with MMC treatment that was absent in both macroaggregates. A significant positive response

to MMC was observed relative to control for activities of CB (peaked days 3-7 in Micro) and XYL (peaked day 14 in Small Macro and Micro). At the end of incubation, MMC treatment significantly decreased activities of BG, CB, and XYL relative to control across all aggregate fractions, whereas a positive response (MMC > control) was observed for AG, LAP, NAG, and PHOS.

Multivariate statistical relationships

Respiration was excluded from multivariate analyses because of the lack of data for day 0. PCA was conducted initially on datasets i) including respiration but excluding all day 0 data (n = 96) and ii) excluding respiration but including all days (n = 120); cumulative variance explained was slightly higher in the later and was therefore used for the Principal Components Analysis (PCA).

Viral abundance had significant ($p < .05$) moderate positive correlation with Bacteria (r = 0.62), VBR (r = 0.56), and activities of AG, NAG, PHOS, and XYL (r = 0.4) (Tables 3.9 and 3.10). VBR had low correlation with Bacteria, indicating greater dependence of VBR on changes in Virus than Bacteria. DOC was negatively correlated with Virus ((r = -0.74), Bacteria (r = -0.84), and activities of NAG (r = -0.31) and XYL (r = 0.41). Moderate-to-high positive correlation was observed between all pairs of enzyme activities except those including LAP which were low and/or not significant. Activities of BG, CB, and PHOS were more correlated with CumResp than RespRate, while activities of AG, NAG, and XYL were more correlated with RespRate than CumResp (Tables 3.11 and 3.12).

The PCA found that three PCs accounted for 78.0 % of the total variability in the dataset, fulfilling criteria of having eigenvalues greater than one and a cumulative fraction of total variance of at least 70% (Jollitte, 2002) (Table 3.13). PC1 explained 40.7 % of total variance with seven variables having high positive loadings: Virus and all enzyme activities except LAP. With PC2, an additional 26.3 % of total variance was explained with Bacteria, DOC, and NH_4 (loading scores of -0.84, 0.74, and -0.83, respectively). PC3 explained an additional 11.1 % of total variance with VBR (loading score = -0.69) and LAP (loading score = 0.62). The position of the loading vector for VBR indicates greater dependence on changes of Virus than Bacteria (Figure 3.9a).

Two-dimensional visualization of the first two components displayed clustering in the score plot by sampling day but not aggregate fraction or MMC treatment. Day 0 formed a separate cluster from the other sampling days (Figure 3.9). These findings are consistent with ANOVA results that found sampling day to be the most influential treatment (i.e., samples measured on a given sampling day were more alike than samples from other days regardless of MMC or Agg). Despite some findings of significant differences using ANOVA, clustering by aggregate size and MMC treatment was not evident from the PCA.

3.4 Discussion

In this study, Mitomycin C (MMC) was used to induce viral lysis in a mixed natural microbial community of aggregate soil slurries. To our knowledge, this work represents the first effort to study virus-microbe interactions on a timescale of weeks and *within* a bulk soil. While we hypothesized that MMC-induction of viral lysis at time zero would

increase respiration, viral and bacterial abundances, enzyme activities, and DOC relative to non-induced control, observed trends in these pools varied significantly by sampling day (except for DOC, which had low sensitivity in response to all treatments). After 28 day incubation, induction treatment significantly increased viral abundance and decreased bacterial abundances relative to control. This lends support to our hypothesis that virus-microbe-DOM cycling would be observed beyond a short hourly timescale. The direction of trends in viral abundance and microbial responses to MMC induction treatments between successive sampling events were similar across aggregate fractions but differed in magnitude. These findings could reflect the influence of overarching controls on virus-microbe interactions at the scale of bulk soil, which are ultimately affected by aggregate-scale habitat properties. In contrast to our third hypothesis, however, the magnitude of microbial responses to MMC induced lysis, as well as background viral abundances under control (non-induced) conditions, tended to scale negatively with aggregate size (MicroAgg > SmallAgg > LargeMacro). These findings indicate the potential for within bulk soil heterogeneity in virus-microbe interactions and viral abundances at the scale of aggregate size fractions, such that the underlying mechanisms explaining our observations warrant further study. Moving beyond the scale of single timepoint measurement of bulk soil will shed light on the scale of virus-microbe-DOM interactions most relevant to microbial functional processes. Establishing this link is critical for placing viral ecology within the context of soil biogeochemical cycling and carbon stabilization.

Temporal Effects of MMC-Induced Viral Lysis

Sampling day was the most influential experimental treatment applied in this controlled incubation study. Under control (non-induced) and lysis induction treatments, these data demonstrate variability in soil native free viral abundance on the timescale of days-to-weeks. Previous studies have observed strong temporal control of viral abundance and diversity in bulk soil with monthly sampling (Roy et al., 2020; Narr et al., 2017). Along with our study, these findings point towards the complex, cross-scale nature of viral ecology and the controls on microbial life in soils. This has been demonstrated in aquatic ecosystems, which exhibit variability at the temporal scale of hours-to-seasons (REFS).

While we hypothesized that induction of viral lysis would increase sizes of the pools included in the viral shunt (i.e., virus and bacteria, extracellular enzyme activities, and DOC), significant interactions between sampling day and MMC complicated interpretation. To disentangle these effects, we have identified three phases in these data that describe general trends observed across all aggregate fractions: i) an initial Stress Response Phase from days 0-7, ii) a Net Lytic Phase from days 7-14, and iii) Net Lysogenic Phase from days 14-28.

Phase I: During the Stress Response Phase, microbes were likely acclimating to the stress of re-wetting of air dry aggregates when slurries were prepared at time zero. Depressed respiration rates were observed in this study for six days with or without MMC treatment, and while these effects are impossible to disentangle in the current study, these data suggest that drying and/or rewetting imposed a stress to the microbial

community that was enhanced in magnitude by MMC addition. Continued growth of bacteria during Phase I is expected from populations not susceptible to MMC induction effects and/or most tolerant to desiccation.

Stress from MMC treatment persisted until day 6, when there was an across-aggregate fraction spike in respiration rates relative to non-induced control from days 6-7. With a lack of new C inputs to the system, the source for the observed CO_2 spike with MMC could reflect consumption of lytic products made available to newly growing microbes during early days of incubation. Although these lytic products should be detectable as an increase in the amount of DOC, a net decrease during the first week was observed that suggests net positive consumption. This timeframe would be consistent with observations by Noble and Fuhrman (1999) that radiolabeled viral lysis products turn over rapidly (1-4 days) in marine water samples. In this study DOC was defined by filtration at 1.0 µm, which could be too large to capture shifts in the < 0.22 µm fraction that lacks microbial cells.

Phase II: The Net Lytic Phase (days 7-14) was characterized by net positive production rates of viruses and bacteria with high CO_2 production, DOC, and activities of all enzymes. High microbial activity and net bacterial production despite high viral abundance could be indicative of low consequences for microbial growth stemming from viral predation pressure. It is also possible that viruses released upon MMC induction had low infection rates towards the actively growing host community on this extended timescale. Recycling of lytic products made available during early Phase I may have fueled ongoing microbial activity and subsequent increases in dissolved substrate supply

and demand. Production of enzymes by microbes is an energy intensive process (Burns et al., 2013; Schimel and Schaeffer, 2012), such that observed increases in activity (especially for C and N targeting enzymes) point towards an increased metabolic investment in enzyme production relative to early incubation (Phase I). This provides evidence of potential changes in resource allocation patterns and growth efficiency of microbial consumers that was especially pronounced with MMC induction treatment. Differing temporal trends between C and N acquiring enzymes and P targeting PHOS suggest key shifts in microbial energy and/or nutrient supply and demand between early, middle, and late incubation across treatments.

Observations of high viral abundance can result from increased production and/or decreased destruction (e.g., stabilization). Major virus production processes would include continued release of viral particles during repeated lysis events associated with drying and/or MMC exposure, environmental stressors imposed on microbes during incubation (e.g., declining oxygen availability between venting events), and low levels of spontaneous induction events (Howard Varona et al., 2017). Abiotic processes that contribute to virus stabilization would include effects of prolonged water saturation and resulting shifts in net sorption/desorption behavior of organic coatings on mineral surfaces (e.g., related to changes in hydrophobicity), destruction of aggregate structures leading to exposure of previously occluded OM and viruses, and transport of viruses and small DOM from nano- and micro-pores to larger pore sizes upon rewetting of air dry soil (Bailey et al., 2019; Kaiser et al., 2015; von Lûtzow et al., 2006; Kalbitz et al., 2000). While sorption and transport of soil viruses have been studied using model systems

(Kimura et al., 2011; Zhuang and Jin, 2003; Jin and Flury, 2002; Bitton, 1975), it remains unclear how such processes affect autochthonous virus infectivity and *in situ* turnover processes. Based on previous experimentation with aggregate fractions, we expect equilibrium of soil water and destruction of large macroaggregate structures to have occurred by Phase II, whereas conformational changes in organomineral associations would likely occur throughout the incubation.

Phase III: During the final Net Lysogenic Phase (days 14-28), there was net negative virus production with net positive bacteria production. Lysis of infected hosts releases daughter phages of the same lineage, such that with repeated cycles of lysis in a closed system the number of viruses overwhelms the supply of susceptible hosts, and the virus population crashes over time (Wommack and Colwell, 2000). In contrast to Phase II, negative net virus production over this two week period reflects a predominance of viral particle destruction/inactivation rather than production processes. In aquatic ecosystems, the turnover time of virus particles has been found to range from 0.1 to 25 days falling within the timeframe of this experiment (Wommack and Colwell, 2000; Suttle, 1994).

Although continued bacterial growth occurred in the absence of viral predation pressure, the drop in activities of all enzymes by day 28 suggests a decline in microbial investment in enzyme production that, along with declining respiration rates, could reflect change in microbial growth patterns (e.g., C and/or substrate use efficiency, dormancy) in response to progressive C or nutrient limitation (Schimel, 2018; Schimel and Schaeffer, 2012). These observed changes in microbial activities over time could reflect a community level shift towards net lysogeny where little to no new viral material

is actively produced via lysis. Lysogenic conversion allows vertical transmission of viral genes while conferring beneficial fitness traits to the host (e.g., via acquisition of phage-encoded traits or superinfection immunity) that promote cell division and growth (Correa et al., 2021; Howard-Varona et al., 2017; Obeng et al., 2016; Zimmerman et al., 2020). In this study, it is possible that we observed a functional shift in the metabolic footprint of the microbial community during late-incubation where viral infection altered central carbon and energy metabolism activities to aid host survival under progressive energy limitation (Howard-Varona et al., 2020; Zimmerman et al., 2020). While we did not study shifts in microbial community structure, these virus-host dynamics were likely to impose a selective pressure that altered the composition of the active microbial community throughout the course of incubation (Chen et al., 2019).

Aggregate effects of MMC-Induced Viral Lysis

While we observed evidence of aggregate level control of these dynamics, the magnitude of the response among aggregate fractions was often unexpected. For example, in control (non-induced) samples, Virus, Bacteria, DOC, and respiration averaged across all days were higher in micro- than macro-aggregates. These findings could be a relic of the dry sieving approach used to isolate aggregate fractions, which is expected to have transferred some OM associated with macroaggregates to the microaggregate fraction. Our findings suggest that microaggregates may harbor greater abundances of bacterial hosts and viral predators relative to macroaggregates,

Although macroaggregates have greater total C and nutrient contents, studies have shown that most microbes in soil inhabit micropores due to benefits of water film

hydration and size exclusion from higher predators (Erktan et al., 2020; Frey, 2015). Our findings support this idea and suggest that at the aggregate scale, microaggregates may harbor greater abundances of bacterial hosts and viral predators relative to macroaggregates. Slurry conditions would equilibrate water potential across the aggregate pore networks, likely disrupting this fine scale spatial distribution of microbes. While these conditions were deliberately applied, they undoubtedly differ from those typically experienced by soil microbes.

In contrast, activities for all enzymes were highest in large macroaggregates. Together these findings could reflect increased growth efficiency in large macroaggregates where a greater proportion of microbial products (e.g., enzymes, exudates, polysaccharides) are produced relative to CO_2 per unit substrate C consumed. This would be consistent with a greater proportion of recently deposited, labile C in the large macroaggregate fraction that would have been made available with the aggregate slaking effect of the soil slurry. Furthermore, MMC induced large macroaggregates showed the largest magnitude spike in respiration rates from days 6-7, along with increased DOC measured relative to control treatment on day 7 that was absent in small macroaggregates and microaggregates. The observed 24 h hot moment of increased microbial activity from days 6-7 with MMC induction is expected to be associated with initially dominant, fast-growing lysogens that were subsequently lysed (or otherwise killed) from days 7-14. The spatiotemporal scale of relevance for community-scale diversity patterns and their relationship to ecosystem functions could be further disentangled with further mechanistic experimentation in combination with advanced ‘omics techniques.

The finding of greater CO_2 production in MMC-treated small aggregates (SmallAgg and MicroAgg) but not Large Macro was also curious. One potential explanation for these results is that consumption of viral lysis products in small aggregates prompted a priming response. Relative to large and small macroaggregates, microaggregates are expected to have less readily available labile substrate in small pores, and as such, may have necessitated mining of endogenous SOM sources in smaller aggregates. A predominance of small pore rather than large pores has been associated with a greater positive priming effect (Toosi et al., 2017). On the other hand, higher rates of virus inactivation have been experimentally associated with the presence of a natural bacterial community and particulate OM (Wommack and Colwell, 2000); both influences are expected to be more pronounced in large macroaggregates, potentially explaining lower viral abundances relative to smaller aggregates.

3.5 Conclusions

Expression of the full viral shunt depends upon spatiotemporal contact between i) a susceptible host and active virus and ii) actively growing microbes, extracellular enzymes, and substrate, both of which would be more easily attained in a well-mixed aquatic habitat. The minimal constraint on physical accessibility for aquatic viruses and microbes likely promote a relatively active viral shunt cycle in these environments relative to soils. While soil viral ecologists have long worked under the assumption that virus-microbe interactions in soils can be explained by knowledge from aquatic ecosystems, there is ample evidence regarding soil-specific controls on microbial functional activity that could likely apply to virus-soil and virus-microbe interactions

across space and time. These fundamental controls in soils will only be revealed with use of creative, mechanistic experimentation informed by emerging conceptual models from both aquatic and terrestrial ecosystems.

Physical fractionation of bulk soil has proven a valuable tool for understanding interactions between soil structure, organic matter characteristics, and microbial activity. Using this approach, we provide the first evidence of potential heterogeneity at the bulk soil scale in viral and microbial community dynamics over time. Our results suggest the presence of some universal controls on virus-microbe interactions across aggregates, as well as unique responses to induction of viral lysis that point toward differences in aggregate-level substrate availability, host abundance, and/or microbial physiology. Our findings suggest that a shift towards net lysogeny occurred alongside a change in microbial activity evident as decreased respiration rates, lower net bacterial abundance, and decreased synthesis of extracellular enzymes despite continued growth. The predominance of lysogeny could increase host fitness during extended periods of low substrate availability in soil. These findings have cross-scale implications for understanding aggregate level controls on microbial processes in soils and ecosystem level influence of viruses on terrestrial ecosystem biogeochemical functions. For example, viral lysis could positively affect soil C stabilization if recycling of viral lysis products is associated with increased long-term production of microbially processed, stabilized organic matter. Conversely, priming responses initiated by hot moments of viral lysis in fine pore spaces could lead to soil C destabilization.

Moving forward, there is need to improve understanding of how soil water content affects viral ecology and virus-microbe interactions across scales. Soil water availability is a dynamic soil property that controls microbial activity in soils across space and time. It is likely that phage production rates and turnover times are also affected by soil water dynamics. Knowledge of how soil water distribution impacts viral transport and survival within the soil is limited but is a necessary next step to understand how shifts in water availability (e.g., with drying and rewetting cycles, extended drought, or flooding) could impact viral abundance and reproductive strategies relative to their microbial hosts under a changing climate.

References

Angers, D. A. & Giroux, M. (1996). Recently Deposited Organic Matter in Soil Water-Stable Aggregates. *Soil Sci. Soc. Am. J.* 60, 1547-1551.

Bach, E.M. & Hofmockel, K.S. (2014). Soil aggregate isolation method affects measures of intra-aggregate extracellular enzyme activity. *Soil Biol. Biochem.* 69, 54-62.

Bailey, V. L., Hicks Pries, C., & Lajtha, K. (2019). What do we know about soil carbon destabilization? *Environ. Res. Lett.* 14, 083004.

Bitton, G., 1975. Adsorption of viruses onto surfaces in soil and water. *Water Res.* 9, 473-484.

Blagodatskaya, E. & Kuzyakov, Y. (2013). Active microorganisms in soil: critical review of estimation criteria and approaches. *Soil B9iol. Biochem.* 67, 192-211.

Boot, C. M., Schaeffer, S. M., & Schimel, J. P. (2013). Static osmolyte concentrations in microbial biomass during seasonal drought in a California grassland. *Soil Biol. Biochem.* 57, 356-361.

Burns, R. G. et al. (2013). Soil enzymes in a changing environment: Current knowledge and future directions. *Soil Biol. Biochem.* 58, 216-234.

Brashear, D. A. & Ward, R. L. (1983). Inactivation of Indigenous Viruses in Raw Sludge by Air Drying. *Appl. Env. Microbiol.* 45, 1943-1945.

Chen, X., Ma, R., Yang, Y., Jiao, N., & Zhang, R. (2019). Viral Regulation on Bacterial Community Impacted by Lysis-Lysogeny Switch: A Microcosm Experiment in Eutrophic Coastal Waters. *Front. Microbiol.* 10, 1763.

Chen, X., Weinbauer, M. G., Jiao, N., & Zhang, R. (2021). Revisiting marine lytic and lysogenic virus-host interactions: Kill-the-Winner and Piggyback-the-Winner. *Science Bulletin* 66, 871-874.

Correa, A., Howard-Varona, C., Coy, S. R., Buchan, A., Sullivan, M. B., & Weitz, J. S. (2021). Revisiting the rules of life for viruses of microorganisms. *Nature Rev. Microbiol.* 19, 501-513.

Doane, T. A., & Horwath, W. R. (2003). Spectrophotometric Determination of Nitrate with a Single Reagent. *Anal. Lett.* 36, 2713-2722.

Doyle, A., Weintraub, M. N., & Schimel, J. P. (2004). Persulfate Digestion and Simultaneous Colorimetric Analysis of Carbon and Nitrogen in Soil Extracts. *Soil Sci. Soc. Am. J.* 68, 669-676.

Elliott, E. T. (1986). Aggregate Structure and Carbon, Nitrogen, and Phosphorus in Native and Cultivated Soils. *Soil Sci. Soc. Am. J.* 50, 627-633.

Erktan, A., Or, D., & Scheu, S. (2020). The physical structure of soil: Determinant and consequence of trophic interactions. *Soil Biol. Biochem.* 148, 107876,

Fierer, N. & Schimel, J.P. (2003). A Proposed Mechanism for the Pulse of Carbon Dioxide Production Commonly Observed Following the Rapid Rewetting of a Dry Soil. *Soil Sci. Soc. Am. J.* 67, 798-805.

Forterre, P., Soler, N., Krupovic, M., Marguet, E., & Ackermann, H.-W. (2013). Fake virus particles generated by fluorescence microscopy. *Trends Microbiol.* 21, 1-5.

Frey, S. D. (2014). The Spatial Distribution of Soil Biota. In: Soil Microbiology, Ecology, and Biochemistry (Paul, E., Ed.), p. 223-244. Academic Press.

Fuhrman, J. A. (1999). Marine viruses and their biogeochemical and ecological effects. *Nature* 399, 541.

Fuhrman, J. A. & Noble, R. T. (1995). Viruses and protists cause similar bacterial mortality in coastal seawater. *Limnol. Oceanogr.* 40, 1236-1242.

Ghosh, D. et al. (2008). Prevalence of Lysogeny among Soil Bacteria and Presence of 16S rRNA and trzN Genes in Viral-Community DNA. *Appl. Environ. Microbiol.* 74, 495-502.

Göransson, H., Godbold, D. L., Jones, D. L., & Rousk, J. (2013). Bacterial growth and respiration responses upon rewetting dry forest soils: impact of drought legacy. *Soil Biol. Biochem.* 57, 477-486.

Gupta, V. V. S. R. & Germida, J. J. (2015). Soil aggregation: Influence on microbial biomass and implications for biological processes. *Soil Biol. Biochem.* 80, A3-A9.

Gupta, V. V. S. R. & Germida, J. J. (1988). Distribution of microbial biomass and activity in different soil aggregates classes as affected by cultivation. *Soil Biol. Biochem.* 20, 777-786.

Herron, P. M., Stark, J. M., Holt, C., Hooker, T., & Cardon, Z. G. (2009). Microbial growth efficiencies across a soil moisture gradient assessed using 13C-acetic acid vapor and 15N-ammonia gas. *Soil Biol. Biochem.* 41(6):1262–69.

Holmfeldt, K., Odic, D., Sullivan, M.B., Middelboe, M., & Riemann, L. (2021). Cultivated Single-Stranded DNA Phages That Infect Marine Bacteroidetes Prove Difficult To Detect with DNA-Binding Stains. *Appl. Env. Microbiol.* 78, 892-894.

Howard-Varona, C., Hargreaves, K. R., Abedon, S. T., & Sullivan, M. B. (2017). Lysogeny in nature: mechanisms, impacts, and ecology of temperate phages. *ISME J.* 11, 1511-1520.

Howard-Varona, C., Lindback, M. M., Bastien, G. E., Solonenko, N., Zayed, A. A., Jang, H., ... & Duhaime, M. B. (2020). Phage-specific metabolic reprogramming of virocells. *ISME J.* 14, 881-895.

Jastrow, J. D. (1996). Soil Aggregate Formation and the Accrual of Particulate and Mineral Associated Organic Matter. *Soil Biol. Biochem.* 28, 665-676.

Jiao, N. et al. (2010). Microbial production of recalcitrant dissolved organic matter: long-term carbon storage in the global ocean. *Nat. Rev. Microbiol.* 8, 593-599.

Jin, Y. & Flury, M. (2002). Fate and transport of viruses in porous media. *Adv. Agron.* 77, 39-102.

Jolliffe, I. T., 2002. Principal component analysis. Springer, London U. K.

Kaiser, M., Kleber, M., & Berhe, A. A. (2015). How air-drying and rewetting modify soil organic matter characteristics: An assessment to improve data interpretation and inference. *Soil Biol. Biochem.* 80, 324-340.

Kalbitz, K., Solinger, S., Park, J. H., Michalzik, B., & Matzner, E. (2000). Controls on the dynamics of dissolved organic matter in soils: a review. *Soil Sci.* 165, 77-304.

Kaletta, J., Pickl, C., Griebler, C., Kling, A., Kurmayer, R., Deng, L. (2020). A rigorous assessment and comparison of enumeration methods for environmental viruses. *Scientific Reports* 10, 18625.

Kimura, M., Jia, Z. J., Nakayama, N., & Asakawa, S. (2008). Ecology of viruses in soils: Past, present, and future perspectives. *J. Soil Sci. Plant Nutr.* 54, 1-32.

Knowles, B., et al., 2016. Lytic to temperate switching of viral communities. *Nature* 531, 466-470.

Kuzyakov, Y. & Blagodatskaya, E. (2015). Microbial hotspots and hot moments in soil: Concept and review. *Soil Biol. Biochem.* 83, 184-199.

Lara, E., et al. (2017). Unveiling the role and life strategies of viruses from the surface to the dark ocean. *Science Advances* 3, e1602565.

Liang, X., et al. (2020). Lysogenic reproductive strategies of viral communities vary with soil depth and are correlated with bacterial diversity. *Soil Biol. Biochem.* 144, 107767.

Manzoni, S. & Katul, G. (2014). Invariant soil water potential at zero microbial respiration explained by hydrological discontinuity in dry soils. *Geophys. Res. Lett.* 41, 7151-7158.

Manzoni, S., Schaeffer, S. M., Katul, G., Porporato, A., & Schimel, J. P. (2014). A theoretical analysis of microbial ecophysiological and diffusion limitations to carbon cycling in drying soils. *Soil Biol. Biochem.* 73:69–83.

Manzoni, S., Schimel, J. P., & Porporato, A. (2012). Responses of soil microbial communities to water stress: results from a meta-analysis. *Ecol.* 93(4):930–38.

Marsh, P. & Wellington, E. M. H. (1994). Phage-host interactions in soil. *FEMS Microbiol. Ecol.* 15, 99-108.

Meisner, A., Leizeaga, A., Rousk, J., & Baath, E. (2017). Partial drying accelerates bacterial growth recovery to rewetting. *Soil Biol. Biochem.* 112, 269-276.

Middelboe, M. & Jørgensen, J. O. G. (2006). Viral lysis of bacteria: an important source of dissolved amino acids and cell wall compounds. *J. Mar. Biol. Ass. U.K.* 86, 605-612.

Middelboe, M., Jørgensen, J. O. G., & Kroer, N. (1996). Effects of Viruses on Nutrient Turnover and Growth Efficiency of Noninfected Marine Bacterioplankton. *Appl. Environ. Microbiol.* 62, 1991-1997.

Moyano, R. E., Manzoni, S., & Chenu, C. (2013). Responses of soil heterotrophic respiration to moisture availability: an exploration of processes and models. *Soil Biol. Biochem.* 59, 72-85.

Nanda, A. M., Thormann, K., & Frunzke, J. (2015). Impact of spontaneous prophage induction on the fitness of bacterial populations and host-microbe interactions. *J. Bacteriol.* 197, 410-419.

Narr, A., Nawaz, A., Wick, L. Y., Harms, H., Chatzinotas, A. (2017). Soil Viral Communities Vary Temporally and along a Land Use Transect as Revealed by Virus-Like Particle Counting and a Modified Community Fingerprinting Approach (fRAPD). *Front. Microbiol.* 8, 1975.

Nimmo, J. R. & Perkins, K. S. (2002). Aggregate stability and size distribution. In: Dane, J. H., Topp, G. C., editors. Methods of Soil Analysis: Part 4—Physical Methods. Madison, Wisconsin, U. S. A.: Soil Science Society of America, Inc., 317-328.

Obeng, N., Pratama, A. A., & van Elsas, J. D. (2016). The significance of mutualistic phages for bacterial ecology and evolution. *Trends Microbiol. 24*, 440-449.

Or, D., Smets, B. F., Wraith, J. M., Dechesne, A., & Friedman, S. P. (2007). Physical constraints affecting bacterial habitats and activity in unsaturated porous media – a review. *Adv. Water Resour.* 30, 1505-1527.

Ortmann, A. C., Lawrence, J. E., & Suttle, C.A. (2002). Lysogeny and Lytic Viral Production during a Bloom of the Cyanobacterium Synechococcus spp. *Microbial Ecology* 43, 225-231.

Otsuji, N., Sekiguchi, M., Iijima, T., & Takagi, Y. (1959). Induction of Phage Formation in the Lysogenic Escherichia coli K-12 by Mitomycin C. *Nature* 184, 1079-1080.

Patel, A., et al. (2007). Virus and prokaryote enumeration from planktonic aquatic environments by epifluorescence microscopy with SYBR Green I. *Nat. Protoc.* 2, 269-276.

Patel, K. F., et al. (2021). Soil carbon dynamics during drying vs. rewetting: Importance of antecedent moisture conditions. *Soil Biol. Biochem.* 156, 108165.

Paul, J. H. & Jiang, S. C. (2001). Lysogeny and transduction. In: *Methods in Microbiology* (Paul, J., Ed.), vol. 30, 105-125. Academic Press, San Diego CA.

Pourtois, J., Tarnita, C. E., & Bonachela, J. A. (2020). Impact of Lytic Phages on Phosphorus- vs. Nitrogen-Limited Marine Microbes. *Front. Microbiol.* 11, 221.

Pradeep Ram, A. S. & Sime-Ngando, T. (2010). Resources drive trade-off between viral lifestyles in the plankton: evidence from freshwater microbial microcosms. *Environ. Microbiol.* 12, 467-479.

Pradeep Ram, A. S. & Sime-Ngando, T. (2008). Functional responses of prokaryotes and viruses to grazer effects and nutrient additions in freshwater microcosms. *ISME J.* 2, 498-509.

Reavy, B. et al. (2015). Distinct Circular Single-Stranded DNA Viruses Exist in Different Soil Types. *Appl. Env. Microbiol.* 81, 3934-3945.

Reavy, B., Swanson, M.M., & Taliansky (2014). Viruses in Soil. In: Interactions in Soil: Promoting Plant Growth, Biodiversity, Community and Ecosystems 1 (Dighton, J., Krumins, J.A., Eds.), 163-180. Spring Science+Business Media Dordrecht.

Rhine, E. D., Sims, G. K., Mulvaney, R. L., & Pratt, E. J. (1998). Improving the Berthelot Reaction for Determining Ammonium in Soil Extracts and Water. *Soil Sci. Soc. Amer. J.* 62, 473-480.

Ripp, S. & Miller, R. V. (1997). The role of pseudolysogeny in bacteriophage-host interactions in a natural freshwater environment. *Microbiol.* 143, 2065-2070.

Roy, K., et al. (2020). Temporal Dynamics of Soil Virus and Bacterial Populations in Agricultural and Early Plant Successional Soils. *Front. Microbiol.* 11, 1404.

Saiya-Cork, K. R., Sinsabaugh, R. L., & Zak, D. F. (2002). The effects of long term nitrogen deposition on extracellular enzyme activity in an Acer saccharum forest soil. *Soil Biol. Biochem.* 34, 1309-1315.

SAS Institute, Inc., 2018. *SAS/STAT® 15.1 User's Guide*. SAS Institute, Inc., Cary, NC U. S. A.

Schimel, J. P. (2018). Life in Dry Soils: Effects of Drought on Soil Microbial Communities and Processes. *Annu. Rev. Ecol. Evol. S.* 49, 409-432.

Schimel, J. P., Balser, T. C., & Wallenstein, M. (2007). Microbial stress-response physiology and its implications for ecosystem function. *Ecology* 88, 1386-1394.

Schimel, J. P. & Schaeffer, S. M. (2012). Microbial control over carbon cycling in soil. *Front. Microbiol.* 3, 348.

Silveira, C. B. & Rohwer, F. L. (2016). Piggyback-the-Winner in host-associated microbial communities. *NPJ Biofilms Microbiomes* 2, 16010.

Six, J., Elliott, E. T., & Paustian, K. (2000). Soil macroaggregate turnover and microaggregate formation: a mechanism for C sequestration under no-tillage agriculture. *Soil Biol. Biochem.* 32, 2099-2103.

Six, J., Bossuyt, H., Degryze, S., & Denef, K. (200)4. A history of research on the link between (micro)aggregates, soil biota, and soil organic matter dynamics. *Soil Till. Res.* 79, 7-31.

Suttle, C. A. (2005). Viruses in the sea. *Nature* 437, 356-361.

Suttle, C. A. (1994). The significance of viruses to mortality in aquatic microbial communities. *Microb. Ecol.* 28, 237-243.

Starr, E. P., Nuccio, E. E., Pett-Ridge, J., Banfield, J. F., & Firestone, M. K. (2020). Metatranscriptomic reconstruction reveals RNA viruses with potential to shape carbon cycling in soil. *Proc. Natl. Acad. Sci U. S. A.* 116, 51.

Srinivasiah, S., Bhavsar, J., Thapar, K., Liles, M., Schoenfeld, T., & Wommack, K. E. (2008). Phages across the biosphere: constrats of viruses in soil and aquatic environments. *Res. Microbiol.* 159, 349-357.

Thingstad, T. F. & Lignell, R. (1997). Theoretical models for the control of bacterial growth rate, abundance, diversity and carbon demand. *Aquat. Microb. Ecol.* 13, 19-27.

Thingstad, T. F., Vage, S., Storesund, J. E., Sandas, R. A., & Giske, J. (2014). A theoretical analysis of how strain-specific viruses can control microbial species diversity. *Proc. Natl. Acad. Sci U. S. A.* 111, 7813-7818.

Tisdall, J. M. & Oades, J. M. (1982). Organic matter and water-stable aggregates in soils. *J. Soil Science* 62, 141-163.

Toosi, E. R., Kravchenko, A. N., Guber, A. K., & Rivers, M. L. (2017). Pore characteristics regulate priming and fate of carbon from plant residue. *Soil Biol. Biochem.* 413, 219-230.

Totsche, K. U. et al. (2018). Microaggregates in soils. *J. Plant Nutr. Soil Sci.* 181, 104-136.

Trubl, G., et al. (2018). Soil Viruses Are Underexplored Players in Ecosystem Carbon Processing. *mSystems* 3, e00076-18.

Trubl, G., Hyman, P., Roux, S., & Abedon, S. T. (2020). Coming-of-Age Characterization of Soil Viruses: A User's Guide to Virus Isolation, Detection within Metagenomes, and Viromics. *Soil Syst.* 4,23.

Tuttle, M. J. & Buchan, A. (2020). Lysogeny in the oceans: Lessons from cultivated model systems and reanalysis of its prevalence. *Environ. Microbiol.* 22, 4919-4933.

von Lûtzow, M. et al. (2006). Stabilization of organic matter in temperate soils: mechanisms and their relevance under different soil conditions—a review. *Eur. J. Soil Sci.* 57, 426-445.

Ward, R. L. & Ashley, C. S. (1977). Inactivation of enteric viruses in wastewater sludge through dewatering by evaporation. *Appl. Environ. Microbiol.* 34, 564-570.

Warren, C. R. (2020). Pools and fluxes of osmolytes in moist soil and dry soil that has been re-wet. *Soil Biol. Biochem.* 150, 108012.

Weitz, J. S. & Wilhelm, S. W. (2012). Ocean viruses and their effects on microbial communities and biogeochemical cycles. *F1000 Biol. Rep.* 4, 17.

Weinbauer, M. G. (2004). Ecology of prokaryotic viruses. *FEMS Microbiol. Rev.* 28, 127-181.

Weinbauer, M. G., Christaki, U., Nedoma, J., & Simek, K. (2003). Comparing the effects of resource enrichment and grazing on viral production in a meso-eutrophic reservoir. *Aquat. Microb. Ecol.* 31, 137-144.

Wilhelm, S. W. & Suttle, C. A. (1999). Viruses and Nutrient Cycles in the Sea. *Bioscience* 49, 781-788.

Williamson, K. E. (2011). Soil Phage Ecology: Abundance, Distribution, and Interactions with Bacterial Hosts. In: *Biocommunication in Soil Microorganisms. Soil Biology* (Witzany, G., Ed.), vol. 23. Springer, Berlin, Heidelberg.

Williamson, K. E., Fuhrmann, J. J., Wommack, K. E., & Radosevich, M. (2017). Viruses in Soil Ecosystems: An Unknown Quantity Within an Unexplored Territory. *Annu. Rev. Virol.* 4, 201-219.

Williamson, K. E., Radosevich, M., Smith, D. W., & Wommack, K. E. (2007). Incidence of lysogeny within temperate and extreme soil environments. *Environ. Microbiol.* 9, 2563-2574.

Williamson, K. E., Radosevich, M., & Wommack, K.E. (2005). Abundance and Diversity of Viruses in Six Delaware Soils. *Appl. Environ. Microbiol.* 71, 3119-3125.

Williamson, K. E., Wommack, K. E., & Radosevich, M. (2003). Sampling natural viral communities from soil for culture-independent analyses. *Appl. Environ. Microbiol.* 69, 6628-6633.

Williamson, K. E., et al. (2013). Estimates of viral abundance in soils are strongly influenced by extraction and enumeration methods. *Biol. Fertil. Soils* 49, 857-869.

Wommack, K. E. & Colwell, R. R. (2000). Virioplankton: Viruses in Aquatic Ecosystems. *Microbiol. Mol. Biol. R.* 64, 69-114.

Wommack, K. E., Nasko, D. J., Chopyk, J., & Sakowski, E. G. (2015). Counts and sequences, observations that continue to change our understanding of viruses in nature. *J. Microbiol.* 53, 181-192.

Zhuang, J. & Jin, Y. (2003). Virus Retention and Transport as Influence by Different Forms of Soil Organic Matter. *J. Environ. Qual.* 32, 816-823.

Zimmerman, A. E., Howard-Varona, C., Needham, D. M., John, S. G., Worden, A. Z., Sullivan, M. B., ... & Coleman, M. L. (2020). Metabolic and biogeochemical consequences of viral infection in aquatic ecosystems. *Nature Rev. Microbiol.* 18, 21-34.

Appendix B

Table 3.1. List of extracellular hydrolytic enzymes assays for maximum potential activities in aggregate size fractions.

Table includes enzyme abbreviation, enzyme commission (EC) number, and the fluorescently labeled substrate used for the assay. Fluorescent labels of substrates are 4-methylumbelliferyl (MUB) and 4-methylcoumarin (MUC). Broad degradation target for enzymes are as follows: sugars (AG, BG), cellulose (CB), protein (LAP), chitin/amino sugar polymer (NAG), organic phosphorous (PHOS), and hemicellulose (XYL).

Enzyme	EC	Substrate
α-Glucosidase (AG)	3.2.1.20	4-MUB-α-D-Glucopyranoside
β-Glucosidase (BG)	3.2.1.21	4-MUB-β-D-Glucopyranoside
β-D-Cellubiosidase (CB)	3.2.1.91	4-MUB-β-D-Cellobioside
Leucine Aminopeptidase (LAP)	3.2.11.1	L-Leucine-MUC Hydrochloride
N-Acetyl-β-D-Glucosaminidase (NAG)	3.2.1.30	4-MUB-N-Acetyl-β-D-Glucosaminide
Acid Phosphatase (PHOS)	3.1.3.2	4-MUB Phosphate
β-Xylosidase (XYL)	3.2.1.37	4-MUB-β-D-Xylopyranoside

Table 3.2. Results of three-way Analysis of Variance (ANOVA) for respiration with fixed effects of Aggregate size fraction (Agg), Mitomycin C (MMC) induction treatment, and sampling day (Day) in the mixed model.

CumResp is Cumulative Respiration and RespRate is daily respiration rate corresponding to destructive sampling events for other analyses (days 3, 7, 14, and 28; $n = 64$). Num DF is Numerator Degrees of Freedom, Denominator DF = 72 for all effects. Statistically significant ($p < .05$) effects are indicated using bold text with an '*' for $p < .0001$.

		CumResp		RespRate	
Source	**Num DF**	**F**	***p***	**F**	***p***
Agg	2	210.1	*****	157.8	*****
MMC	1	98.2	*****	256.7	*****
Day	3	12245.2	*****	1210.0	*****
Agg*MMC	2	3.4	**0.040**	0.6	0.529
Agg*Day	6	45.6	*****	13.3	*****
MMC*Day	3	11.4	*****	34.9	*****
Agg*MMC*Day	6	3.5	**0.004**	1.9	0.102

Table 3.3. Results of one-way Analysis of Variance for high frequency respiration data (RESP28) by Aggregate size fraction.

The ANOVA model included fixed effect of sampling day. SS is Sum of Squares, DF is Degrees of Freedom, MS is Mean Squares.

Aggregate	Source	SS	DF	MS	F	*p*
Large Macro	Between	17.5	18	0.97051	27.17	3.22E-50
	Within	9.6	269	0.03572		
	Total	27.1	287			
Small Macro	Between	9.6	18	0.53157	12.36	3.93E-26
	Within	11.6	269	0.04298		
	Total	21.1	287			
Micro	Between	16.5	18	0.91743	24.78	6.38E-47
	Within	9.9	269	0.03702		
	Total	26.5	287			

Table 3.4. Results of Tukey's Least Significant Difference (LSD) test for one-way Analysis of Variance of control-normalized high frequency respiration (RESP28) data for Large Macroaggregates.

The ANOVA model included fixed effect of sampling day. Significance levels (Signif) are indicated as follows: ***** (p = .00001), **** (p = .0001, *** (p = .001), ** (p = .01), and * (p = .05). Comparisons where $p > .05$ are excluded from the list.

Groups	Means	*p*	Signif
Large1 vs Large10	[0.781465992802098, 1.0709504271976]	0.0002	***
Large1 vs Large18	[0.781465992802098, 1.07673881829271]	0.0130	*
Large1 vs Large24	[0.781465992802098, 1.11161896956293]	0.0021	**
Large1 vs Large27	[0.781465992802098, 1.10596208120471]	0.0029	**
Large1 vs Large7	[0.781465992802098, 1.83275913928629]	0.0000	*****
Large1 vs Large9	[0.781465992802098, 1.0491411565024]	0.0009	***
Large10 vs Large2	[1.0709504271976, 0.848725448314829]	0.0193	*
Large10 vs Large4	[1.0709504271976, 0.806658859503594]	0.0030	**
Large10 vs Large6	[1.0709504271976, 0.662302036358485]	0.0000	*****
Large10 vs Large7	[1.0709504271976, 1.83275913928629]	0.0000	*****
Large14 vs Large6	[0.986895082075044, 0.662302036358485]	0.0000	****
Large14 vs Large7	[0.986895082075044, 1.83275913928629]	0.0000	*****
Large15 vs Large6	[1.00539896984327, 0.662302036358485]	0.0019	**
Large15 vs Large7	[1.00539896984327, 1.83275913928629]	0.0000	*****
Large16 vs Large6	[0.941720956690329, 0.662302036358485]	0.0402	*
Large16 vs Large7	[0.941720956690329, 1.83275913928629]	0.0000	*****
Large18 vs Large6	[1.07673881829271, 0.662302036358485]	0.0000	****
Large18 vs Large7	[1.07673881829271, 1.83275913928629]	0.0000	*****
Large2 vs Large6	[0.848725448314829, 0.662302036358485]	0.0363	*
Large2 vs Large7	[0.848725448314829, 1.83275913928629]	0.0000	*****
Large21 vs Large7	[0.904131961456802, 1.83275913928629]	0.0000	*****
Large22 vs Large6	[1.04061728629801, 0.662302036358485]	0.0003	***
Large22 vs Large7	[1.04061728629801, 1.83275913928629]	0.0000	*****
Large24 vs Large4	[1.11161896956293, 0.806658859503594]	0.0130	*
Large24 vs Large6	[1.11161896956293, 0.662302036358485]	0.0000	*****

Table 3.4 continued

Groups	Means	*p*	Signif
Large24 vs Large7	[1.11161896956293, 1.83275913928629]	0.0000	*****
Large25 vs Large7	[0.868783760546445, 1.83275913928629]	0.0000	*****
Large27 vs Large4	[1.10596208120471, 0.806658859503594]	0.0168	*
Large27 vs Large6	[1.10596208120471, 0.662302036358485]	0.0000	*****
Large27 vs Large7	[1.10596208120471, 1.83275913928629]	0.0000	*****
Large28 vs Large6	[1.00763508329645, 0.662302036358485]	0.0017	**
Large28 vs Large7	[1.00763508329645, 1.83275913928629]	0.0000	*****
Large3 vs Large6	[0.874944570072689, 0.662302036358485]	0.0158	*
Large3 vs Large7	[0.874944570072689, 1.83275913928629]	0.0000	*****
Large4 vs Large7	[0.806658859503594, 1.83275913928629]	0.0000	*****
Large4 vs Large9	[0.806658859503594, 1.0491411565024]	0.0119	*
Large6 vs Large7	[0.662302036358485, 1.83275913928629]	0.0000	*****
Large6 vs Large8	[0.662302036358485, 0.914376747264162]	0.0066	**
Large6 vs Large9	[0.662302036358485, 1.0491411565024]	0.0000	*****
Large7 vs Large8	[1.83275913928629, 0.914376747264162]	0.0000	*****
Large7 vs Large9	[1.83275913928629, 1.0491411565024]	0.0000	*****

Table 3.5. Results of Tukey's Least Significant Difference (LSD) test for one-way Analysis of Variance of control-normalized high frequency respiration (RESP28) for Small Macroaggregates.

The ANOVA model included fixed effect of sampling day. Significance levels (Signif) are indicated as follows: ***** (p = .00001), **** (p = .0001, *** (p = .001), ** (p = .01), and * (p = .05). Comparisons where p > .05 are excluded from the list.

Groups	Means	*p*	Signif
Small1 vs Small10	[0.789335517824309, 1.13589443214766]	0.0000	****
Small1 vs Small14	[0.789335517824309, 1.09308084115641]	0.0004	***
Small1 vs Small16	[0.789335517824309, 1.35828710350645]	0.0000	*****
Small1 vs Small21	[0.789335517824309, 1.18207282913165]	0.0004	***
Small1 vs Small22	[0.789335517824309, 1.1698251856488]	0.0008	***
Small1 vs Small24	[0.789335517824309, 1.11722010459826]	0.0109	*
Small1 vs Small25	[0.789335517824309, 1.38165302334503]	0.0000	*****
Small1 vs Small7	[0.789335517824309, 1.04877475117638]	0.0079	**
Small1 vs Small9	[0.789335517824309, 1.05290421352864]	0.0062	**
Small10 vs Small2	[1.13589443214766, 0.819087464796337]	0.0002	***
Small10 vs Small3	[1.13589443214766, 0.702611971147124]	0.0000	*****
Small10 vs Small4	[1.13589443214766, 0.779977087576375]	0.0000	****
Small10 vs Small6	[1.13589443214766, 0.775098550139145]	0.0000	****
Small14 vs Small2	[1.09308084115641, 0.819087464796337]	0.0032	**
Small14 vs Small3	[1.09308084115641, 0.702611971147124]	0.0000	*****
Small14 vs Small4	[1.09308084115641, 0.779977087576375]	0.0007	***
Small14 vs Small6	[1.09308084115641, 0.775098550139145]	0.0005	***
Small15 vs Small3	[1.03777293339034, 0.702611971147124]	0.0126	*
Small16 vs Small18	[1.35828710350645, 0.983814022356807]	0.0413	*
Small16 vs Small2	[1.35828710350645, 0.819087464796337]	0.0000	*****
Small16 vs Small3	[1.35828710350645, 0.702611971147124]	0.0000	*****
Small16 vs Small4	[1.35828710350645, 0.779977087576375]	0.0000	*****
Small16 vs Small6	[1.35828710350645, 0.775098550139145]	0.0000	*****
Small16 vs Small8	[1.35828710350645, 0.92176056302573]	0.0003	***
Small18 vs Small25	[0.983814022356807, 1.38165302334503]	0.0195	*

Table 3.5 continued

Groups	Means	*p*	Signif
Small2 vs Small21	[0.819087464796337, 1.18207282913165]	0.0020	**
Small2 vs Small22	[0.819087464796337, 1.1698251856488]	0.0037	**
Small2 vs Small24	[0.819087464796337, 1.11722010459826]	0.0381	*
Small2 vs Small25	[0.819087464796337, 1.38165302334503]	0.0000	*****
Small2 vs Small7	[0.819087464796337, 1.04877475117638]	0.0406	*
Small2 vs Small9	[0.819087464796337, 1.05290421352864]	0.0328	*
Small21 vs Small3	[1.18207282913165, 0.702611971147124]	0.0000	*****
Small21 vs Small4	[1.18207282913165, 0.779977087576375]	0.0005	***
Small21 vs Small6	[1.18207282913165, 0.775098550139145]	0.0004	***
Small22 vs Small3	[1.1698251856488, 0.702611971147124]	0.0000	****
Small22 vs Small4	[1.1698251856488, 0.779977087576375]	0.0010	***
Small22 vs Small6	[1.1698251856488, 0.775098550139145]	0.0008	***
Small24 vs Small3	[1.11722010459826, 0.702611971147124]	0.0003	***
Small24 vs Small4	[1.11722010459826, 0.779977087576375]	0.0115	*
Small24 vs Small6	[1.11722010459826, 0.775098550139145]	0.0093	**
Small25 vs Small3	[1.38165302334503, 0.702611971147124]	0.0000	*****
Small25 vs Small4	[1.38165302334503, 0.779977087576375]	0.0000	*****
Small25 vs Small6	[1.38165302334503, 0.775098550139145]	0.0000	*****
Small25 vs Small7	[1.38165302334503, 1.04877475117638]	0.0303	*
Small25 vs Small8	[1.38165302334503, 0.92176056302573]	0.0001	****
Small25 vs Small9	[1.38165302334503, 1.05290421352864]	0.0352	*
Small27 vs Small3	[1.05920775083344, 0.702611971147124]	0.0049	**
Small28 vs Small3	[1.03136890371223, 0.702611971147124]	0.0165	*
Small3 vs Small7	[0.702611971147124, 1.04877475117638]	0.0001	****
Small3 vs Small9	[0.702611971147124, 1.05290421352864]	0.0001	****
Small4 vs Small7	[0.779977087576375, 1.04877475117638]	0.0102	*
Small4 vs Small9	[0.779977087576375, 1.05290421352864]	0.0081	**
Small6 vs Small7	[0.775098550139145, 1.04877475117638]	0.0078	**
Small6 vs Small9	[0.775098550139145, 1.05290421352864]	0.0062	**

Table 3.6. Results of Tukey's Least Significant Difference (LSD) test for one-way Analysis of Variance of control-normalized high frequency respiration (RESP28) data for Microaggregates (Micro).

The ANOVA model included fixed effect of sampling day. Significance levels (Signif) are indicated as follows: ***** (p = .00001), **** (p = .0001, *** (p = .001), ** (p = .01), and * (p = .05). Comparisons where $p > .05$ are excluded from the list.

Groups	Means	*p*	Signif
Micro1 vs Micro10	[0.718008489196876, 1.09242718967109]	0.0000	*****
Micro1 vs Micro14	[0.718008489196876, 1.13896068196585]	0.0000	*****
Micro1 vs Micro15	[0.718008489196876, 1.05515470071612]	0.0020	**
Micro1 vs Micro16	[0.718008489196876, 1.56190481943208]	0.0000	*****
Micro1 vs Micro18	[0.718008489196876, 0.989921528555483]	0.0465	*
Micro1 vs Micro21	[0.718008489196876, 1.31393980158063]	0.0000	*****
Micro1 vs Micro22	[0.718008489196876, 1.27262133499054]	0.0000	*****
Micro1 vs Micro24	[0.718008489196876, 1.0799205760224]	0.0005	***
Micro1 vs Micro25	[0.718008489196876, 1.28229327119522]	0.0000	*****
Micro1 vs Micro27	[0.718008489196876, 1.20743751635096]	0.0000	*****
Micro1 vs Micro7	[0.718008489196876, 1.29849460164956]	0.0000	*****
Micro1 vs Micro9	[0.718008489196876, 1.2520834048145]	0.0000	*****
Micro10 vs Micro16	[1.09242718967109, 1.56190481943208]	0.0000	*****
Micro10 vs Micro2	[1.09242718967109, 0.821250474027316]	0.0010	***
Micro10 vs Micro3	[1.09242718967109, 0.768534978428061]	0.0001	****
Micro10 vs Micro4	[1.09242718967109, 0.725892277741727]	0.0000	*****
Micro10 vs Micro6	[1.09242718967109, 0.716282020039069]	0.0000	*****
Micro10 vs Micro8	[1.09242718967109, 0.845731138497659]	0.0395	*
Micro14 vs Micro16	[1.13896068196585, 1.56190481943208]	0.0001	***
Micro14 vs Micro2	[1.13896068196585, 0.821250474027316]	0.0000	****
Micro14 vs Micro3	[1.13896068196585, 0.768534978428061]	0.0000	*****
Micro14 vs Micro4	[1.13896068196585, 0.725892277741727]	0.0000	*****
Micro14 vs Micro6	[1.13896068196585, 0.716282020039069]	0.0000	*****
Micro14 vs Micro8	[1.13896068196585, 0.845731138497659]	0.0033	**

Table 3.6 continued

Groups	Means	*p*	Signif
Micro22 vs Micro8	[1.27262133499054, 0.845731138497659]	0.0001	****
Micro24 vs Micro3	[1.0799205760224, 0.768534978428061]	0.0124	*
Micro24 vs Micro4	[1.0799205760224, 0.725892277741727]	0.0015	**
Micro24 vs Micro6	[1.0799205760224, 0.716282020039069]	0.0009	***
Micro25 vs Micro28	[1.28229327119522, 0.922004273955404]	0.0268	*
Micro25 vs Micro3	[1.28229327119522, 0.768534978428061]	0.0000	*****
Micro25 vs Micro4	[1.28229327119522, 0.725892277741727]	0.0000	*****
Micro25 vs Micro6	[1.28229327119522, 0.716282020039069]	0.0000	*****
Micro25 vs Micro8	[1.28229327119522, 0.845731138497659]	0.0001	****
Micro27 vs Micro3	[1.20743751635096, 0.768534978428061]	0.0000	*****
Micro27 vs Micro4	[1.20743751635096, 0.725892277741727]	0.0000	*****
Micro27 vs Micro6	[1.20743751635096, 0.716282020039069]	0.0000	*****
Micro27 vs Micro8	[1.20743751635096, 0.845731138497659]	0.0029	**
Micro28 vs Micro7	[0.922004273955404, 1.29849460164956]	0.0014	**
Micro28 vs Micro9	[0.922004273955404, 1.2520834048145]	0.0125	*
Micro3 vs Micro7	[0.768534978428061, 1.29849460164956]	0.0000	*****
Micro3 vs Micro9	[0.768534978428061, 1.2520834048145]	0.0000	*****
Micro4 vs Micro7	[0.725892277741727, 1.29849460164956]	0.0000	*****
Micro4 vs Micro9	[0.725892277741727, 1.2520834048145]	0.0000	*****
Micro6 vs Micro7	[0.716282020039069, 1.29849460164956]	0.0000	*****
Micro6 vs Micro9	[0.716282020039069, 1.2520834048145]	0.0000	*****
Micro7 vs Micro8	[1.29849460164956, 0.845731138497659]	0.0000	*****
Micro8 vs Micro9	[0.845731138497659, 1.2520834048145]	0.0000	*****

Table 3.7. Results of three-way Analysis of Variance (ANOVA) for viral abundance, bacterial abundance, Virus-Bacteria Ratio (VBR), dissolved organic carbon (DOC), and ammonium (NH_4) by aggregate size fraction (Agg), Mitomycin C (MMC) induction treatment, and sampling day (Day).

Num DF is Numerator Degrees of Freedom and Denominator DF = 90 for all effects. Statistically significant ($p < .05$) effects are highlighted using bold text with an '*' for $p < .0001$.

Source	**Num DF**	Virus		Bacteria		VBR	
		F	***p***	**F**	***p***	**F**	***p***
Agg	2	4.6	**0.012**	1.0	0.367	1.7	0.191
MMC	1	2.0	0.163	17.9	*	5.7	**0.020**
Day	4	369.2	*	578.8	*	96.6	*
Agg*MMC	2	3.1	**0.049**	1.3	0.290	1.8	0.167
Agg*Day	8	1.4	0.227	2.2	**0.031**	1.4	0.197
MMC*Day	4	3.6	**0.009**	13.4	*	11.0	*
Agg*MMC*Day	8	1.3	0.277	1.3	0.266	2.1	**0.046**

Table 3.7 continued

Source	Num DF	DOC F	DOC *p*	NH_4 F	NH_4 *p*
Agg	2	9.9	**0.000**	111.0	*
MMC	1	17.9	*	0.6	0.426
Day	4	399.8	*	1249.8	*
Agg*MMC	2	2.2	0.122	1.1	0.354
Agg*Day	8	2.1	**0.046**	2.1	**0.040**
MMC*Day	4	24.3	*	2.7	**0.037**
Agg*MMC*Day	8	1.5	0.172	0.5	0.859

Table 3.8. Results of three-way Analysis of Variance (ANOVA) for seven extracellular enzyme activities.

Fixed effects of Aggregate size fraction (Agg), Mitomycin C (MMC) induction treatment, and Day were included in the ANOVA model along with all two- and three-way interactions. Num DF is Numerator Degrees of Freedom, Denominator DF = 90 for all effects. Statistically significant ($p < .05$) effects are highlighted by bold text.

		AG		BG		CB		LAP	
Source	**Num DF**	**F**	***p***	**F**	***p***	**F**	***p***	**F**	***p***
Agg	2	1.0	0.378	7.4	**0.001**	0.5	0.608	0.5	0.635
MMC	1	0.9	0.348	1.5	0.224	0.2	0.658	3.2	**0.077**
Day	4	17.9	*	25.5	*	11.2	*	5.1	**0.001**
Agg*MMC	2	8.0	**0.001**	24.6	*	16.2	*	5.8	**0.004**
Agg*Day	8	0.8	0.580	1.5	0.164	0.9	0.544	1.5	0.156
MMC*Day	4	0.5	0.758	0.2	0.960	0.5	0.716	1.2	0.307
Agg*MMC*Day	8	1.7	0.106	1.5	0.174	1.5	0.176	0.7	0.712

Abbreviations: α-Glucosidase (AG), β-Glucosidase (BG), β-D-Cellubiosidase (CB), Leucine Aminopeptidase (LAP), N-Acetyl- β-Glucosaminidase (NAG), Acid Phosphatase (PHOS), and β-Xylosidase (XYL).

Table 3.8 continued

Source	Num DF	NAG F	NAG *p*	PHOS F	PHOS *p*	XYL F	XYL *p*
Agg	2	1.4	0.263	10.1	**0.0001**	1.1	0.346
MMC	1	2.8	**0.097**	6.3	**0.014**	0.2	0.686
Day	4	26.3	*	83.6	*	27.0	*
Agg*MMC	2	21.8	*	41.3	*	10.7	*
Agg*Day	8	0.8	0.596	1.7	0.108	0.7	0.734
MMC*Day	4	2.4	**0.055**	15.9	*	3.7	**0.008**
Agg*MMC*Day	8	1.2	0.309	1.6	0.142	1.6	0.132

Table 3.9. Correlation matrix used for the Principal Components Analysis (PCA) (*n* = 120).

NS is Not Significant at $p < .1$ and an '*' indicates significance at $p < .1$; all other correlations are significant at $p < .05$. Probability (p) values are available in Table 3.10.

	Virus	Bacteria	VBR	DOC	NH_4
Bacteria	0.62				
VBR	0.56	-0.15*			
DOC	-0.74	-0.84	NS		
NH_4	0.36	0.83	-0.25	-0.65	
AG	0.36	NS	0.23	-0.22	NS
BG	0.28	NS	0.29	NS	-0.26
CB	0.17*	NS	0.25	NS	-0.25
LAP	NS	NS	NS	0.18*	NS
NAG	0.45	0.23	0.22	-0.31	NS
PHOS	0.45	-0.10	0.52	NS	-0.31
XYL	0.43	0.27	0.26	-0.41	NS

Abbreviations: α-Glucosidase (AG), ammonium (NH_4), bacterial cell abundance (Bacteria), β-Glucosidase (BG), β-D-Cellubiosidase (CB), dissolved organic carbon (DOC), Leucine Aminopeptidase (LAP), N-Acetyl-β-Glucosaminidase (NAG), Acid Phosphatase (PHOS), respiration (Resp), viral abundance (Virus), Virus-Bacteria Ratio (VBR), and β-Xylosidase (XYL).

Table 3.9 continued

	AG	BG	CB	LAP	NAG	PHOS
Bacteria						
VBR						
DOC						
NH_4						
AG						
BG	0.62					
CB	0.55	0.83				
LAP	0.21	0.29	0.32			
NAG	0.60	0.61	0.44	0.35		
PHOS	0.50	0.66	0.52	0.10	0.57	
XYL	0.55	0.62	0.50	0.18	0.67	0.47

Table 3.10. Probability (p) values for the correlation matrix used for the Principal Components Analysis (PCA) (excluding respiration data, *n* = 120).

Significant *p* values at 95% confidence levels are indicated by bold text with an '*' for $p < .0001$.

	Virus	Bacteria	VBR	DOC	NH_4
Bacteria	*****				
VBR	*****	0.094			
DOC	*****	*****	0.218		
NH_4	*****	*****	**0.005**	*****	
AG	*****	0.266	**0.011**	**0.018**	0.710
BG	**0.002**	0.448	**0.002**	0.306	**0.004**
CB	0.059	0.123	**0.006**	0.703	**0.006**
LAP	0.225	0.149	0.202	0.050	0.108
NAG	*****	**0.013**	**0.015**	**0.001**	0.313
PHOS	*****	0.280	*****	0.304	**0.001**
XYL	*****	**0.003**	**0.005**	*****	0.174

Abbreviations: α-Glucosidase (AG), β-Glucosidase (BG), β-D-Cellubiosidase (CB), dissolved organic carbon (DOC), Leucine Aminopeptidase (LAP), N-Acetyl- β-Glucosaminidase (NAG), ammonium (NH_4), Acid Phosphatase (PHOS), Virus-Bacteria Ratio (VBR), and β-Xylosidase (XYL).

Table 3.10 continued

	AG	BG	CB	LAP	NAG	PHOS
Bacteria						
VBR						
DOC						
NH_4						
AG						
BG	*					
CB	*	*				
LAP	**0.020**	**0.002**	**0.001**			
NAG	*	*	*	*		
PHOS	*	*	*	0.263	*	
XYL	*	*	*	**0.046**	*	*

Table 3.11. Correlation matrix including cumulative respiration (CumResp) and daily respiration rates (RespRate) (excluding day 0, *n* = 96).

NS is Not Significant at $p < .1$ and an '*' indicates significance at $p < .1$; all other correlations are significant at $p < .05$. Probability (*p*) values are provided in Table 3.12.

	CumResp	RespRate
RespRate	0.68	
Virus	-0.23	0.24
Bacteria	0.89	0.61
VBR	-0.68	-0.21
DOC	-0.59	-0.66
NH_4	0.92	0.73
AG	NS	NS
BG	-0.34	NS
CB	-0.30	NS
LAP	NS	NS
NAG	NS	NS
PHOS	-0.65	-0.39
XYL	NS	0.33

Abbreviations: α-Glucosidase (AG), β-Glucosidase (BG), β-D-Cellubiosidase (CB), dissolved organic carbon (DOC), Leucine Aminopeptidase (LAP), N-Acetyl- β-Glucosaminidase (NAG), ammonium (NH_4), Acid Phosphatase (PHOS), Virus-Bacteria Ratio (VBR), and β-Xylosidase (XYL).

Table 3.12. Probability (*p*) values for correlation coefficients calculated between variable pairs including cumulative respiration (CumResp) and daily respiration rates (RespRate).

Statistically significant ($p < .05$) values are highlighted by bold text with an '*' indicating $p < .0001$.

	CumResp	RespRate
RespRate	*****	
Virus	**0.025**	**0.019**
Bacteria	*****	*****
VBR	*****	**0.037**
DOC	*****	*****
NH_4	*****	*****
AG	0.186	0.324
BG	**0.001**	0.836
CB	**0.003**	0.499
LAP	0.528	0.508
NAG	0.397	0.155
PHOS	*****	*****
XYL	0.561	**0.001**

Abbreviations: α-Glucosidase (AG), β-Glucosidase (BG), β-D-Cellubiosidase (CB), cumulative respiration (CO_2 production; CumResp), dissolved organic carbon (DOC), Leucine Aminopeptidase (LAP), N-Acetyl- β-Glucosaminidase (NAG), ammonium (NH_4), Acid Phosphatase (PHOS), respiration rate (RespRate), Virus-Bacteria Ratio (VBR), and β-Xylosidase (XYL).

Table 3.13. Eigenanalysis for Principal Components (PCs) 1, 2, and 3 from the PC Analysis (PCA).

Additional PCs had eigenvalues less than one. All experimental treatments were included (*n* = 120) in the analysis. Variables contributing to each PC based on the magnitude of loading scores are indicated by bold text. CumPercent is Cumulative Percent of variance explained with successive addition of each PC.

Eigenanalysis	**PC1**	**PC2**	**PC3**
Eigenvalue	4.88	3.15	1.33
Percent	40.7	26.3	11.1
Cum Percent	40.7	67.0	78.0
Loading scores	**PC1**	**PC2**	**PC3**
Virus	**0.762**	-0.474	-0.301
Bacteria	0.398	**-0.845**	0.271
VBR	0.592	0.157	**-0.690**
DOC	-0.568	**0.739**	-0.050
NH_4	0.474	**-0.826**	0.099
AG	**0.723**	0.260	0.126
BG	**0.749**	0.502	0.084
CB	**0.612**	0.549	0.128
LAP	0.182	0.414	**0.616**
NAG	**0.790**	0.144	0.269
PHOS	**0.714**	0.375	-0.376
XYL	**0.788**	0.074	0.211

Abbreviations: α-Glucosidase (AG), β-Glucosidase (BG), β-D-Cellubiosidase (CB), cumulative respiration (CO_2 production; CumResp), dissolved organic carbon (DOC), Leucine Aminopeptidase (LAP), N-Acetyl- β-Glucosaminidase (NAG), ammonium (NH_4), Acid Phosphatase (PHOS), respiration rate (RespRate), Virus-Bacteria Ratio (VBR), and β-Xylosidase (XYL).

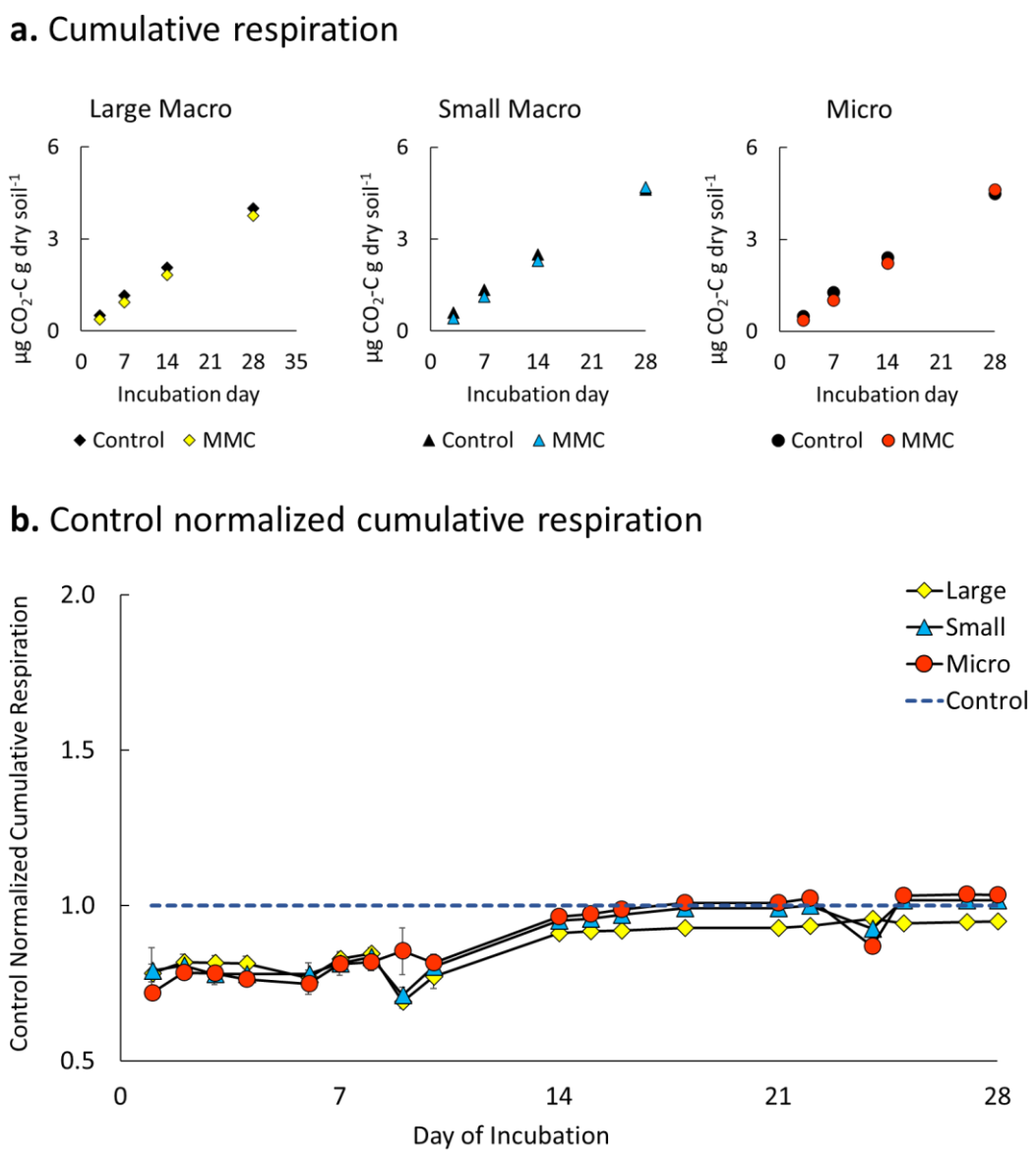

Figure 3.1. Mean cumulative heterotrophic respiration (i.e., CO_2 production) by aggregate size fraction, Mitomycin C (MMC) induction treatment, and sampling day.

Data presented include cumulative respiration used for the three-way ANOVA model (a) and control-normalized cumulative respiration (b). Control normalization reflects the response of MMC relative to control calculated as mean of MMC treatments divided by mean of control treatments. Error bars represent standard error of n = 4 replications for non-normalized data and propagated standard error of n = 8 replications for normalized data.

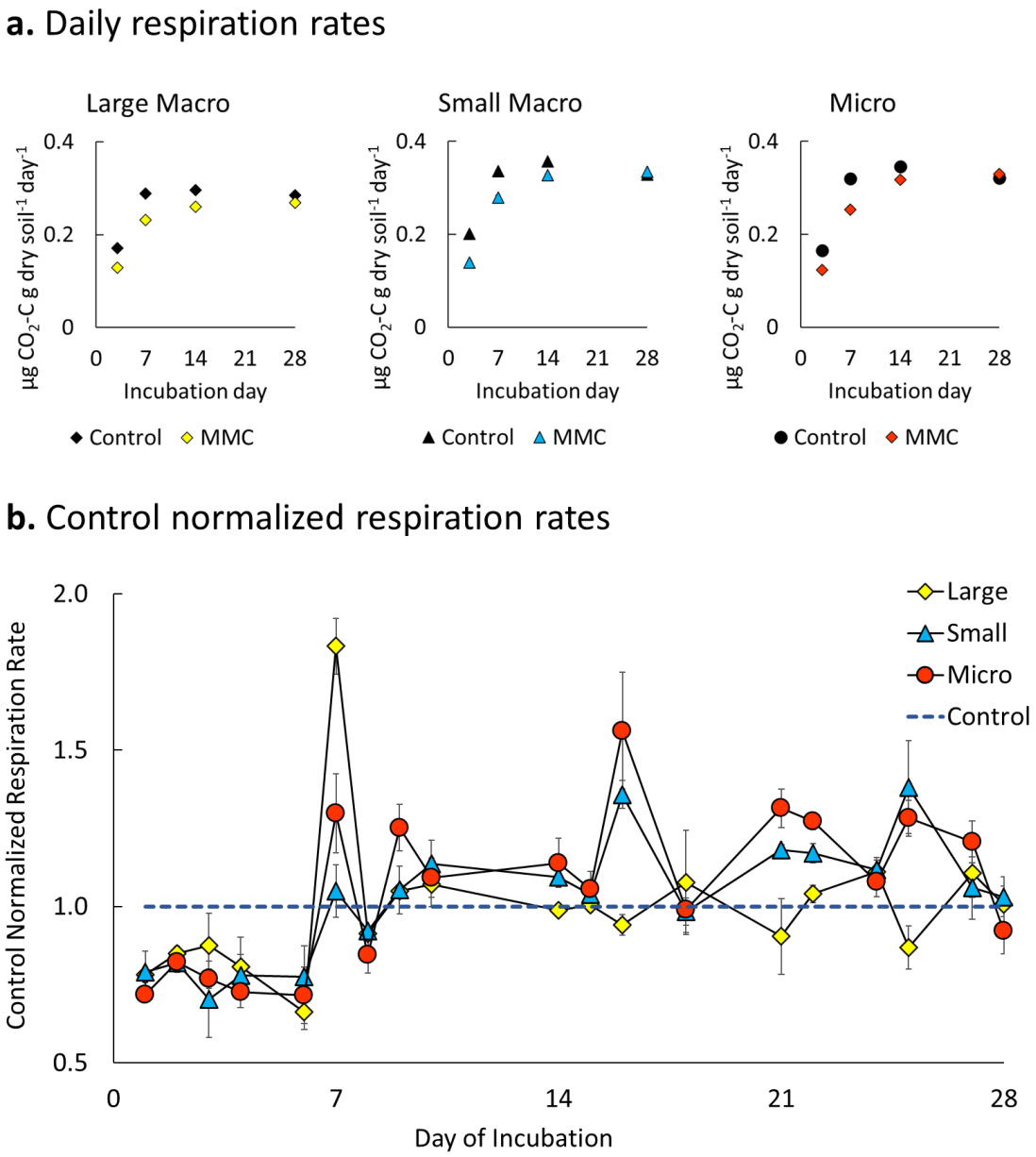

Figure 3.2. Mean daily heterotrophic respiration (i.e., CO_2 production) rates by aggregate size fraction, Mitomycin C (MMC) induction treatment, and sampling day.

Data presented include daily respiration rates used for the three-way ANOVA model (a) and control-normalized daily respiration rates (b). Control normalization reflects the response of MMC relative to control calculated as mean of MMC treatments divided by mean of control treatments. Error bars represent standard error of n = 4 replications for non-normalized data and propagated standard error of n = 8 replications for normalized data.

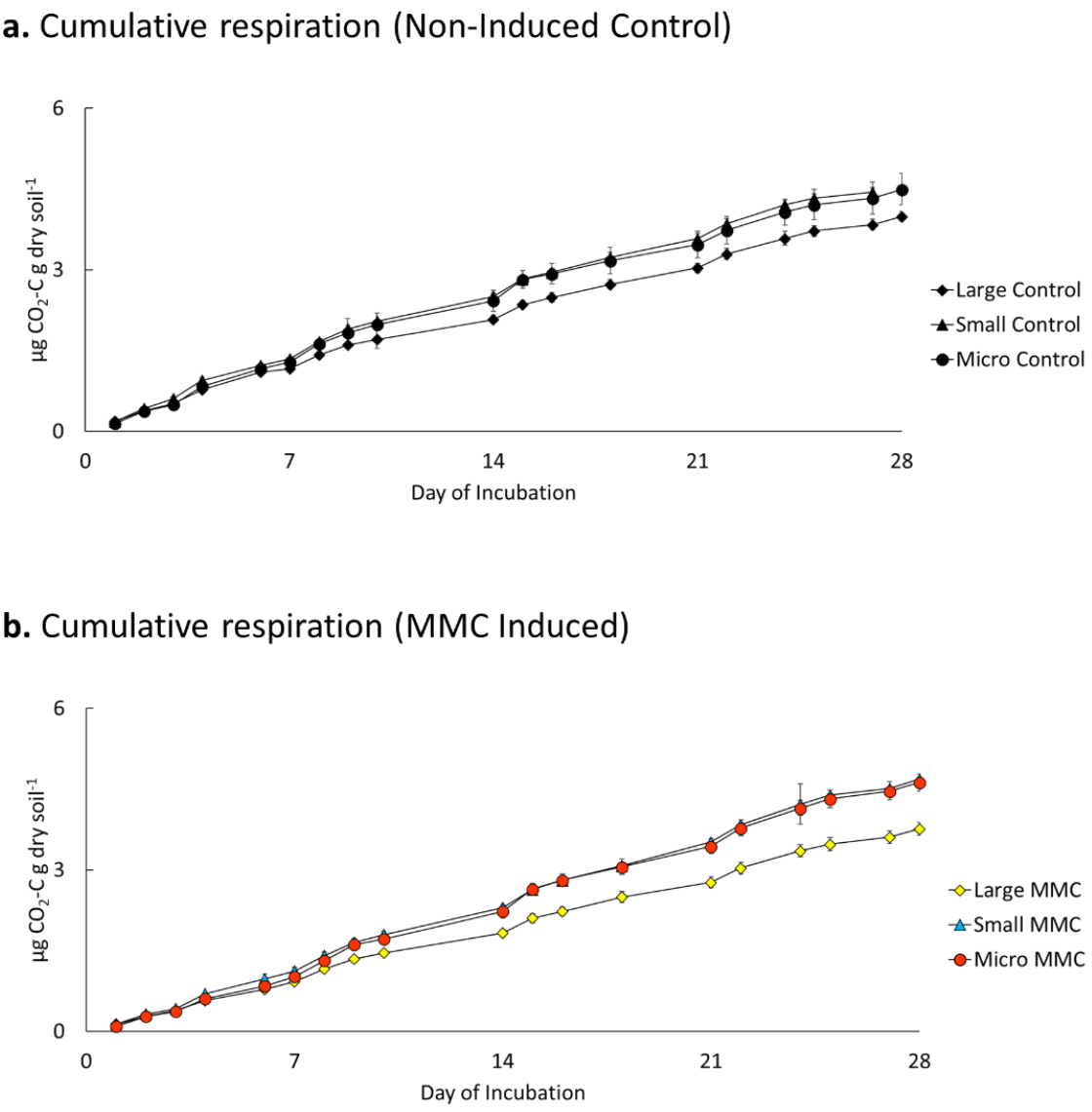

Figure 3.3. High frequency data of cumulative respiration (i.e., total CO_2 production) by aggregate size fraction for control (non-induced) (a) and Mitomycin C (MMC) induced (b) samples.

Error bars represent standard error of $n = 4$ replications per treatment combination.

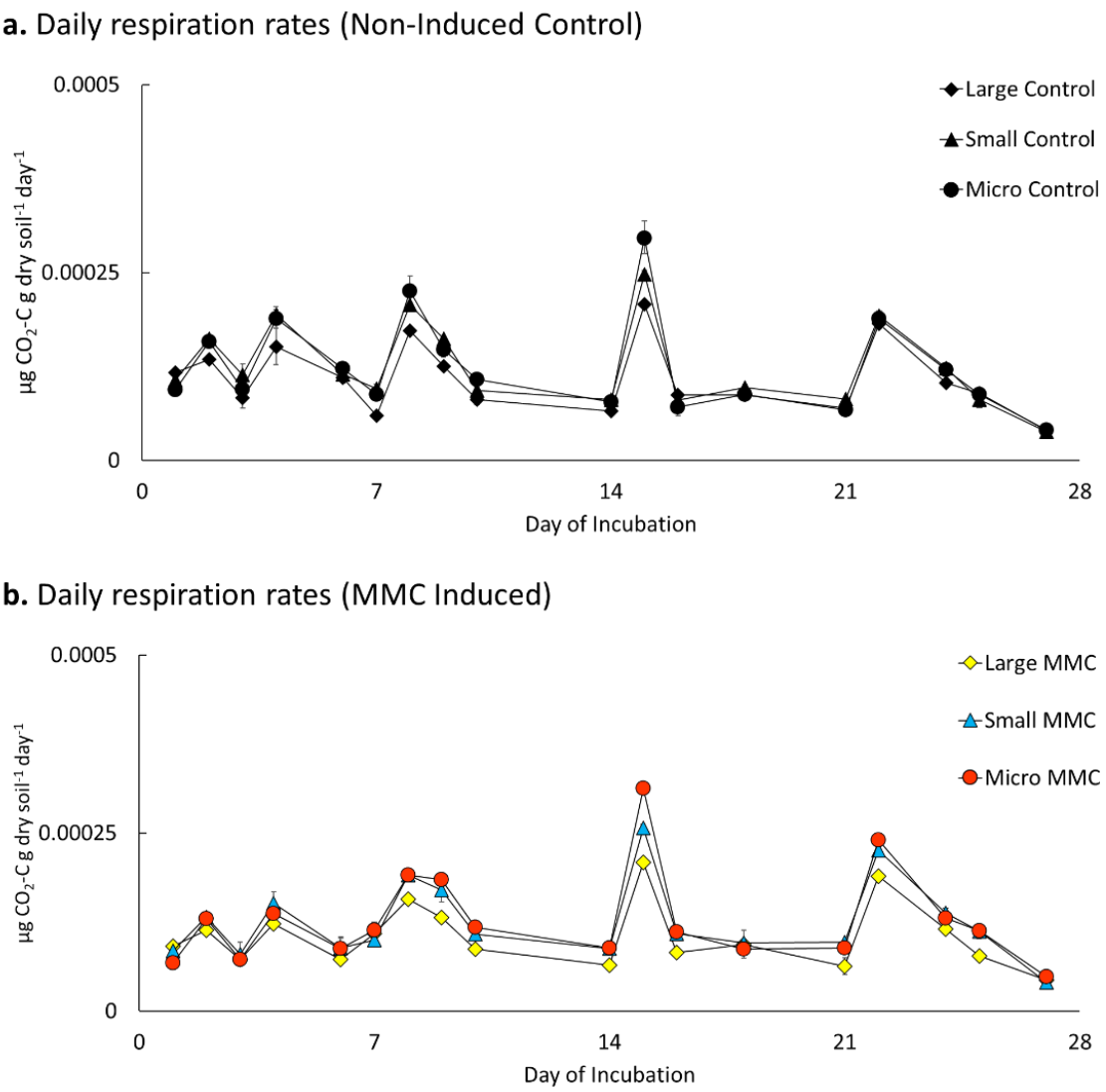

Figure 3.4. High frequency data of daily respiration rates calculated between successive headspace sampling events by aggregate size fraction for control (non-induced) (a) and Mitomycin C (MMC) induced (b) samples.

Error bars represent standard error of $n = 4$ replications per treatment combination.

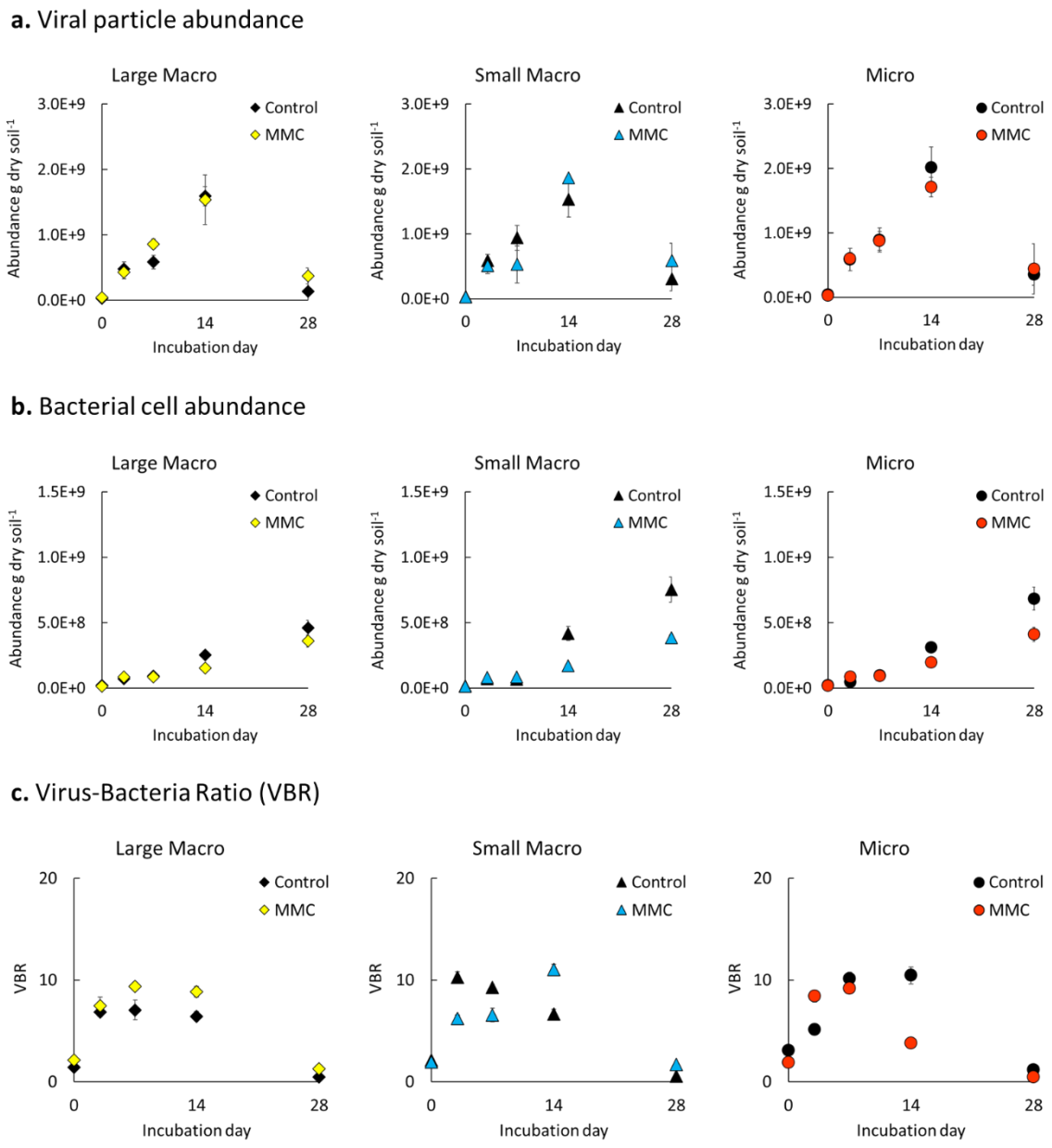

Figure 3.5. Mean viral particle abundance (a), bacterial cell abundance (b), and Virus-Bacteria Ratio (VBR) (c) by aggregate size fraction, Mitomycin C (MMC) induction treatment, and sampling day.

Error bars represent standard error of n = 4 replications per treatment combination.

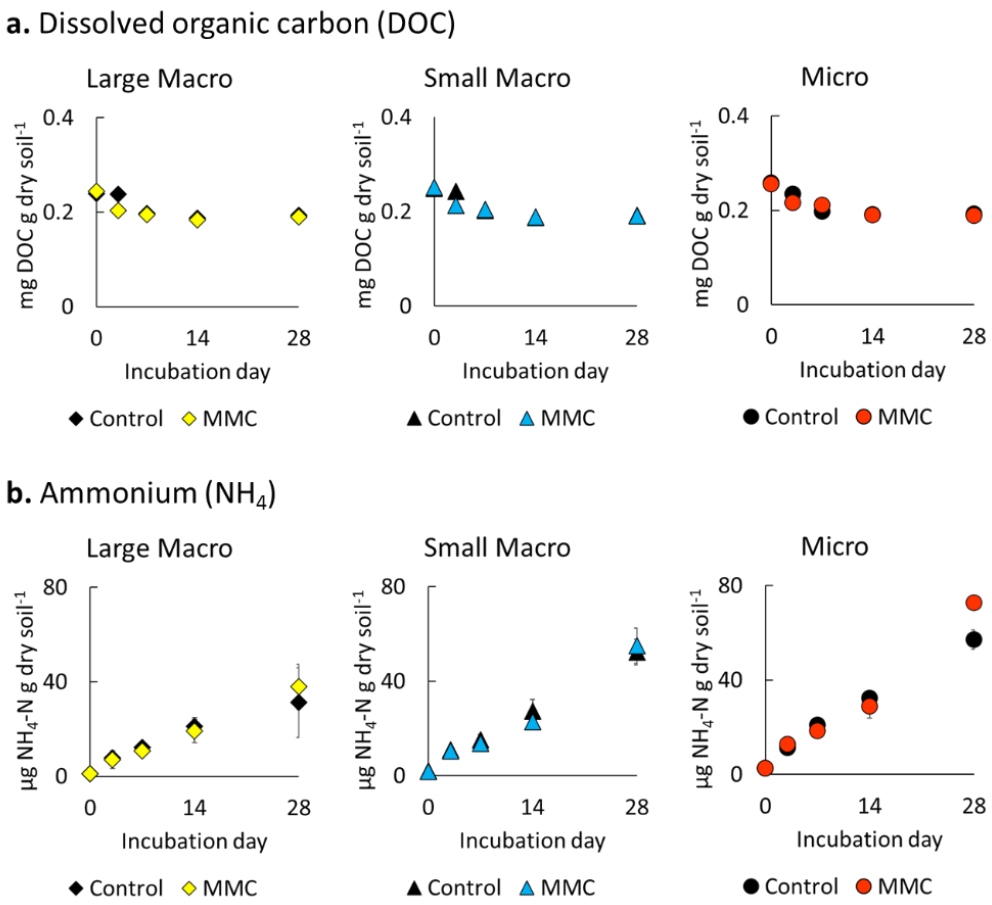

Figure 3.6. Mean extractable dissolved organic carbon (DOC) (a) and ammonium nitrogen (NH_4-N) (b) by aggregate size fraction, Mitomycin C (MMC) induction treatment, and sampling day.

Nitrate (NO_3) was below 1 µg NO_3-N g dry soil^{-1} for the entire experiment. Error bars represent standard error of n = 4 replications per treatment combination.

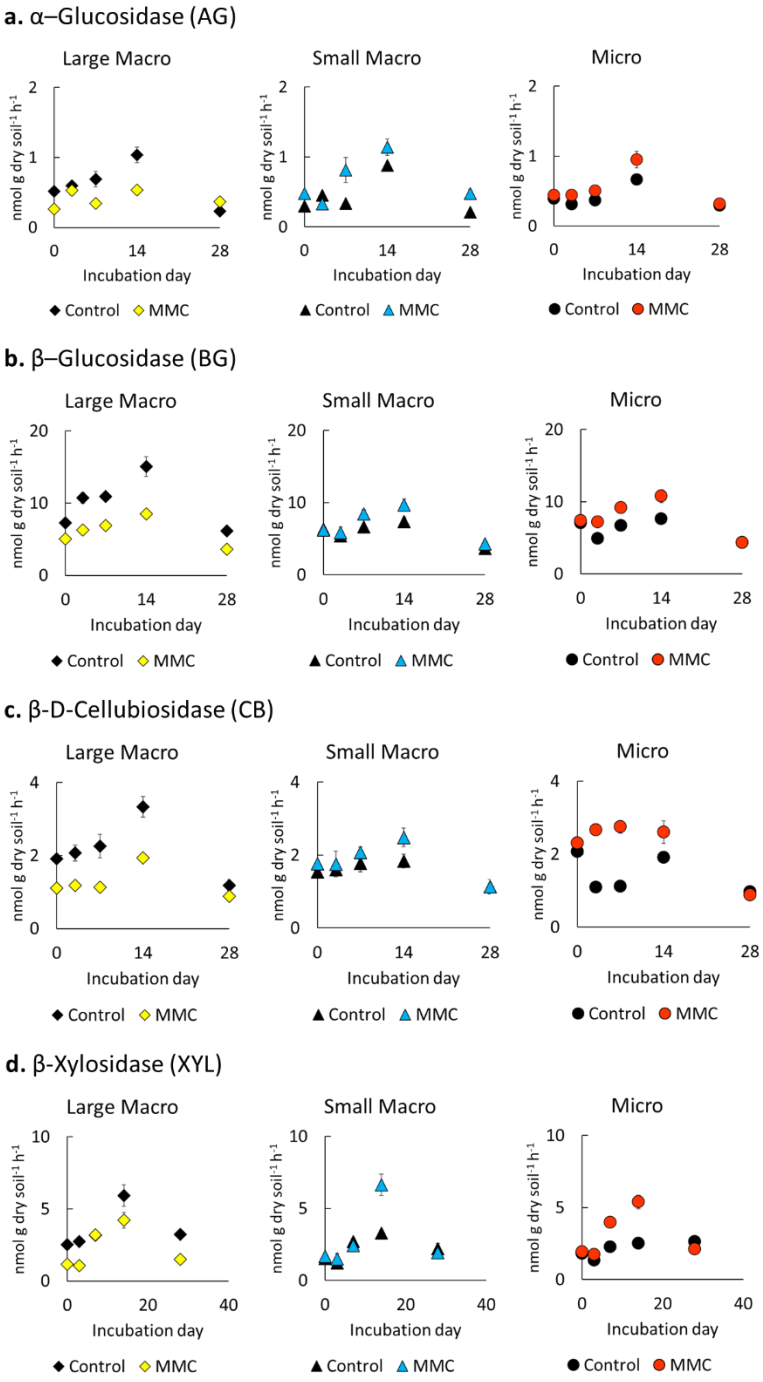

Figure 3.7. Mean activities of C targeting extracellular enzymes by aggregate size fraction, Mitomycin C (MMC) induction treatment, and sampling day.

Enzymes assayed include AG (a), BG (b), CB (c), and XYL (d). Error bars represent standard error of $n = 4$ replications per treatment combination.

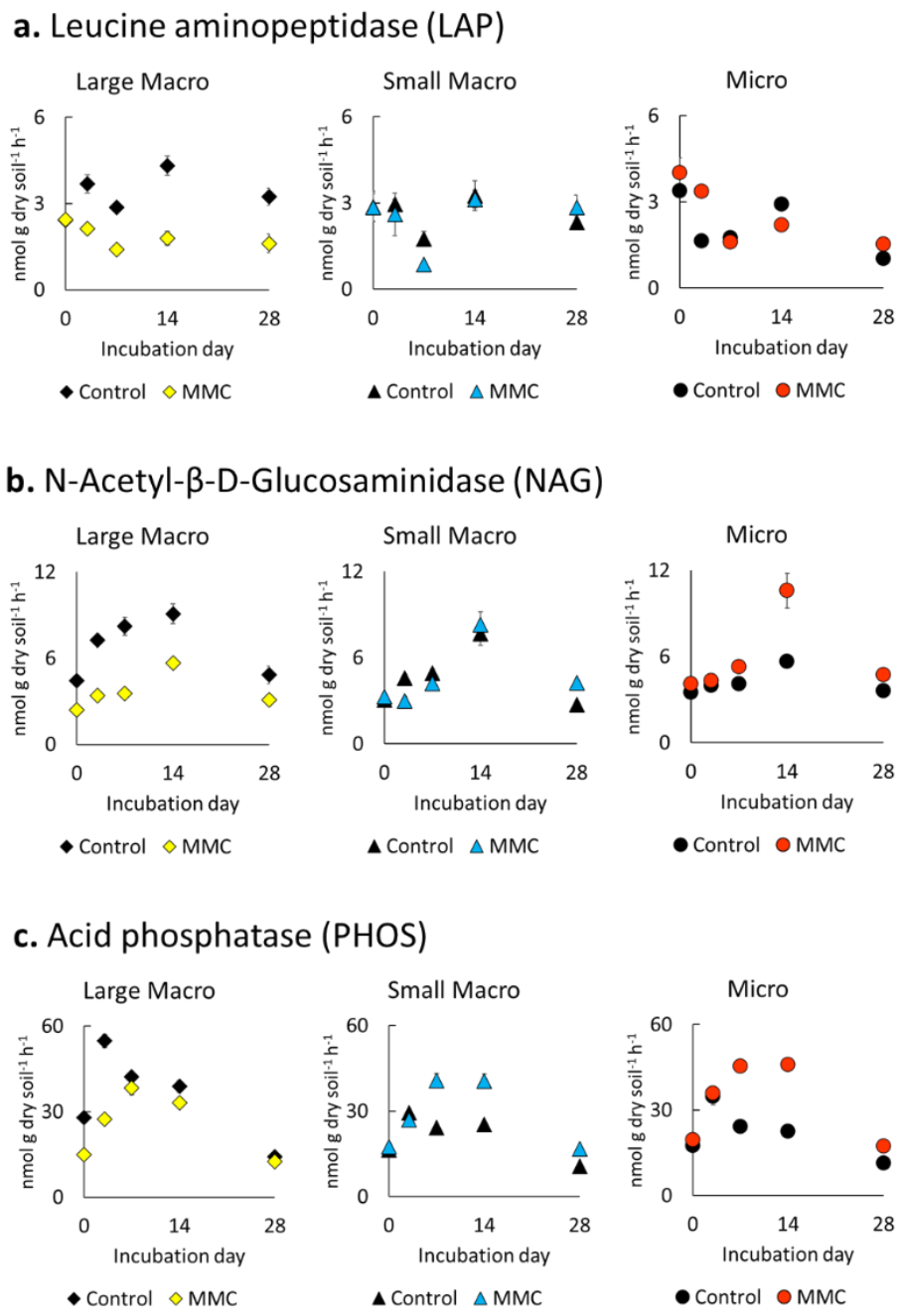

Figure 3.8. Mean activities of N and P targeting extracellular enzymes by aggregate size fraction, Mitomycin C (MMC) induction treatment, and sampling day.

Enzymes assayed include LAP (a), NAG (b), and PHOS (c). Error bars represent standard error of n = 4 replications per treatment combination.

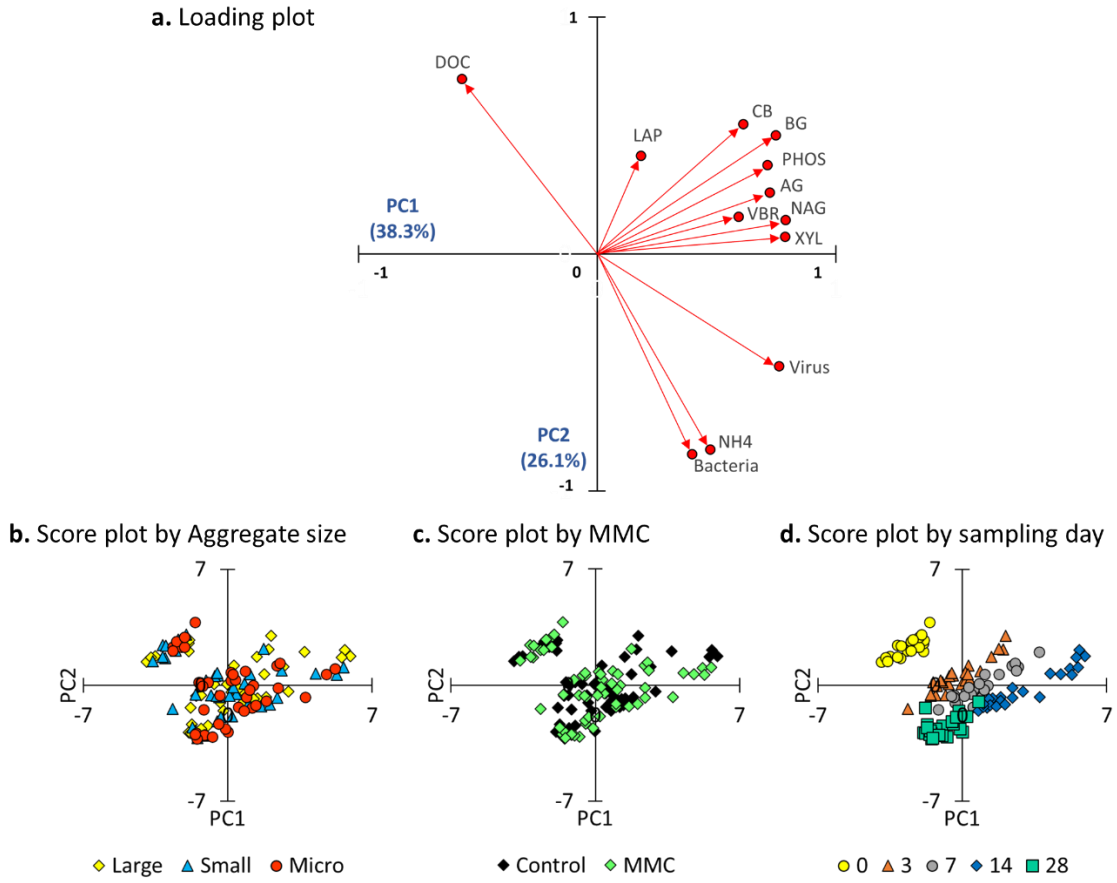

Figure 3.9. Loading plot (a) and score plots from the Principal Components Analysis (PCA) with observations displayed by aggregate size fraction (b), Mitomycin C (MMC) induction treatment (c), and sampling day (d).

Principal Components (PCs) 1 and 2 explain a cumulative 64.4% of variability (lacking respiration data but including all sampling days; n = 120). Abbreviations: α-glucosidase (AG), ammonium (NH_4), bacterial cell abundance (Bacteria), β-glucosidase (BG), β-D-cellubiosidase (CB), dissolved organic carbon (DOC), leucine aminopeptidase (LAP), N-acetyl- β-glucosaminidase (NAG), nitrate (NO_3), acid phosphatase (PHOS), respiration (Resp), viral abundance (Virus), Virus-Bacteria Ratio (VBR), and β-xylosidase (XYL).

CHAPTER FOUR

FREE VIRAL ABUNDANCE IN SOIL RESPONDS TO DRYING AND REWETTING: INFLUENCE OF DROUGHT LENGTH AND RELATION TO MICROBIAL ACTIVITY

A version of this chapter will be originally submitted to *Soil Biology and Biochemistry* by Aubrey K. Fine[a], Mark Radosevich[a], Jie Zhuang[a], Melanie Mayes[b], Sean M. Schaeffer[a]*

[a]Department of Biosystems Engineering and Soil Science, University of Tennessee, Knoxville, TN 37996, United States.
[b]Environmental Sciences Division & Climate Change Institute, Oak Ridge National Laboratory, Oak Ridge, TN, United States.

*Corresponding author: sschaef5@utk.edu

Acknowledgements: This research was supported by the United States Department of Agriculture National Institute of Food and Agriculture (Award 2018-67019-27792).

Abstract

Viral lysis and infection processes have been demonstrated to affect microbially-mediated ecosystem function in the oceans. In soils, limited water availability is unique habitat property that imposes unique constraints on microbial communities. Despite its potential to affect host growth patterns and virus-host contact in space and time, dynamic wetting processes have yet to be mechanistically explored in the field of soil viral ecology. To address this key knowledge gap, an extended incubation study was conducted where we tested the broad hypotheses that i) free viral abundance would be negatively impacted by soil drought and ii) rewetting of dry soil would be associated with a burst of microbial activity and lytic production of viral particles. Multifactorial treatments were applied to test effects of induced viral lysis, drought length, and soil rewetting on free viral abundance, dissolved C and N availability, and microbial activity (respiration, extracellular enzyme activities, and cell abundance). Using this approach, we present empirical evidence that soil drying beyond 20% water by weight is associated with a significant decline of free viral abundance and microbial activity. Regardless of length of drought, rewetting pulses were associated with i) a 200 to 3000-fold burst of microbial respiration that was positively correlated with drought length and ii) increases in all enzyme activities and cell abundance. Within 24 h of rewetting, abundance of free viral particles increased 15 to 37-fold relative to non-rewetted soil; magnitude of increases were greater with induction of viral lysis and unaffected by drought length. These data suggest that soil drying functions as a control on free viral abundance and of an increase of lytic viral reproduction upon rewetting. The establishment of a link

between soil viral abundance and dynamic soil rewetting processes points towards potential sensitivity of soil virus-microbe interactions to climate change, while providing context for mechanistic understanding of soil-specific abiotic controls on microbial functional activities.

4.1 Introduction

Mixed microbial communities mediate key biogeochemical processes across the globe that directly affect the net accumulation of organic matter. While microbes across ecosystems are generally energy limited (Soong et al., 2020; Lever et al., 2015; Hoeler and Jørgensen, 2013), soils are especially harsh microbial habitats that feature low and/or fluctuating water availability. Microbial functions are dependent upon water as a metabolic resource, but also as a solvent and transport medium that governs soil dissolution, diffusion, and transport processes in space and time (Schimel, 2018). Pore connectivity and hydrologic conductivity increasingly declines with soil drying and imposes a limit on physical accessibility of microbe-enzyme-substrate systems (Manzoni and Katul, 2014; Moyano et al., 2013; Schimel et al., 2007). Under extreme dryness, microbial stress responses lead to physiological consequences that further constrain microbial activity (e.g., shifts in carbon (C) allocation patterns, dormancy, death) (Schimel, 2018; Schimel et al., 2007). Rewetting of dry soil is associated with a characteristic burst of C and nitrogen (N) mineralization (known as the Birch effect) most commonly observed as a large pulse of carbon dioxide (CO_2) production (Schimel, 2018; Birch, 1958). The source of substrate fueling this enhanced microbial activity upon rewetting has been attributed to increased availability of microbial biomass and

cytoplasmic constituents (e.g., osmolytes) due to microbial lysis (Kieft et al., 1987) as well as abiotic factors that increase organic matter (OM) availability such as aggregate slaking, release of dissolved organic matter (DOM) from fine pores, and through desorption from mineral surfaces (Navaro-García et al., 2012; Borken and Matzner, 2009; Xiang et al., 2008; Fierer and Schimel, 2003). Disentangling effects of the coupled stressors of drought and rewetting on soil biogeochemical processes remains an active area of research and have direct relevance to shifting global precipitation patterns associated with climate change.

Extensive study of aquatic microbial ecology highlights the role of viral infection in directly affecting the metabolic activity of aquatic microbial populations and communities while indirectly influencing ecosystem properties including substrate availability, nutrient turnover, and potentially the net stabilization of organic C (Weitz et al., 2015; Jiao et al., 2011; Suttle, 2005). The field of viral ecology broadly recognizes two contrasting viral reproductive strategies: lysogeny and lysis, where the former is considered a chronic, dormant infection that facilitates viral proliferation during host cell division without active production and release of viral particles (Weinbauer, 2004). Lysogenic infection is increasingly viewed as a mutualistic relationship because of beneficial traits conferred to the host (i.e., lysogenic conversion e.g., regulation of host gene expression, introduction of new or altered metabolic functions, superinfection immunity, horizontal gene transfer, etc.) (Zimmerman et al., 2020; Howard-Varona et al., 2017; Feiner et al., 2015; Obeng et al., 2015). Lysis can be induced from a state of lysogeny in response to a variety of poorly understood genetic and environmental cues

and stressors (Zimmerman et al., 2020; Howard-Varona et al., 2017; Casjens and Hendrix, 2015; Wommack and Colwell, 2000). Viral lysis is characterized by viral reprogramming of host cell metabolism towards production of viral progeny and enzymes that causes the host cell to burst or lyse (Zimmerman et al., 2020; Weinbauer, 2004). Released viral particles can infect susceptible members of metabolically active microbial community, while host cell components released to the dissolved OM (DOM) pool can be enzymatically degraded and utilized as substrate by newly growing microbes (termed the 'viral shunt') (Wommack et al., 2015; Weitz and Wilhelm, 2012; Suttle, 2005; Wilhelm and Suttle, 1999). Viral infection functionally shifts microbial metabolic activities, which can affect rates of key microbially-mediated biogeochemical reactions (e.g., carbon (C), nitrogen (N), and phosphorus (P) mineralization), but also potentially the biochemical composition of DOM and microbial biomass residues that serve as inputs to the soil organic matter (SOM) pool (Zimmerman et al., 2020; Bonetti et al., 2019; Wommack et al., 2015).

Soil water-virus relationships have been widely speculated but remain an understudied mechanism impacting soil microbial and viral ecology. Studies from the late twentieth century reported that key soil properties (i.e., pH, microbial activity, organic matter, soil type, clay mineralogy) affected the fate of radiolabeled model bacteriophages and pathogenic viruses (e.g., poliovirus, coxsachievirus, etc.) applied to sewage sludge and soils (Fuhs et al., 1985; Hurst et al., 1980; Yeager and O'Brien, 1979a; Burge and Enkiri, 1978). Notably, these early experiments also pointed towards the role of soil drying as a mechanism of viral particle inactivation (i.e., loss of infectivity) and physical

destruction (Zhao et al., 2000; Brashear and Ward, 1993; Sobsey et al., 1980; Yeager and O'Brien, 1979b). Study of native, autochthonous soil viral communities in the past two decades using enumeration and molecular sequencing approaches have provided further evidence supporting these early findings. Specifically, low viral abundances (from below detection up to 10^3-10^5 viral particles per g soil dry weight) have consistently been observed in hyperarid desert soils (Williamson et al., 2017; Zablocki et al., 2016; Williamson, 2011; Prestel et al., 2008; Fierer et al., 2007; Prigent et al., 2005). These trends have been supported by observations of an increase in viral abundance with increasing mean annual precipitation across a grassland precipitation gradient in China (Cao et al., 2022). Under controlled incubation, soil collected from a midwestern U. S. prairie had relatively lower transcriptional activity and a 20-fold increase in transcripts for lysogenic markers in air dried relative to saturated soil (Wu et al., 2021). Together, these lines of evidence suggest that dry soil functions as a constraint on lytic viral production and favors a lysogenic strategy. However, given that measured viral abundances represent the net balance between viral reproduction and decay processes, as well as physiochemical inputs and outputs, the complex (a)biotic controls underlying these dynamics (as well as influence on host communities) remain unclear. Closing this knowledge gap will require mechanistic investigation into the role of water availability in controlling virus-microbe interactions under equilibrium conditions (e.g., at a single water content across the full range from dry to saturated) but also dynamic drying-rewetting processes that occur with varying frequency and magnitude across spatiotemporal scales and soil types.

With this study, we sought to answer two broad questions: first, to assess how the abundance of free, extractable viral particles respond to rewetting of dry soil after varying length of drought, and second, how the response of viral abundance to drying-rewetting treatments interacts with multiple measures of microbial activity (respiration, cell/biomass production, extracellular enzyme activities) and dissolved organic C and N availability. A viral lysis pre-incubation treatment was included to manipulate viral abundances, microbial mortality, and substrate availability relative to non-induced control, shedding light on the potential for biochemical shifts resulting from viral lysis induction to have extended temporal effects on virus-host-DOM relationships. Based on our literature review and preliminary experimentation, it was hypothesized that measured viral abundances will decrease with soil air drying and increase within 24 h of rewetting air dry soil irrespective of drought length. Furthermore, we expected greater microbial response to drought and rewetting treatments and higher correlation among viral abundance and measures of microbial activity under conditions of enhanced lytic activity. Our overall aim with this work is to provide additional context for existing studies of soil viral ecology and future experimental exploration into soil-specific controls on virus-microbe-OM dynamics in terrestrial ecosystems.

4.2 Materials and Methods

Soil description and processing

Bulk surface soil (0-20 cm; A horizon) was collected in August 2019 from an upland forest site located at the East Tennessee Research and Education Center in Knoxville,

Tennessee U. S. A. Soils are classified as Fine, mixed, semiactive, thermic Typic Paleudults with a silt loam texture (10 % sand, 75-80 % silt, 10-15 % clay). Soils were formed in clayey residuum weathered from shale/interbedded sandstone and shale. Slope of the site was measured at 9% with southeast aspect of 160°. Soil pH (10 g soil: 20 mL) was 3.9 in water and 4.0 in 0.01 M calcium chloride. Loss on ignition (24 h at 400 °C) was measured on triplicate samples and calculated as 6.0 ± 0.1 % organic matter. Soil color was determined on moist soil as 10 YR 4/3. Water holding capacity (WHC) was estimated at 0.64 g water per g dry soil by saturating sieved soil (~10 cm^3) inside a filter funnel with deionized water and determining mass of water retained by the soil after drainage for 6 h.

Bulk soil was dried to optimal moisture conditions (15% gravimetric water content) over four days at 4 °C (Bach and Hofmockel, 2014). Soil was sieved (2 mm) and thoroughly mixed by hand then weighed (30.0 g) into an aluminum pan (6.35 cm diameter) with 12 1 mm holes punched in the bottom. Pans containing soil were carefully placed on top of a glass microfiber filter in the bottom of pint-sized glass incubation jars with lids equipped with rubber septa for headspace gas sampling.

Experimental design and pre-incubation induction treatment

This experiment was carried out in a fully factorial design including pre-incubation induction of viral lysis treatment followed by incubation with varying duration of drought before rewetting (Figure 4.1Figure 4.1; all Figures for Chapter 4 are available in Appendix C). At the start of pre-incubation, 40.0 mL sterile, 0.22 µm filtered milliQ (18.2 Ω) water ± 2.5 ppm Mitomycin C (MMC) was slowly pipetted along the inside of

the jar. Mitomycin C is an antibiotic widely demonstrated to induce viral lysis of infected microbial cells when applied at a non-lethal exposure level (Paul and Jiang, 2001; Otsuji et al., 1959). Dosage of Mitomycin C was adjusted after preliminary experimentation (unpublished data, A. Fine) and applied as pre-incubation treatment to manipulate viral abundance, host mortality, and substrate availability relative to non-induced control. An induction response was expected from a subset of MMC-inducible populations, rather than the whole microbial community (Levine, 1961).

Immediately following addition of ± MMC solution, jars were sealed, and a pre-incubation time zero (t0) measurement of headspace carbon dioxide (CO_2) was measured using an infrared gas analyzer (IRGA; LI-COR Biosciences, NE U. S. A.). Samples were incubated overnight (25 °C) to allow gradual uptake of solution via capillary rise through the holes of the pan, with the goal of minimizing destabilization of macroaggregate structure (Smith et al., 2017) while saturating soil pores with solution to maximize the induction response. After 24 h, a second CO_2 measurement was made for calculation of cumulative respiration (i.e., total CO_2 production) (24hRESP). Sample pans were removed from incubation jars and placed over a funnel to allow drainage of gravitational water for 2 h to approximate field capacity water content (i.e., approximately half of water holding capacity). After drainage of excess water, samples were weighed, subsampled for measurement of gravimetric water content, and returned to incubation jars. Lids were sealed immediately before collecting a second t0 headspace CO_2 measurement followed by incubation under moist but unsaturated conditions (± MMC)

for an additional five days (25 °C) (referred to as 'wet pre-incubation', lasting a total of seven days) (Figure 4.1).

At the end of the wet pre-incubation, five day cumulative respiration measurements were made (5dRESP) and destructive sampling was performed for viral and bacterial abundances, extracellular enzyme activities, and extractable organic C and inorganic N as described below. Remaining jars were opened, and samples were allowed to air dry for seven days (25 °C) (referred to as 'dry pre-incubation'). Respiration was not measured during dry pre-incubation to allow sample jars to stay open. The one week dry pre-incubation period was meant to completely air dry soil samples and is therefore not considered in calculations of drought length (i.e., when Weeksdry = 1, samples went through wet and dry pre-incubation totaling 14 days plus an additional 1, 2, 4, and 8 weeks of drought-not *drying*- conditions). The following occurred for each sampling event: i) soil was rewetted (or left dry) to 50% water holding capacity, ii) jars were sealed and background CO_2 was measured with an IRGA, iii) samples were incubated for 24 h, iv) CO_2 was measured after 24 h (RESP), and v) samples were destructively sampled for viral and bacterial abundances, extracellular enzyme activities, and extractable organic C and inorganic N.

Due to equipment malfunction mid-experiment, experimental incubations occurred at 25 °C conditions through Weeksdry = 2 and at 21 °C for Weeksdry = 4 and 8. It was determined during sample analysis that the seven days of dry pre-incubation was insufficient to completely air dry soils. Soils destructively sampled for Weeksdry = 1

were therefore wetter (24 % gravimetric water content) than soils for Weeksdry = 2, 4, and 8 (2 % gravimetric water content) at the time rewetting treatment was applied.

Laboratory analyses

Virus and bacteria extraction and enumeration

Sterile potassium phosphate buffer was added to incubated soil slurry to achieve a final concentration of 1% (pH 7.0). Buffered slurries were blended for one minute using a high speed commercial blender. Virus extract was obtained by centrifuging blended soil slurry at 10,000 x*g* (4 °C, 20 minutes) and filtering the supernatant using a Millex-GV 0.22 µm pore size syringe filter (EMD Millipore, MA U. S. A.) (Williamson et al., 2003). Bacterial cells were extracted from soil slurry using a 60% Nycodenz® density gradient (Accurate Chemical and Scientific Co., NY U. S. A.) (2 mL + 9 mL slurry) (Williamson et al., 2007). Bacterial extracts were diluted 20% with glycerol to decrease freezing stress. All extracts were immediately frozen in liquid nitrogen and stored at -80 °C until analysis.

Thawed virus and bacteria extracts were treated with DNase I enzyme (RNA-free; Fisher Bioreagents) for 20 minutes to remove free DNA (Williamson et al., 2003). Virus extracts were vacuum filtered through 0.02 µm pore size Whatman® Anodisc filters (Cytiva Life Sciences, Buckinghamshire, U. K.), retaining the fraction greater than 20 nm and defining viral particles as having diameter of 20-200 nm (Williamson et al., 20003; Patel et al., 2007). Bacteria extracts were vacuum filtered through 0.22 µm pore size Whatman® Nuclepore™ Track-Etched Polycarbonate Membrane filters (Cytiva Life Sciences, Buckinghamshire, U. K.). Virus and bacteria retained on their respective filters

were directly stained for 20 minutes in the dark using 500 µL of 2x SYBR™ Gold Nucleic Acid Gel Stain (Molecular Probes-Invitrogen, OR U. S. A.). Filters were mounted using anti-fade reagent (Patel et al., 2007).

Stained viruses and bacteria were counted using a Nikon Eclipse E600 Epifluorescence Microscope (EFM) with a fluorescein isothiocyanate excitation (467-498 nm) and emission (513-556 nm) filter set at 1000x magnification. Ten randomly selected fields of view were digitally photographed using a Retiga™ Ex-I CCD camera (Qimaging, BC Canada). After user image normalization, fluorescent particles were counted using IP Laboratory software (BD Biosciences, CA U. S. A.). The mean count from all ten fields was used to calculate abundance per g dry soil using equation (1) (Patel et al., 2007), where RSF is the microscope grid-reticle scaling factor (59,000 for this setup) and volume of extract filtered ranged from 0.15-0.30 mL. Virus-to-Bacteria Ratio (VBR) was calculated as mean viral abundance divided by mean bacterial abundance.

$$\boldsymbol{Abundance} = \frac{\boldsymbol{Mean\ count * RSF}}{\boldsymbol{Volume\ extract\ filtered\ (mL)}} * \frac{\boldsymbol{100\ mL\ extractant}}{\boldsymbol{35.0\ g * (1 - \frac{g\ water}{g\ soil})}} \qquad (1)$$

Dissolved Organic Carbon and Inorganic Nitrogen

Aliquots of soil slurry were filtered through glass microfiber filters 1.0 size (Whatman GF/B, 1.0 µm pores) and frozen at 4 °C until analysis. Extracts were adjusted to 1% potassium sulfate to facilitate clay flocculation. Dissolved OC was quantified by reacting extracts with a potassium persulfate reagent overnight (80 °C) in sealed glass vials equipped with rubber septa for headspace gas analysis using an Infrared Gas Analyzer (IRGA, LI820, LiCor Inc., Lincoln, NE U. S. A.) (Doyle et al., 2004). A series

of potassium hydrogen phthalate calibration standards was included for calculation of persulfate-oxidized DOC in samples. Soil extracts were carried through colorimetric assays to quantify concentrations of extractable nitrate (NO_3^-; Doane and Horwath, 2003) and ammonium (NH_4^+; Rhine et al., 1998) using a 96-well microplate reader (Synergy H1 Hybrid Reader, Biotek Inc., Winooski, VT U. S. A.).

Extracellular Enzyme Activities

Maximum potential activities for seven major C, N, and P hydrolytic enzymes were assayed using fluorometric methods (Burns et al., 2013; Bell et al., 2013). The following enzymes were assayed: α-glucosidase (AG), β-glucosidase (BG), β-D-cellubiosidase (CB), leucine aminopeptidase (LAP), N-acetyl-glucosaminidase (NAG), acid phosphatase (PHOS), and β-xylosidase (XYL) (Table 4.1; all tables for Chapter 4 are available in Appendix C). A subsample of incubated soil slurry was adjusted to 50 mM sodium acetate buffer (pH 5.0) for control of pH during incubation with enzyme substrates. Variability in soil matrix effects was accounted for with standard additions of fluorescent MUC (7-amino-4-methylcoumarin) and MUB (4-methylumbelliferone) made to each soil slurry. Soil slurries were incubated with standards and labeled substrates (200 µl of 200 µM solution) at 25 °C in the dark for 3 hours. Fluorescence (365 nm excitation, 450 nm emission) was measured using a microplate reader under optimal gain settings. Enzyme activity was calculated in nmol g dry $soil^{-1}$ h^{-1}, with higher activities indicating a greater amount of fluorescently labeled substrate degraded under ideal conditions of incubation.

Statistical analyses

Data were analyzed as a three-factorial completely randomized design using a mixed model Analysis of Variance (ANOVA) with drought length, MMC treatment, and rewetting treatment (including all interactions) as fixed effects (total n = 64 plus soil and no soil blanks). Least squares (LS) means were separated using Tukey's least significant difference test with statistical significance indicated at the 95% ($p < .05$) confidence level. All data were confirmed to meet ANOVA assumptions after AG, BG, LAP, NAG, PHOS, Bacteria, Virus, and VBR were log10 transformed and are reported in back-transformed format. All ANOVA calculations were performed using the GLIMMIX procedure in SAS v. 9.4 (SAS Institute, Inc., NC U. S. A.).

Calculation of pairwise correlation coefficients and Principal Components Analysis (PCA) were conducted using JMP® Pro v. 15.0.0 (SAS Institute, Inc., NC U. S. A.) to investigate multivariate relationships in the dataset. All variables that were log10 transformed to meet ANOVA assumptions were transformed prior to standardization for PCA (subtraction of the mean and division by the standard deviation).

4.3 Results

Pre-incubation induction treatment

Pre-incubation induction treatment (± MMC) was applied before the experiment to induce viral lysis, with data collected at the end of the wet pre-incubation (seven days exposure to MMC) representing an initial baseline before soil drying and rewetting treatments. One-way ANOVA of pre-incubation data revealed a lack of statistically

significant differences ($p < .05$) resulting from pre-induction treatment for all measured variables (Table 4.2). Relaxation of the confidence level indicates influence on NAG ($p = 0.1$; higher in control) and PHOS ($p = 0.16$, higher in control) activities, 24hResp ($p = 0.16$; higher in MMC), Bacteria ($p = 0.19$, higher in control), and Virus-to-Bacterium Ratio (VBR; $p = 0.21$; higher in MMC) (Table 4.2). Across all samples, mean DOC was 0.17 mg C g dry soil^{-1}, NO_3 was undetectable, and NH_4 ranged from 22.6-23.2 ± 0.7 µg NH_4-N g dry soil^{-1}. Cumulative respiration was similar between control and MMC treatments (0.1 ± 0.002 µg CO_2-C g dry soil^{-1} for 24hResp and 0.42 ± 0.006 µg CO_2-C g dry soil^{-1} for 5dResp. Mean bacterial abundance at the end of wet pre-incubation was calculated at 9.1 x 10^7 cells g dry soil^{-1} for control and 8.7 x 10^7 cells g dry soil^{-1} for MMC (both with 2 x 10^6 standard error). Abundance of free viruses was measured at 4.0 x 10^8 viral particles g dry soil^{-1} for control and 4.1 x 10^8 viral particles g dry soil^{-1} for MMC (both with 1.7 x 10^7 standard error). Calculated Virus-to-Bacterium Ratio (VBR) was 0.63 ± 0.02 for control and 0.68 ± 0.02 for MMC.

ANOVA results (main treatment effects)

Three-way interactions from the ANOVA were statistically significant ($p < .05$) for activities of AG, BG, and NAG, Respiration, Bacteria, and Virus (as well as CB, LAP, PHOS, and XYL at $p < .1$) (Tables 4.3, 4.4, 4.5, and 4.6). The prevalence of these three-way interactions points towards variability in response to both induction and wetting treatments that differed by drought length (Weeksdry). Taking these interactions into account, significant effects ($p < .05$) of all three main treatments were found across the

dataset. Relative to control, MMC induction treatment increased activities of AG, LAP, and PHOS, RESP, Bacteria, and Virus while decreasing NO_3 and NH_4. (Figures 4.2, 4.3, 4.4, and 4.5).

Rewetting was associated with an increase in all measured variables ($p < .0001$; $p = 0.0153$ for NO_3); drought length treatment had significant ($p < .0001$) effect on all variables with a lack of clear trends across the four drought length treatments. Relative to Weeksdry =1 and across rewetting and MMC treatments, the highest intensity drought (Weeksdry = 8) decreased LAP, PHOS, DOC, respiration, and NH_4 and increased AG, BG, CB, XYL, Bacteria, Virus, VBR, and NO_3 (NAG was unchanged). All measured variables had at least one significant ($p < .05$) two-way interaction, most commonly between Weeksdry and Rewet (Tables 4.3, 4.4, 4.5, and 4.6).

The largest magnitude of response to rewetting (Rewet divided by Dry) was observed for RESP and Virus when Weeksdry = 2, 4, and 8. At 2 weeks drought, wetting increased RESP by 200x and Virus by 37x (MMC) and 32x (control) relative to non-wetted samples. High intensity drought (4 and 8 weeks dry) was associated with more than a 3000 fold increase in 24 h CO_2 production (both MMC + control) and 15-to-30 fold increase in free viral abundance upon rewetting. Bacteria increased by 1-4x with rewetting across MMC and Weeksdry treatments (Figure 4.2).

Correlations and Principal Components Analysis

Calculated correlation coefficients (r) were significant ($p < .05$) for 67 of 94 pairs of variables (71 %) with an additional seven variable pairs showing significant correlation at

$p < .1$ (Table 4.7 and 4.8). Positive correlations were observed between all pairs of enzyme activities. Virus was correlated Bacteria ($r = 0.6$) and activities of BG ($r = 0.5$), CB ($r = 0.7$), NAG ($r = 0.6$), and XYL ($r = -0.6$). Bacteria was moderately correlated with post-wetting respiration (Resp) ($r = 0.7$), CB ($r = 0.6$), and XYL ($r = -0.6$). Virus-to-Bacteria Ratio (VBR) was more correlated with Virus ($r = 0.9$) than with Bacteria ($r = 0.3$), suggesting that changes in viral abundance largely drove shifts in VBR. DOC was positively correlated with LAP, PHOS, and RESP ($r = 0.6$) and NH_4 ($r = 0.54$). Nitrate had moderate negative correlation with Virus ($r = -0.4$), VBR and NAG ($r = -0.5$), and DOC ($r = -0.3$). Ammonium was positively correlated with activities of LAP and PHOS and RESP ($r = 0.5$).

Principal Components Analysis (PCA) indicated that variance in the overall dataset is adequately explained by three Principal Components (PCs) with eigenvalues greater than one (Jolliffe, 2002; Table 4.9). Distribution of loading scores showed influence of enzyme activities, Virus, and VBR (and secondarily Resp and Bacteria) for PC1 (eigenvalue = 6.4; 46.0%); LAP, DOC, and NH_4 for PC2 (eigenvalue = 2.7; 19.0%); and Respiration, Bacteria, and NO_3 for PC3 (eigenvalue = 1.6; 11.4%). These findings point towards the greater role of viral abundance and enzyme activities relative to other measured properties in controlling across-treatment variability. Together, the first three PCs explain a cumulative 76.5% of observed variance that was distributed predominantly in quadrants I and IV for all variables except NO_3 (Figure 4.6). High positive correlations across many variables, especially enzyme activities, is supported by the small angles formed between variable loading vector pairs. With representation of individual

observations in two-dimensional PC space, clustering of points is observed between Wet and Dry samples, with the later forming two clusters associated with Weeksdry = 1 and Weeksdry = 2, 4, and 8; observations did not cluster by MMC treatment (Figure 4.6).

4.4 Discussion

With this controlled incubation study, we present evidence that the abundance of free viruses in soils exhibits dynamic response to drying-rewetting of bulk soil. This finding has impact from the perspective of general knowledge of soil viral ecology while being directly applicable to understanding the effects of soil drying-rewetting on the biochemical character of DOM and microbial functional processes. Establishment of a relationship between lytic viral production and soil wetting points towards an unexplored role of viral lysis in the Birch effect as well as potential for sensitivity of virus-microbe interactions to changing precipitation patterns in terrestrial ecosystems. Ultimately, this knowledge is viewed as a key initial step towards the eventual incorporation of soil viruses into conceptual and computational models of biogeochemical processes in terrestrial ecosystems.

Methodological considerations

Viral particle enumeration using epifluorescence microscopy

Epifluorescence microscopy (EFM) has been a widely used direct counting method for bacterial cell and virus particle enumeration in water, sediment, and soil samples since the late 20th century. While gaining in utility, state-of-the-art metagenomic and viromic analyses remain subject to similar biases towards dsDNA, interference from non-

virus particles of microbial origin, and interactions with the soil matrix that affect extraction efficiency (Trubl et al., 2020; Wommack et al., 2015). The use of 'omics techniques can provide information of relative abundance that is dependent upon total number of nucleic acids sequenced; however, these approaches do not assess total abundance of cells or free viral particles as was the goal of this study (Alteio et al., 2021; Sommers et al., 2021; Trubl et al., 2020; Alrasheed et al., 2019; Gloor et al., 2017). Similar to analytical all methods, EFM has important limitations that were noted in this study. First, SYBR^{TM} dye preferentially binds to double stranded DNA (dsDNA) (Forterre et al., 2013; Holmfeldt et al., 2012). High abundances of single stranded DNA and RNA viruses have been observed in environmental samples (e.g., Hillary et al., 2022; Wu et al., 2021; Starr et al., 2019; Reavy et al., 2014), leading to potential underestimation of total viral abundance across samples (Kaletta et al., 2020; Trubl et al., 2020; Williamson et al., 2017; Wommack et al., 2015).

Second, potential interference in virus enumeration could arise from microbially-derived, non-viral particles including gene transfer agents and membrane vesicles (MV) (Forterre et al., 2013). The presence and predominance of these 'fake viruses' in natural environmental samples (especially soils) remain largely uninvestigated (Forterre et al., 2013). Third, viruses enumerated represent an *extractable* fraction dependent upon extraction efficiency that likely displays between and within bulk soil heterogeneity. Physical or chemical association with soil inorganic minerals and/or organic matter (including microbial cells) could decrease extraction efficiency and lead to underestimation of abundance although use of a neutral phosphate extraction buffer was

meant to minimize such interactions. While it is impossible to determine absolute abundance, data from sequential extractions suggest ~70% of total extractable viruses are extracted during a single extraction event (Williamson et al., 2013; Williamson et al., 2005). We note that biases and inefficiencies are also relevant for extraction of microbial cells (Lombard et al., 2011)). With a lack of data indicating otherwise, extraction efficiency is assumed to be constant across samples. Lastly, we have no way to determine whether enumerated viral particles are actively infective, as it is possible that only a proportion of counted viruses are activated. Finally, the equation used to calculate viral abundance from EFM readings has a minimum detection limit of 1.7×10^6 viral particles g dry soil^{-1}. Abundances lower than this value were not detectable due to method limitations.

Pre-incubation induction of viral lysis

We attribute the failure of the one-way ANOVA to recognize significant ($p < .05$) effects of MMC pre-incubation treatment for all measured variables to a few experimental factors. First, destructive sampling was done one week from the pre-incubation time zero when ± MMC solution was added. An additional sampling time point at 24 h may have better assessed efficacy of MMC treatment missed with the present sampling design. Second, our ability to capture microbial dynamics that operate at the microscale remains largely limited by analytic techniques that target macroscale processes. This is also likely to be the case for soil viruses that are smaller than bacterial cells and can therefore potentially access the finest of soil pore spaces. Finally, high background abundance of free viral particles could limit the ability to detect increases in

abundance with induction treatment. With short-term (< 24 h) induction assays, this issue has been addressed using the dilution approach in aquatic samples (Dell'Anno et al., 2009; Wilhelm et al., 2002; Jiang and Paul, 2008) by exposing virus-free cell soil extracts to MMC post-extraction (rather than application of induction treatment pre-extraction) (Williamson et al., 2007). Estimation of inducible fraction was outside of the scope of the current study, and detection of significant treatment effects of MMC during the experiment suggest that our goal of shifting biogeochemical dynamics during pre-incubation was successful.

Microbial activity and free viral abundance respond to soil drought

Depending on soil texture and structure, loss of hydrologic connectivity and solute diffusivity in the soil pore network occurs when soil water potential drops to -0.1 to -1 MPa (more negative for finer textured soil) (Manzoni and Katul, 2014). Under these conditions, microbial activity can persist via physiological shifts away from resource acquisition and growth yield strategies and towards expression of stress tolerance traits (e.g., productive of osmolytes, secretion of extracellular polymeric substances (EPS), spore formation, dormancy) (Malik and Bouskill, 2022; Malik et al., 2020; Schimel, 2018; Schimel et al., 2007). The ability of microbes to invoke drought adaptations is an evolved life history trait that varies within members of the microbial community but also across microbial communities due to biogeographic differences in drought legacy as an evolutionary pressure (Müller and Bahn, 2022; Wang and Allison, 2021; Schimel, 2018). Across soil types, microbial activity ceases at the water stress threshold (-15 MPa) which represents dryness so extreme that adaptive strategies are unable to overcome the

physiological stress (Manzoni and Katul, 2014). The high depression of respiration rates under extreme dryness indicates limited microbial activity but we are unable to distinguish between effects of physiological stress versus resource inaccessibility.

Consistent with our findings, extended soil drought is generally associated with an accumulation of DOC and decreased microbial activity (Kaiser et al., 2015). We did not observe clear trends in influence of drought length on measured variables, possibly reflecting the lower incubation temperature at high intensity of drought (Weeksdry = 1 and 2 at 25 °C and Weeksdry = 4 and 8 incubated at 21 °C). Increased DOC with drying has been attributed to the activity of extracellular enzymes, which persists under dry conditions even when microbial activity is constrained (Malik and Bouskill, 2022; Blankinship et al., 2014). Active production of extracellular enzymes is not viewed as successful strategy under drought conditions due to the large energy investment required and the inaccessibility of substrates to non-motile microbial cells (Schimel, 2018; Burns et al., 2013). Interestingly, in this incubation an increase in activities of extracellular enzymes (except CB and XYL that degrade cellulose and hemicellulose, respectively) was observed in dry soil with increasing length of drought. These findings are supported by some observations (Yan et al., 2022; Bouskill et al., 2016; Alster et al., 2013), although reports of decreased enzyme activities under drought are more common (Gao et al., 2021; Acosta-Martinez et al., 2014; Burns et al., 2013; Steinweg et al., 2012; Sardans and Peñuelas, 2005). These inconsistencies (and results from this study) could be attributed to a variety of factors associated with drought conditions including decreased enzyme efficiencies, slower enzyme turnover, and mobilization of mineral-associated or

physically occluded enzymes (Alster et al., 2013; Burns et al., 2013; Schimel and Schaeffer, 2012). Finally, the drought length treatments were chosen because these are common conditions encountered in east Tennessee; however, the native microbial community may be somewhat adapted to these conditions and able to invest in resource acquisition strategies at low levels of water availability. Our data suggests limited lytic viral particle production under dry conditions, but also little influence of MMC induction treatment on microbial activity under dry conditions or upon rewetting suggesting quick utilization of lysis products or potential stabilization with the soil matrix.

Data from this study supports our hypothesis that soil viral abundance is negatively affected by extreme soil drying. The pre-incubation was deliberately designed to maintain soil water content above 15 % before experimental drying treatments, allowing us to establish baseline conditions before soil was air dried. Although it was intended for soil to fully air dry for all drought length treatments (1, 2, 4, and 8 weeks), the incomplete drying at 1 week (without the sharp drop in viral abundances observed at 2, 4, and 8 weeks dry) suggests that these effects were observed as soil dried from 24 % to 2 % (air dry) gravimetric water content. This is supported by observations of raw sludge where viral infectivity was gradually lost (i.e., viral inactivation increased) as water content decreased to ~20 % then rapidly declined with additional water loss resulting from irreversible particle disintegration at highly negative soil water potential (Brashear and Ward, 1983; Ward and Ashley, 1977). Presumably, physical disintegration would act as a non-evolutionary selective force that functionally resets the total abundance and infectivity of the viral community. With a lack of ability to actively adapt to drought

conditions like their microbial hosts, we expect that limitations on physical accessibility of virus-host systems would occur at water potentials where low hydrologic connectivity decreases diffusion rates (-0.1 to -1 MPa). The water potential corresponding to viral particle activation would vary across soil types and would likely occur before drying to the water stress threshold (-15 MPa) where microbial activity stops.

Viral lysis and the Birch effect

The burst of microbial activity upon soil rewetting is perhaps the most widely recognized yet unexplained phenomena characteristic of soils. Rewetting of dry soil functions as a hot moment of increased microbial activity that has a disproportional impact on ecosystem processes despite its transient nature (typically days) (Borken and Matzner, 2009). Hot moments were conceptualized for understanding of riparian zone ecosystems where the frequency and intensity of precipitation events affect hydrologic connectivity among physically isolated patches at the landscape scale (Bernhardt et al., 2017; McClain et al., 2003). Similar dynamics at present at the scale of soil pores where rewetting alleviates multiple constraints on microbial activity, functioning as an activated control point where conditions are optimized for growth yield and resource acquisition (Malik and Bouskill, 2022; Bernhardt et al., 2017). The hot moment associated with rewetting is transient in nature (hours-to-days) with spatial influence (i.e., the hot spot) varying with extent and intensity of rewetting with a soil profile.

In this study, free viral particle abundance measured within 24 h of rewetting (~10^8) was lower than during pre-incubation (before soil was dried past 15 % gravimetric water content) and falls on the low range of values (reaching ~10^9 viral particles g dry soil^{-1})

reported across all but the most extreme soils. Turnover of viral particles on the order of hours-to-days, as suggested by literature from aquatic ecosystems (Bongiorni et al., 2005; Noble and Fuhrman, 1997; Suttle and Chen, 1992), that favors net production over destruction processes are expected to further increase free viral abundances over time. Our data suggests that soil drought imposes a limit on virus-host interactions and lysis while also functioning as a control on free viral abundance via viral particle disintegration with drying.

We hypothesize that the burst of microbial growth upon rewetting induces a shift of an integrated virus towards a productive lytic strategy. After a delay to allow for intracellular production of viral material (i.e., latent period), lysis events would release additional substrate from dead microbial biomass that could fuel additional microbial growth. Viral lysis would therefore function to prolong the duration of hot moments by increasing microbial activity and potentially result in priming of native soil OM. Testing of this hypothesis would shed light on the role hydrologically fueled hot moments (which occur in spatially localized hot spots) as a natural inducer of viral lysis in soils. Increases in DOC observed upon rewetting, therefore, would reflect an increasing contribution from newly produced viruses but also viral protein and nucleic building blocks released upon viral particle destruction within fine pore spaces during extreme soil drying. Viral lysis-mediated microbial mortality could also obscure assessment of microbial physiological responses (including death) to coupled drought and rewetting stress depending on sampling frequency.

4.5 Conclusions

Climate change is predicted to fundamentally alter global precipitation and temperature regimes, expanding the global-scale distribution of drought-prone soils while also increasing the intensity and frequency of extreme weather events. These environmental changes control patterns in net primary productivity and organic matter accumulation across terrestrial ecosystems while also affecting water availability at the scale of microbial habitats. As intrinsically coupled processes, drought and rewetting impose unique constraints on microbial physiology and resource accessibility in bulk soil that have yet to be explored as mechanisms affecting viral proliferation and survival in soil.

Three key findings from this study provide valuable context for understanding of viral abundance and virus-microbe interactions in soil. First, the observed influence of soil drying on free viral abundance is a soil-specific mechanism affecting viral particle persistence across soil types that is supported by previous research using radiolabeled model pathogenic viruses. Second, under drought conditions there is a lack of new viral particle production corresponding to depressed microbial activity. With constrained microbial physiology and low resource accessibility, viral lysis is not likely a successful survival strategy for viruses that rely upon growth of their host but also spatiotemporal accessibility to initiate new infections. These findings shed light on low water availability as a mechanism controlling viral production in dessert and drought-prone soils. Finally, the observation that rewetting of dry soil is associated with a ~40-fold increase in viral abundance along with a spike in microbial activity supports the idea that lytic viral

production could play an unexplored role in the Birch effect. This new piece of information has potential to advance fundamental knowledge of the Birch effect, which despite decades of intensive research remains the most widely recognized yet still unexplained phenomenon characteristic of soils. Ultimately, these results propose a link between soil free viral abundance and infection processes with dynamic environmental conditions driven by water availability.

Study of soil microbes and viruses has always been methodologically challenging due to the intimate association of microbial cells and viral particles with soil inorganic and organic components. Consequently, initial progress in the fields of microbial and viral ecology were coupled and largely focused on aquatic ecosystems, with over a decade gap between the first published reports of high viral abundances in the ocean water column and soils. During this decade, data from extensive observational and experimental study focused on aquatic systems laid the foundation for development of a tentative ecological framework incorporating microbial activity and virus-microbe-organic matter feedbacks This framework has inspired continued mechanistic research both within and across aquatic systems, the findings of which have been largely assumed to also apply to soils. While working under this assumption has provided valuable direction to soil viral ecologists, incorporation of virus-microbe interactions into current models of soil organic matter cycling will require careful investigation into the role of soil-specific habitat properties in affecting viral persistence and infection processes relative to microbial functional activities. Such mechanistic knowledge has potential to fundamentally advance the fields of soil viral and microbial ecology while closing a key gap in

representation of native free viruses in cross-ecosystem models of global biogeochemical cycles.

References

Acosta-Martinez, V., Moore-Kucera, J., Cotton, J., Gardner, T., & Wester, D. (2014). Soil enzyme activities during the 2011 Texas record drought/heat wave and implications to biogeochemical cycling and organic matter dynamics. *Appl. Soil Ecol. 75*, 43-51.

Allison, S. D. (2005). Cheaters, diffusion and nutrients constrain decomposition by microbial enzymes in spatially structured environments. *Ecol. Lett.* 8, 626-635.

Alrasheed, H., Jin, R., & Weitz, J. S. (2019). Caution in inferring viral strategies from abundance correlations in marine metagenomes. *Nature Comm.* 10, 1-4.

Alster, C. J., German, D. P., Lu, Y., & Allison, S. D. (2013). Microbial enzymatic responses to drought and to nitrogen addition in a southern California grassland. *Soil Biol. Biochem.* 64, 68-79.

Alteio, L. V., et al. (2021). A critical perspective on interpreting amplicon sequen cing data in soil ecological research. *Soil Biol. Biochem.* 160, 108357.

Asplund, M., Kjartansdóttir, K. R., Mollerup, S., Vinner, L., Fridholm, H., Herrera, J. A., ... & Hansen, A. J. (2019). Contaminating viral sequences in high-throughput sequencing viromics: a linkage study of 700 sequencing libraries. *Clin. Microbiol. Infect.* 25, 1277-1285.

Bach, E. M. & Hofmockel, K. S. (2014). Soil aggregate isolation method affects measures of intra-aggregate extracellular enzyme activity. *Soil Biol. Biochem.* 69, 54-62.

Bell, C. W., Fricks, B. E., Rocca, J. D., Steinweg, J. M., McMahon, S. K., & Wallenstein, M. D. (2013). High-throughput Fluorometric Measurement of Potential Soil Extracellular Enzyme Activities. *J. Vis. Exp.* 81, e50961.

Bernhardt, E. S., Blaszczak, J. R., Ficken, C. D., Fork, M. L., Kaiser, K. E., & Seybold, E. C. (2017). Control points in ecosystems: moving beyond the hot spot hot moment concept. *Ecosystems* 20, 665-682.

Birch, H. (1958). The effect of soil drying on humus decomposition and nitrogen availability. *Plant Soil* 10: 9-31.

Blankinship, J. C., Becerra, C. A., Schaeffer, S. M., & Schimel, J. P. (2014). Separating cellular metabolism from exoenzyme activity in soil organic matter decomposition. *Soil Biol. Biochem.* 71, 68-75.

Bolan, N. S., Adriano, D. C., Kunhikrishnan, A., James, T., McDowell, R., & Senesi, N. (2011). Dissolved organic matter: biogeochemistry, dynamics, and environmental significance in soils. *Adv. Agron.* 110, 1-75.

Bonetti, G., Trevathan-Tackett, S. M., Carnell, P. E., & Macreadie, P. I. (2019). Implication of Viral Infections for Greenhouse Gas Dynamics in Freshwater Wetlands: Challenges and Perspectives. *Front. Microbiol.* 10, 1962.

Bongiorni, L., Magagnini, M., Armeni, M., Noble, R., & Danovaro, R. (2005). Viral production, decay rates, and life strategies along a trophic gradient in the North Adriatic Sea. *Appl. Environ. Microbiol.* 71, 6644-6650.

Borken, W., & Matzner, E. (2009). Reappraisal of drying and wetting effects on C and N mineralization and fluxes in soils. *Glob. Change Biol.* 15, 808-824.

Bouskill, N. J., et al. (2016). Belowground response to drought in a tropical forest soil. I. Changes in microbial functional potential and metabolism. *Front. Microbiol. 7*, 525.

Brashear, D. A., & Ward, R. L. (1983). Inactivation of indigenous viruses in raw sludge by air drying. *Appl. Env. Microbiol.* 45, 1943-1945.

Burge, W. D., & Enkiri, N. K. (1978). *Virus adsorption by five soils* (Vol. 7, No. 1, pp. 73-76). American Society of Agronomy, Crop Science Society of America, and Soil Science Society of America.

Burns, R. G., et al. (2013). Soil enzymes in a changing environment: current knowledge and future directions. *Soil Biol. Biochem.* 58, 216-234.

Cao, M. M., et al. (2022). Distribution Characteristics of Soil Viruses Under Different Precipitation Gradients on the Qinghai-Tibet Plateau. *Front. Microbiol.* 13, 848305-848305.

Casjens, S. R., & Hendrix, R. W. (2015). Bacteriophage lamda: early pioneer and still relevant. *Virol. J.* 479, 310.

Dell'Anno, A., Corinaldesi, C., Magagnini, M., & Danovaro, R. (2009). Determination of viral production in aquatic sediments using the dilution-based approach. *Nat. Protoc.* 4, 1013-1022.

Doane, T. A., & Horwath, W. R. (2003). Spectrophotometric Determination of Nitrate with a Single Reagent. *Anal. Lett.* 36, 2713-2722.

Doyle, A., Weintraub, M. N., & Schimel, J. P. (2004). Persulfate Digestion and Simultaneous Colorimetric Analysis of Carbon and Nitrogen in Soil Extracts. *Soil Sci. Soc. Am. J.* 68, 669-676.

Feiner, R., Argov, T., Rabinovich, L., Sigal, N., Borovok, I., & Herskovits, A. A. (2015). A new perspective on lysogeny: prophages as active regulatory switches of bacteria. *Nat. Rev. Microbiol.* 13, 641-650.

Fierer, N., et al. (2007). Metagenomic and small-subunit rRNA analyses reveal the genetic diversity of bacteria, archaea, fungi, and viruses in soil. *Appl. Environ. Microbiol.* 73, 7059-7066.

Fierer, N., & Schimel, J. P. (2003). A proposed mechanism for the pulse in carbon dioxide production commonly observed following the rapid rewetting of a dry soil. *Soil Sci. Soc. Amer*. J. 67, 798-805.

Forterre, P., Soler, N., Krupovic, M., Marguet, E., & Ackermann, H. W. (2013). Fake virus particles generated by fluorescence microscopy. *Trends Microbiol.* 21, 1-5.

Fuhs, G. W., Chen, M., Sturman, L. S., & Moore, R. S. (1985). Virus adsorption to mineral surfaces is reduced by microbial overgrowth and organic coatings. *Microb. Ecol.* 11, 25-39.

Gao, W., et al. (2021). Responses of soil extracellular enzyme activities and bacterial community composition to seasonal stages of drought in a semiarid grassland. *Geoderma* 401, 115327.

Geyer, K. M., Kyker-Snowman, E., Grandy, A. S., & Frey, S. D. (2016). Microbial carbon use efficiency: accounting for population, community, and ecosystem-scale controls over the fate of metabolized organic matter. *Biogeochem.* 127, 173-188.

Gloor, G. B., Macklaim, J. M., Pawlowsky-Glahn, V., & Egozcue, J. J. (2017). Microbiome datasets are compositional: and this is not optional. *Front. Microbiol.* 8, 2224.

Hansell, D. A., Carlson, C. A., Repeta, D. J., & Schlitzer, R. (2009). Dissolved organic matter in the ocean: A controversy stimulates new insights. *Oceanography*, *22*, 202-211.

Heinrichs, M. E., Heyerhoff, B., Arslan-Gatz, B. S., Seidel, M., Niggemann, J., & Engelen, B. (2022). Deciphering the Virus Signal Within the Marine Dissolved Organic Matter Pool. *Front. Microbiol.* 13, 863686

Heinrichs, M. E., Tebbe, D. A., Wemheuer, B., Niggemann, J., & Engelen, B. (2020). Impact of viral lysis on the composition of bacterial communities and dissolved organic matter in deep-sea sediments. *Viruses* 12, 922.

Hillary, L. S., Adriaenssens, E. M., Jones, D. L., & McDonald, J. E. (2022). RNA-viromics reveals diverse communities of soil RNA viruses with the potential to affect grassland ecosystems across multiple trophic levels. *ISME Comm.* 2, 1-10.

Hoehler, T. M., & Jørgensen, B. B. (2013). Microbial life under extreme energy limitation. *Nat. Rev. Microbiol.* 11, 83-94.

Holmfeldt, K., Odić, D., Sullivan, M. B., Middelboe, M., & Riemann, L. (2012). Cultivated single-stranded DNA phages that infect marine Bacteroidetes prove difficult to detect with DNA-binding stains. *Appl. Environ. Microbiol.* 78, 892-894.

Howard-Varona, C., Hargreaves, K. R., Abedon, S.T., & Sullivan, M.B. (2017). Lysogeny in nature: mechanisms, impact and ecology of temperate phages. *ISME J.* 11, 1511-1520.

Hurst, C. J., Gerba, C. P., & Cech, I. (1980). Effects of environmental variables and soil characteristics on virus survival in soil. *Appl. Env. Microbiol.* 40, 1067-1079.

Jiang, S. C., & Paul, J. H. (1998). Significance of lysogeny in the marine environment: studies with isolates and a model of lysogenic phage production. *Microb. Ecol.* 35, 235-243.

Jiao, N. et al. (2011). The microbial carbon pump and the oceanic recalcitrant dissolved organic matter pool. *Nat. Rev. Microbiol.* 9, 555.

Jolliffe, I. T. (2002). Principal component analysis. Springer, London U. K.

Jover, L. F., Effler, T. C., Buchan, A., Wilhelm, S. W., & Weitz, J. S. (2014). The elemental composition of virus particles: implications for marine biogeochemical cycles. *Nat. Rev. Microbiol.* 12, 519-528.

Kaiser, K., & Kalbitz, K. (2012). Cycling downwards–dissolved organic matter in soils. *Soil Biol. Biochem. 52*, 29-32.

Kaiser, M., Kleber, M., & Berhe, A. A. (2015). How air-drying and rewetting modify soil organic matter characteristics: an assessment to improve data interpretation and inference. Soil Biol. Biochem. 80, 324-340.

Kaletta, J., Pickl, C., Griebler, C., Klingl, A., Kurmayer, R., & Deng, L. (2020). A rigorous assessment and comparison of enumeration methods for environmental viruses. *Sci. Rep.* 10, 1-12.

Kieft, T. L., Soroker, E., & Firestone, M. K. (1987). Microbial biomass response to a rapid increase in water potential when dry soil is wetted. *Soil Biol. Biochem.* 19, 119-126.

Lever, M.A., et al. (2015). Life under extreme energy limitation: a synthesis of laboratory- and field-based investigations. *FEMS Microbiol. Rev.* 5, 688–728,

Levine, M. (1961). Effect of Mitomycin C on Interactions between Temperate Phages and Bacteria. *Virol. J.* 13, 493-499.

Malik, A. A., & Bouskill, N. J. (2022). Drought impacts on microbial trait distribution and feedback to soil carbon cycling. *Funct. Ecol.* 36, 1442-1456.

Malik, A. A., Martiny, J. B. H., Brodie, E. L., Martiny, A. C., Treseder, K. K., & Allison, S. D. (2020). Defining trait-based microbial strategies with consequences for soil carbon cycling under climate change. *ISME J.* 14, 1-19.

Manzoni, S., & Katul, G. (2014). Invariant soil water potential at zero microbial respiration explained by hydrological discontinuity in dry soils. *Geophys. Res. Lett.* 41, 7151-7158.

Manzoni, S., Moyano, F., Kätterer, T., & Schimel, J.P. (2016). Modeling coupled enzymatic and solute transport controls on decomposition in drying soils. *Soil Biol. Biochem.* 95, 275-287.

Manzoni, S., Schaeffer, S. M., Katul, G., Porporato, A., & Schimel, J. P. (2014). A theoretical analysis of microbial eco-physiological and diffusion limitations to carbon cycling in drying soils. *Soil Biol. Biochem.* 73, 69-83.

McClain, M. E., et al. (2003). Biogeochemical hot spots and hot moments at the interface of terrestrial and aquatic ecosystems. *Ecosystems*, 301-312.

Moyano, F. E., Manzoni, S., & Chenu, C. (2013). Responses of soil heterotrophic respiration to moisture availability: An exploration of processes and models. *Soil Biol. Biochem.* 59, 72-85.

Müller, L. M., & Bahn, M. (2022). Drought legacies and ecosystem responses to subsequent drought. *Global Change Biology* 28, 5086-5103.

Navarro-García, F., Casermeiro, M. Á., & Schimel, J. P. (2012). When structure means conservation: effect of aggregate structure in controlling microbial responses to rewetting events. *Soil Biol. Biochem.* 44, 1-8.

Noble, R. T., & Fuhrman, J. A. (1999). Breakdown and microbial uptake of marine viruses and other lysis products. *Aquat. Microb. Ecol. 20*, 1-11.

Obeng, N., Pratama, A. A., & van Elsas, J. D. (2015). The significant of Mutualistic Phages for Bacterial Ecology and Evolution. *Trends Microbiol.* 24, 440-449.

Otsuji, N., Sekiguchi, M., Iijima, T., & Takagi, Y. (1959). Induction of Phage Formation in the Lysogenic *Escherichia coli* K-12 by Mitomycin C. *Nature* 184, 1079-1080.

Patel, A., et al. (2007). Virus and prokaryote enumeration from planktonic aquatic environments by epifluorescence microscopy with SYBR Green I. *Nat. Protoc.* 2, 269-276.

Paul, J. H. & Jiang, S. C. Lysogeny and transduction. In: *Methods in Microbiology* (Paul, J., Ed.), vol. 30, 105-125. Academic Press, San Diego CA (2001).

Prestel, E., Salamitou, S., & DuBow, M. S. (2008). An examination of the bacteriophages and bacteria of the Namib desert. *J. Microbiol.* 46, 364-372.

Prigent, M., Leroy, M., Confalonieri, F., Dutertre, M., & DuBow, M. S. (2005). A diversity of bacteriophage forms and genomes can be isolated from the surface sands of the Sahara Desert. *Extremophiles* 9, 289–296

Reavy, B., et al. (2015). Distinct circular single-stranded DNA viruses exist in different soil types. *Appl. Environ. Microbiol.* 81, 3934-3945.

Rhine, E. D., Sims, G. K., Mulvaney, R. L., & Pratt, E. J. (1998). Improving the Berthelot Reaction for Determining Ammonium in Soil Extracts and Water. *Soil Sci. Soc. Amer. J.* 62, 473-480.

Sardans, J., & Peñuelas, J. (2005). Drought decreases soil enzyme activity in a Mediterranean *Quercus ilex* L. forest. *Soil Biol. Biochem.* 37, 455-461.

Schimel, J. P. (2018). Life in Dry Soils: Effects of Drought on Soil Microbial Communities and Processes. *Ann. Rev. Ecol. Evol. Syst.* 49, 409-432.

Schimel, J., Balser, T. C., & Wallenstein, M. (2007). Microbial stress-response physiology and its implications for ecosystem function. *Ecol.* 88, 1386-1394.

Schimel, J. P., & Schaeffer, S. M. (2012). Microbial control over carbon cycling in soil. *Front. Microbiol.* 3, 348.

Sinsabaugh, R. L., Manzoni, S., Moorhead, D. L., & Richter, A. (2013). Carbon use efficiency of microbial communities: stoichiometry, methodology and modelling. *Ecol. Lett.* 16, 930-939.

Smith, A. P., et al. (2017). Shifts in pore connectivity from precipitation versus groundwater rewetting increases soil carbon loss after drought. *Nat. Comm.* 8, 1-11.

Sobsey, M. D., Dean, C. H., Knuckles, M. E., & Wagner, R. A. (1980). Interactions and survival of enteric viruses in soil materials. *Appl. Environ. Microbiol.* 40, 92-101.

Sommers, P., Chatterjee, A., Varsani, A., & Trubl, G. (2021). Integrating viral metagenomics into an ecological framework. *Annu. Rev. Virol.* 8, 133-158.

Soong, J. L., et al. (2020). Microbial carbon limitation: The need for integrating microorganisms into our understanding of ecosystem carbon cycling. *Glob. Change Biol*. 26: 1953– 1961.

Starr, E. P., Nuccio, E. E., Pett-Ridge, J., Banfield, J. F., & Firestone, M. K. (2019). Metatranscriptomic reconstruction reveals RNA viruses with the potential to shape carbon cycling in soil. *Proc. Natl. Acad. Sci. U. S. A.* 116, 25900-25908.

Steinweg, J. M., Dukes, J. S., & Wallenstein, M. D. (2012). Modeling the effects of temperature and moisture on soil enzyme activity: linking laboratory assays to continuous field data. *Soil Biol. Biochem.* 55, 85-92.

Steward, G. F. et al. (2007). Microbial biomass and viral infections of heterotrophic prokaryotes in the sub-surface layer of the central Arctic Ocean. *Deep-Sea Res. I* 54, 1744–1757.

Srinivasiah, S., Bhavsar, J., Thapar, K., Liles, M., Schoenfeld, T. & Wommack, K., E. (2008). Phages across the biosphere: contrasts of viruses in soil and aquatic environments. *Res. Microbiol.* 159, 349-357.

Sutela, S., Poimala, A., & Vainio, E. J. (2019). Viruses of fungi and oomycetes in the soil environment. *FEMS Microbiol. Ecol. 95,* fiz119.

Suttle, C. A. (2005). Viruses in the sea. *Nature* 437, 356-361.

Suttle, C. A., & Chen, F. (1992). Mechanisms and rates of decay of marine viruses in seawater. *Appl. Env. Microbiol.* 58, 3721-3729.

Trubl, G., Hyman, P., Roux, S., & Abedon, S. T. (2020). Coming-of-age characterization of soil viruses: a user's guide to virus isolation, detection within metagenomes, and viromics. *Soil Syst.* 4, 23.

Wang, B., & Allison, S. D. (2021). Drought legacies mediated by trait trade-offs in soil microbiomes. *Ecosphere* 12, e03562.

Ward, R. L., & Ashely, C. S. (1977). Inactivation of enteric viruses in wastewater slude through dewatering by evaporation. *Appl. Environ. Microbiol.* 34, 564-570.

Weinbauer, M. G. (2004). Ecology of prokaryotic viruses. *FEMS Microbiol. Rev.* 28, 127-181.

Weitz, J. S., et al. (2015). A multitrophic model to quantify the effects of marine viruses on microbial food webs and ecosystem processes. *ISME J.* 9, 1352-1364.

Weitz, J. S., & Wilhelm, S. W. (2012). Ocean viruses and their effects on microbial communities and biogeochemical cycles. *F1000 Rep. Biol.* 4, 17.

Wilhelm, S. W., Brigden, S. M., & Suttle, C. A. (2002). A dilution technique for the direct measurement of viral production: a comparison in stratified and tidally mixed coastal waters. *Microb. Ecol.* 43, 168-173.

Wilhelm, S. W., & Suttle, C. A. (1999). Viruses and nutrient cycles in the sea. *Biosciences* 49, 781–788.

Williamson, K. E. (2011). Soil phage ecology: abundance, distribution, and interactions with bacterial hosts. In *Biocommunication in Soil Microorganisms* (pp. 113-136). Springer, Berlin, Heidelberg.

Williamson, K. E., Corzo, K. A., Drissi, C. L., Buckingham, J. M., Thompson, C. P., & Helton, R. R. (2013). Estimates of viral abundance in soils are strongly influenced by extraction and enumeration methods. *Biol. Fert. Soil* 49, 857-869.

Williamson, K. E., Fuhrmann, J. J., Wommack, K. E., & Radosevich, M. (2017). Viruses in soil ecosystems: an unknown quantity within an unexplored territory. *Annu. Rev. Virol*. *4*, 201-219.

Williamson, K. E., Radosevich, M., & Wommack, K. E. (2005). Abundance and diversity of viruses in six Delaware soils. *Appl. Environ. Microbiol.* 71, 3119-3125.

Williamson, K. E., Radosevich, M., Smith, D. W., & Wommack, K. E. (2007). Incidence of lysogeny within temperate and extreme soil environments. *Environ. Microbiol.* 9, 2563-2574.

Williamson, K. E., Wommack, K. E., & Radosevich, M. (2003). Sampling natural viral communities from soil for culture-independent analyses. *Appl. Environ. Microbiol.* 69, 6628-6633.

Wommack, K. E., & Colwell, R. R. (2000). Virioplankton: viruses in aquatic ecosystems. *Microbiol. Mol. Biol. Rev.* 64, 69-114.

Wommack, K.E., Nasko, D.J., Chopyk, J., & Sakowski, E.G. (2015). Counts and sequences, observations that continue to change our understanding of viruses in nature. *J. Microbiol.* 53, 181-192.

Wu, R., et al. (2021). Moisture modulates soil reservoirs of active DNA and RNA viruses. *Commun. Biol.* 4, 1-11.

Xiang, S. R., Doyle, A., Holden, P. A., & Schimel, J. P. (2008). Drying and rewetting effects on C and N mineralization and microbial activity in surface and subsurface California grassland soils. *Soil Biol. Biochem.* 40, 2281-2289.

Yan, Z., Li, Y., Wu, H., Zhang, K., Hao, Y., Wang, J., ... & Kang, X. (2020). Different responses of soil hydrolases and oxidases to extreme drought in an alpine peatland on the Qinghai-Tibet Plateau, China. *Eur. J. Soil Biol.* 99, 103195.

Yeager, J. G., & O'Brien, R. T. (1979a). Enterovirus inactivation in soil. *Appl. Env. Microbiol.* 38, 694-701.

Yeager, J. G., & O'Brien, R. T. (1979b). Structural changes associated with poliovirus inactivation in soil. *Appl. Env. Microbiol.* 38, 702-709.

Zablocki, O., Adriaenssens, E. M., & Cowan, D. (2016). Diversity and ecology of viruses in hyperarid desert soils. *Appl. Env. Microbiol.* 82, 770-777.

Zhao, B., Zhang, H., Zhang, J., & Jin, Y. (2008). Virus adsorption and inactivation in soil as influenced by autochthonous microorganisms and water content. *Soil Biol. Biochem.* 40, 649-659.

Zhao, Z., Gonsior, M., Schmitt-Kopplin, P. *et al.* Microbial transformation of virus-induced dissolved organic matter from picocyanobacteria: coupling of bacterial diversity and DOM chemodiversity. *ISME J.* 13, 2551–2565 (2019).

Zimmerman, A. E., et al. (2020). Metabolic and biogeochemical consequences of viral infection in aquatic ecosystems. *Nat. Rev. Microbiol.* 18, 21-34.

Appendix C

Table 4.1. List of extracellular hydrolytic enzyme activities assayed on aggregate fractions.

Table includes enzyme abbreviation, commission (EC) number, fluorescently labeled substrate used for the assay, and the broad type of organic compound each enzyme degrades. Fluorescent labels are 4-MUB (4-methylumbelliferyl) and 4-MUC (4-methylcoumarin). Broad degradation target for enzymes are as follows: sugars (AG, BG), cellulose (CB), protein (LAP), chitin/amino sugar polymer (NAG), organic phosphorous (PHOS), and hemicellulose (XYL).

Enzyme	EC	Substrate
β-Glucosidase (BG)	3.2.1.21	4-MUB-β-D-Glucopyranoside
β-D-Cellubiosidase (CB)	3.2.1.91	4-MUB-β-D-Cellobioside
β-Xylosidase (XYL)	3.2.1.37	4-MUB-β-D-Xylopyranoside
α-Glucosidase (AG)	3.2.1.20	4-MUB-α-D-Glucopyranoside
Leucine Aminopeptidase (LAP)	3.2.11.1	L-Leucine-MUC Hydrochloride
N-Acetyl-β-D-Glucosaminidase (NAG)	3.2.1.30	4-MUB-N-Acetyl-β-D-Glucosaminide
Acid Phosphatase (PHOS)	3.1.3.2	4-MUB Phosphate

Table 4.2. Results of one-way Analysis of Variance (ANOVA) on pre-incubation induction treatment with calculated means and standard errors (SE) for control (non-induced) and Mitomycin C (MMC) induced samples.

For all variables, numerator degrees of freedom = 1 and Den DF (denominator degrees of freedom) is indicated for the one-way ANOVA model. Induction treatment had insignificant effect on all variables the 95% confidence level ($p < .05$). Nitrate (NO_3) was not detectable in extracts collected during pre-incubation.

Variable	Den DF	F	*p*
24h Resp	62	1.98	0.16
5d Resp	62	1.4	0.24
Virus	6	0.08	0.79
Bacteria	6	2.15	0.19
VBR	6	2	0.21
DOC	6	0	0.95
NO_3	--	--	--
NH_4	6	0.27	0.62
AG	6	0.61	0.46
BG	6	0.59	0.47
CB	6	0.04	0.84
LAP	6	1.14	0.33
NAG	6	3.66	0.1
PHOS	6	2.55	0.16
XYL	6	0.97	0.36

Table 4.2 continued

Variable	Mean Control	SE	Mean MMC	SE
24h Resp	0.1	0.002	0.103	0.002
5d Resp	0.426	0.006	0.415	0.006
Virus	4.04E+08	1.72E+07	4.11E+08	1.75E+07
Bacteria	9.10E+07	2.03E+06	8.69E+07	1.94E+06
VBR	0.626	0.024	0.675	0.024
DOC	29.37	0.71	29.31	0.71
NO_3	--	--	--	--
NH_4	22.63	0.72	23.16	0.72
AG	0.8	0.06	0.87	0.06
BG	2.13	0.01	2.15	0.01
CB	60.79	1.11	61.11	1.11
LAP	1.03	0.01	1.01	0.01
NAG	1.93	0.04	1.82	0.04
PHOS	2.43	0.01	2.4	0.01
XYL	39.99	3.2	44.45	3.2

Table 4.3. Results of three-way Analysis of Variance (ANOVA) for viral abundance (Virus), bacterial cell abundance (Bacteria), and Virus-Bacteria Ratio (VBR).

Main treatment effects included in the ANOVA model were Mitomycin C (MMC) induction treatment (± MMC), drought length (WeeksDry), and rewetting (Rewet) plus all two- and three-way interactions. For all variables, denominator degrees of freedom = 48 and numerator degrees of freedom (Num DF) is indicated. Statistically significant effects ($p < .05$) are indicated by bold text with an "*" used for $p < .0001$.

Source	**Num DF**	Virus		Bacteria		VBR	
		F	***p***	**F**	***p***	**F**	***p***
MMC	1	6.3	**0.015**	17.3	**0.0001**	2.1	0.152
WeeksDry	3	1052.2	*	85.1	*	131.8	*
Rewet	1	5222.5	*	595.6	*	432.2	*
WeeksDry*MMC	3	0.9	0.458	8.8	*	3.0	**0.041**
Rewet*MMC	1	5.3	**0.025**	6.0	**0.018**	0.0	0.889
WeeksDry*Rewet	3	1268.0	*	24.0	*	221.1	*
WeeksDry*Rewet*MMC	3	2.8	**0.0472**	7.4	**0.0004**	1.2	0.3

Table 4.4. Results of three-way Analysis of Variance (ANOVA) for respiration (Resp), dissolved organic carbon (DOC), and ammonium (NH_4).

Main treatment effects included in the ANOVA model were Mitomycin C (MMC) induction treatment (± MMC), drought length (WeeksDry), and rewetting (Rewet) plus all two- and three-way interactions. For all variables, denominator degrees of freedom = 48 and numerator degrees of freedom (Num DF) is indicated. Statistically significant effects ($p < .05$) are indicated by bold text with an "*" used for $p < .0001$.

Source	Num DF	Resp		DOC		NH_4	
		F	***p***	**F**	***p***	**F**	***p***
MMC	1	4.4	**0.041**	0.6	0.456	301.0	*
WeeksDry	3	15.2	*	158.6	*	186.0	*
Rewet	1	14196.0	*	315.9	*	615.0	*
WeeksDry*MMC	3	5.8	**0.002**	1.6	0.215	35.7	*
Rewet*MMC	1	4.0	0.051	2.7	0.11	13.8	**0.001**
WeeksDry*Rewet	3	67.0	*	68.0	*	171.5	*
WeeksDry*Rewet*MMC	3	3.2	**0.033**	1.1	0.358	49.0	*

Table 4.5. Results of the three-way Analysis of Variance (ANOVA) for C-degrading extracellular enzymes (AG, BG, CB, and XYL).

Main treatment effects included in the ANOVA model were Mitomycin C (MMC) induction treatment (± MMC), drought length (WeeksDry), and rewetting (Rewet) plus all two- and three-way interactions. For all variables, denominator degrees of freedom = 48 and numerator degrees of freedom (Num DF) is indicated. Statistically significant effects ($p < .05$) are indicated by bold text with an "*" used for $p < .0001$.

Source	**Num DF**	AG		BG		CB	
		F	***p***	**F**	***p***	**F**	***p***
MMC	1	81.3	*****	0.2	0.631	0	0.970
WeeksDry	3	15.6	*****	18.9	*****	53.8	*****
Rewet	1	64.8	*****	75.2	*****	27.9	*****
WeeksDry*MMC	3	14.7	*****	0.4	0.776	1.1	0.349
Rewet*MMC	1	51.3	*****	12.7	**0.001**	0.3	0.600
WeeksDry*Rewet	3	27.3	*****	19.4	*****	4.9	**0.005**
WeeksDry*Rewet*MMC	3	18.7	*****	5.8	**0.002**	2.3	0.094

Abbreviations: α-glucosidase (AG), β-glucosidase (BG), β-D-cellubiosidase (CB), and β-xylosidase (XYL).

Table 4.5 continued

Source	Num DF	XYL F	XYL *p*
MMC	1	1.4	0.245
WeeksDry	3	11.2	*
Rewet	1	56.7	*
WeeksDry*MMC	3	2.9	**0.046**
Rewet*MMC	1	5.8	**0.020**
WeeksDry*Rewet	3	7.6	**0.000**
WeeksDry*Rewet*MMC	3	2.4	0.081

Table 4.6. Results of the three-way Analysis of Variance (ANOVA) for N- and P-degrading enzymes (LAP, NAG, and PHOS).

Main treatment effects included in the ANOVA model were Mitomycin C (MMC) induction treatment (± MMC), drought length (WeeksDry), and rewetting (Rewet) plus all two- and three-way interactions. For all variables, denominator degrees of freedom = 48 and numerator degrees of freedom (Num DF) is indicated. Statistically significant effects ($p < .05$) are indicated by bold text with an "*" used for $p < .0001$.

Source	**Num DF**	LAP		NAG		PHOS	
		F	***p***	**F**	***p***	**F**	***p***
MMC	1	6.8	**0.012**	2.7	0.105	4.5	**0.039**
WeeksDry	3	45.8	*	21.7	*	23.6	*
Rewet	1	140.8	*	12.6	**0.001**	95.9	*
WeeksDry*MMC	3	6.1	**0.001**	0.4	0.783	3.6	**0.020**
Rewet*MMC	1	5.8	**0.020**	11.4	**0.001**	3.4	0.072
WeeksDry*Rewet	3	12.5	*	17.1	*	18.7	*
WeeksDry*Rewet*MMC	3	2.5	0.071	3	**0.039**	2.3	0.089

Abbreviations: leucine aminopeptidase (LAP), N-scetyl- β-glucosaminidase (NAG), and acid phosphatase (PHOS).

Table 4.7. Correlation coefficients (*r*) calculated for all pairs of variables.

All probabilities provided in Table 4.8. Pre-incubation data was excluded from correlation analysis ($n = 64$).

	AG	BG	CB	LAP	NAG	PHOS	XYL
BG	0.56						
CB	0.42	0.65					
LAP	0.50	0.70	NS				
NAG	0.38	0.76	0.49	0.55			
PHOS	0.47	0.86	0.27	0.90	0.69		
XYL	0.51	0.82	0.70	0.47	0.60	0.59	
Resp	0.40	0.48	0.33	0.51	0.26	0.52	0.57
DOC	0.44	0.38	NS	0.63	0.33	0.59	NS
NO_3	NS	NS	NS	NS	-0.51	NS	NS
NH_4	NS	0.32	NS	0.55	NS	0.50	NS
Bacteria	0.28	0.43	0.64	NS	0.30	0.27	0.61
VBR	NS	0.56	0.64	NS	0.67	0.33	0.48
Virus	NS	0.55	0.74	NS	0.64	0.30	0.57

Abbreviations: α-glucosidase (AG), ammonium (NH_4), bacterial cell abundance (Bacteria), β-glucosidase (BG), β-D-cellubiosidase (CB), dissolved organic carbon (DOC), leucine aminopeptidase (LAP), N-acetyl-β-glucosaminidase (NAG), nitrate (NO_3), acid phosphatase (PHOS), respiration (Resp), viral abundance (Virus), Virus-Bacteria Ratio (VBR), and β-xylosidase (XYL).

Table 4.7 continued

	Resp	DOC	NO_3	NH_4	Bacteria	VBR
BG						
CB						
LAP						
NAG						
PHOS						
XYL						
Resp						
DOC	0.56					
NO_3	NS	-0.32				
NH_4	0.46	0.54	NS			
Bacteria	0.75	NS	NS	NS		
VBR	NS	NS	-0.47	NS	0.35	
Virus	0.32	NS	-0.44	NS	0.65	0.89

Table 4.8. Probability (*p*) values for correlation coefficients (*r*).

Statistically significant *p*-values (< 0.05) are indicated by bold text with an '* for $p < .0001$.

	AG	BG	CB	LAP	NAG	PHOS	XYL
BG	*						
CB	**0.0005**	*					
LAP	*	*	0.7503				
NAG	**0.0021**	*	*	*			
PHOS	**0.0001**	*	**0.0337**	*	*		
XYL	*	*	*	*	*	*	
Resp	**0.0011**	*	**0.0081**	*	**0.0367**	*	*
DOC	**0.0003**	**0.0021**	0.8125	*	**0.0081**	*	0.1131
NO_3	0.0653	0.0678	0.699	0.0906	*	0.1005	0.0895
NH_4	0.0904	**0.009**	0.894	*	0.2179	*	0.3372
Bacteria	**0.0247**	**0.0004**	*	0.3265	**0.015**	**0.0319**	*
VBR	0.0598	*	*	0.3843	*	**0.0083**	*
Virus	**0.0332**	*	*	0.5592	*	**0.016**	*

Abbreviations: α-glucosidase (AG), ammonium (NH_4), bacterial cell abundance (Bacteria), β-glucosidase (BG), β-D-cellubiosidase (CB), dissolved organic carbon (DOC), leucine aminopeptidase (LAP), N-acetyl-β-glucosaminidase (NAG), nitrate (NO_3), acid phosphatase (PHOS), respiration (Resp), viral abundance (Virus), Virus-Bacteria Ratio (VBR), and β-xylosidase (XYL).

Table 4.8 continued

	Resp	DOC	NO_3	NH_4	Bacteria	VBR
BG						
CB						
LAP						
NAG						
PHOS						
XYL						
Resp						
DOC	*					
NO_3	0.9414	**0.0104**				
NH_4	**0.0001**	*	0.2273			
Bacteria	*	0.1493	0.6937	0.861		
VBR	0.2636	0.1098	*	0.3625	**0.0042**	
Virus	**0.0097**	0.1764	**0.0002**	0.1517	*	*

Table 4.9. Eigenanalysis and loading scores for Principal Components (PCs) 1, 2, and 3 generated from the Principal Components Analysis (PCA) (*n* = 64).

Additional PCs had eigenvalues less than 1. Percent is percent contribution of each individual PC and Cum Percent is the cumulative percent contribution to total explained variance.

EIGENANALYSIS	**PC1**	**PC2**	**PC3**
Eigenvalue	7.49	2.15	1.50
Percent	53.5	15.3	10.7
Cum Percent	53.5	68.8	79.6
LOADING SCORES	**PC1**	**PC2**	**PC3**
AG	**0.699**	-0.073	-0.260
BG	**0.912**	-0.080	0.008
CB	0.652	**-0.615**	0.166
LAP	0.707	**0.622**	-0.064
NAG	**0.758**	-0.014	-0.429
PHOS	**0.852**	0.341	-0.052
XYL	**0.808**	-0.287	0.065
Resp	**0.741**	0.183	0.463
DOC	0.579	**0.616**	-0.073
NO_3	-0.345	0.001	**0.835**
NH_4	0.365	**0.715**	0.346
Bacteria	**0.753**	-0.335	0.400
VBR	**0.880**	-0.231	-0.100
Virus	**0.900**	-0.288	0.083

Abbreviations: α-glucosidase (AG), ammonium (NH_4), bacterial cell abundance (Bacteria), β-glucosidase (BG), β-D-cellubiosidase (CB), dissolved organic carbon (DOC), leucine aminopeptidase (LAP), N-acetyl-β-glucosaminidase (NAG), nitrate (NO_3), acid phosphatase (PHOS), respiration (Resp), viral abundance (Virus), Virus-Bacteria Ratio (VBR), and β-xylosidase (XYL).

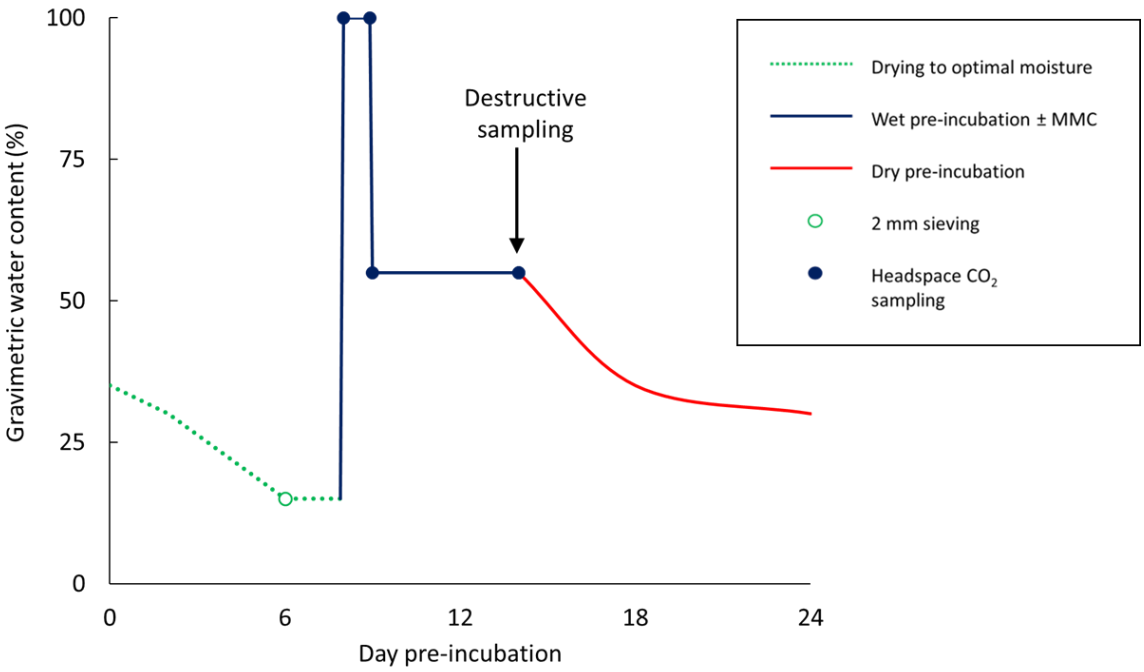

Figure 4.1. Soil processing and schedule of pre-incubation treatment showing how gravimetric water content (GWC) was manipulated ± Mitomycin C (MMC).

Soil was collected from the field and dried to optimal moisture for sieving (15% GWC) over a period of six days at 4 °C. Sieved soil was saturated with MMC overnight, drained to field capacity, then incubated under moist conditions for one week (wet pre-incubation). After one week, jars were opened to begin the drying process (dry pre-incubation).

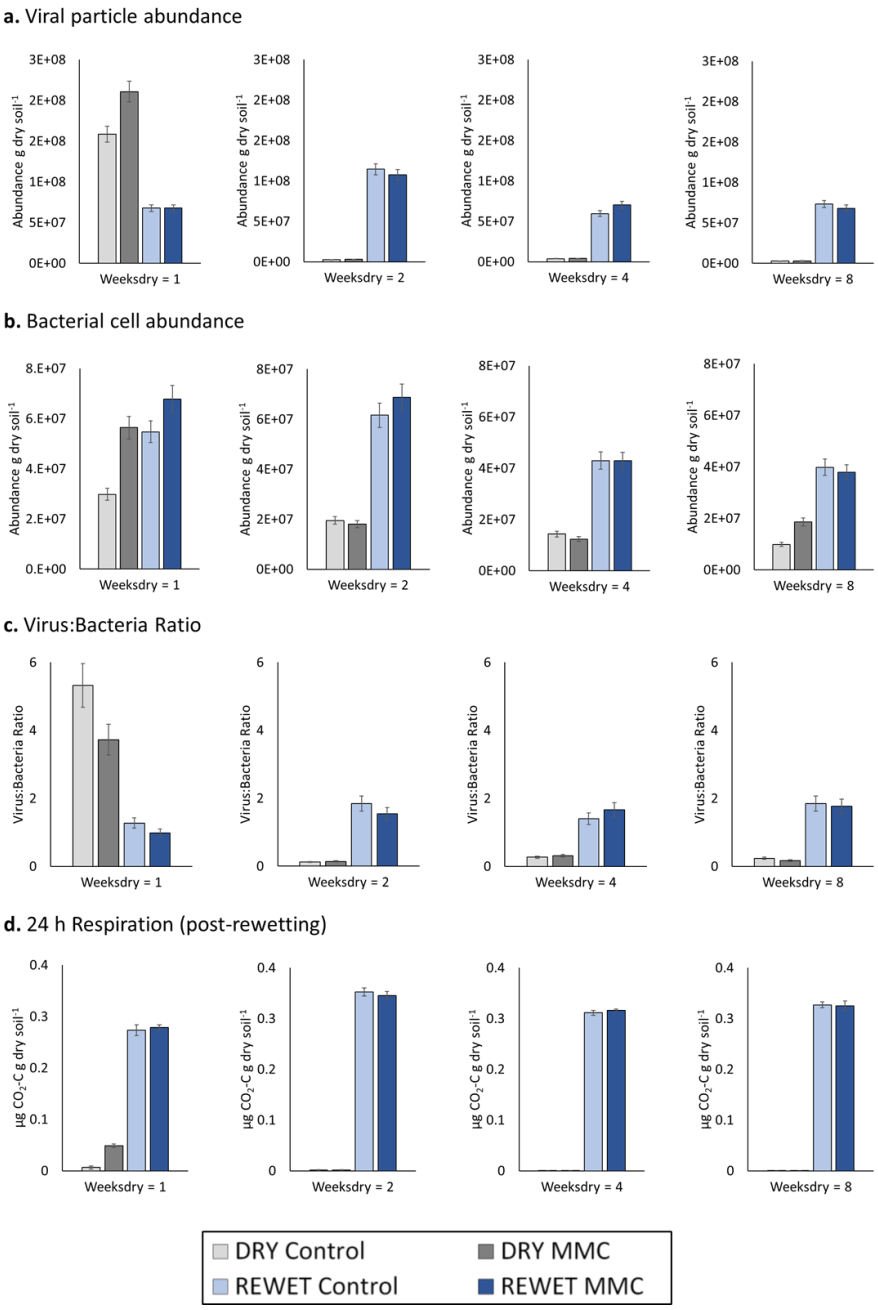

Figure 4.2. Mean Viral particle abundance (a), Bacterial cell abundance (b), Virus-Bacteria Ratio (c), and 24 h Respiration (i.e., CO_2 production) measured post-rewetting of dry soil (d).

Panels are separated by drought length treatment (Weeksdry), with Dry samples in gray and Rewetted samples in blue; darker colors indicate application of pre-incubation induction treatment with Mitomycin C (MMC). Error bars represent standard error of $n = 4$ replications per treatment combination.

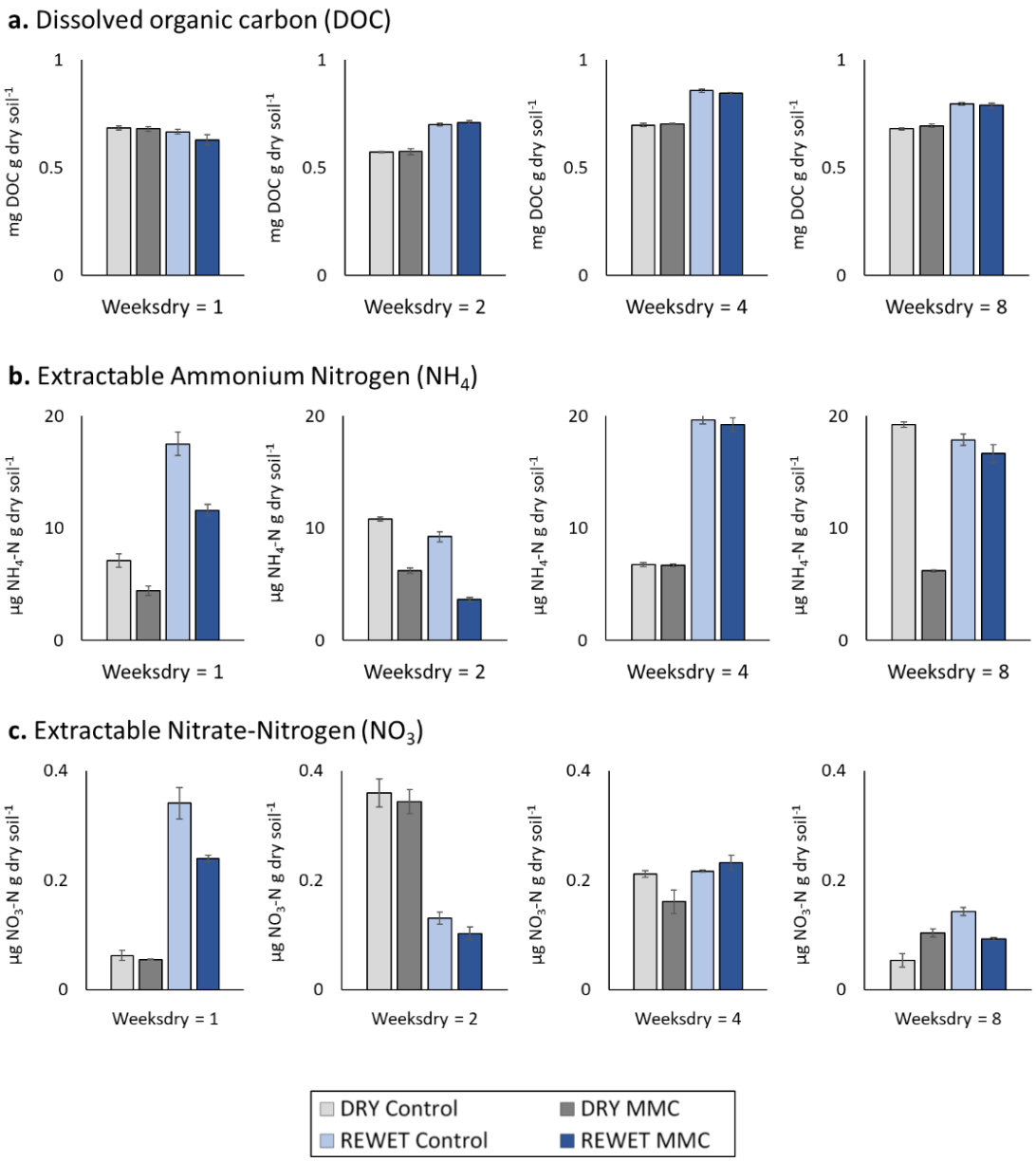

Figure 4.3. Mean concentrations of extractable dissolved organic carbon (DOC) (a), ammonium (b), and nitrate (c) by Mitomycin C induction treatment (MMC), drought length (Weeksdry), and rewetting (Rewet).

Panels are separated by drought length treatment (Weeksdry), with Dry samples in gray and Rewetted samples in blue; darker colors indicate application of pre-incubation MMC induction treatment. Error bars represent standard error of $n = 4$ replications per treatment combination.

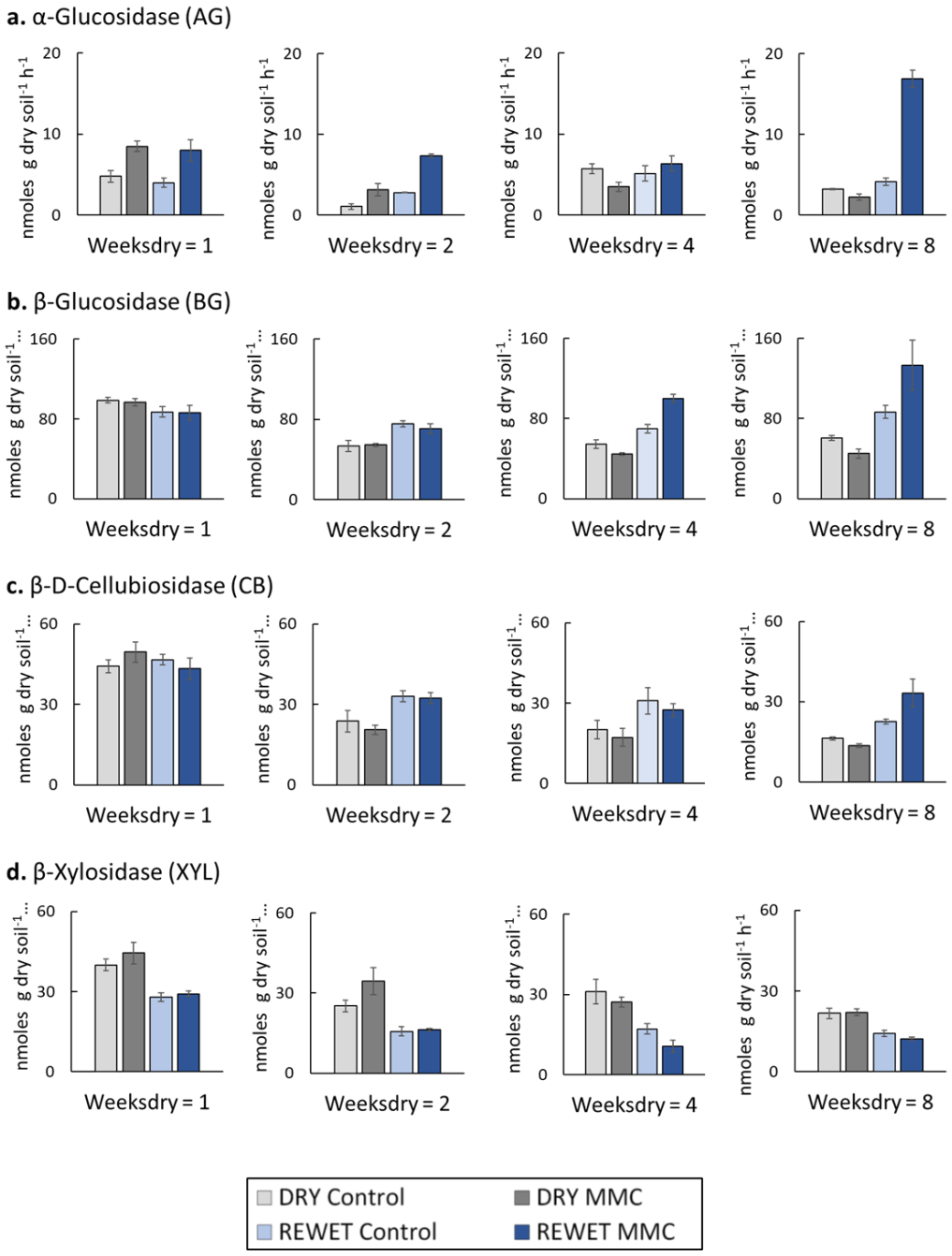

Figure 4.4. Mean activities of C-degrading extracellular enzymes (AG (a), BG (b), CB (c), and XYL (d) by Mitomycin C induction treatment (MMC), drought length (Weeksdry), and rewetting (Rewet).

Panels are separated by drought length treatment (Weeksdry), with Dry samples in gray and Rewetted samples in blue; darker colors indicate application of pre-incubation MMC induction treatment. Error bars represent standard error of $n = 4$ replications per treatment combination.

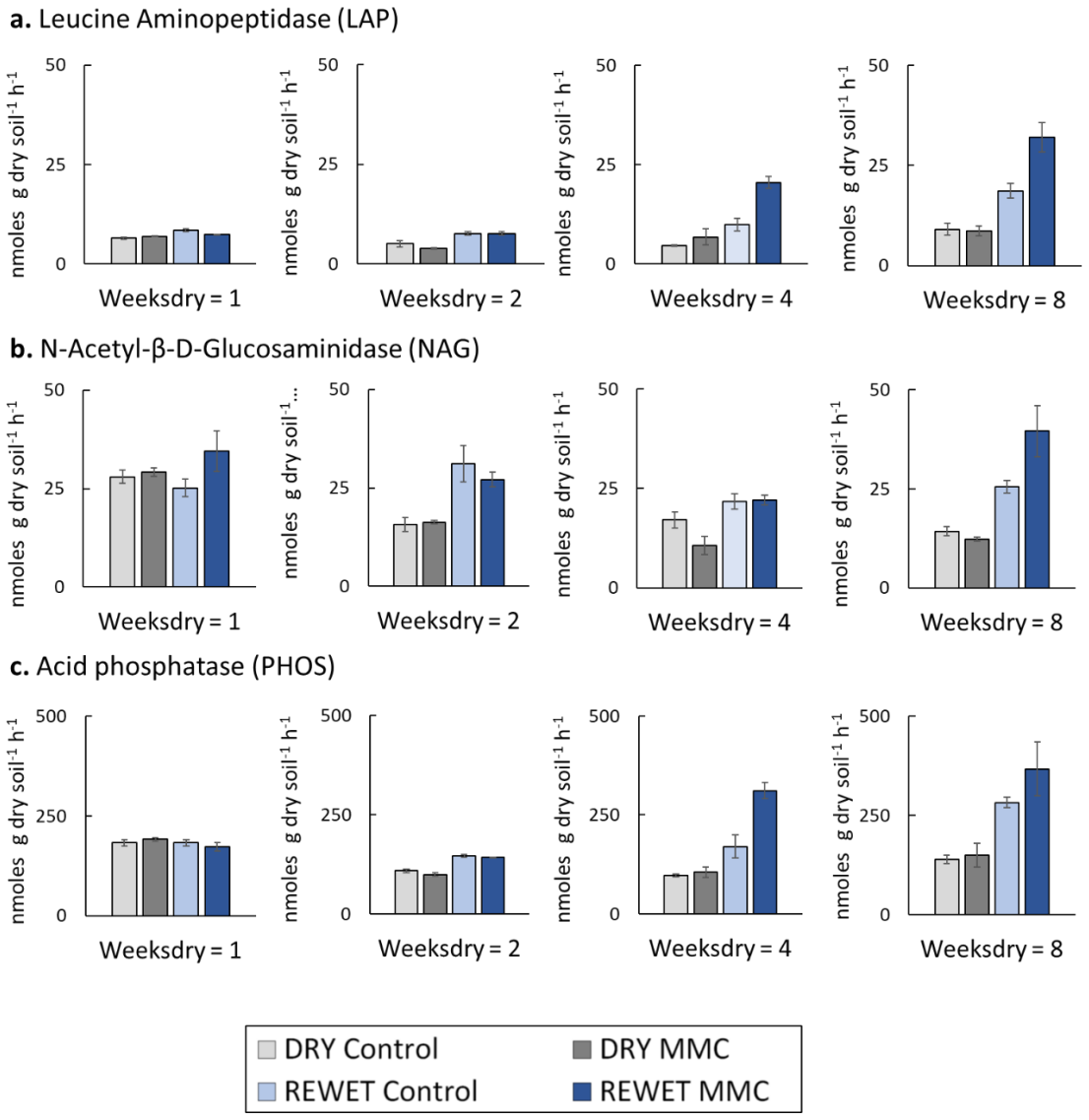

Figure 4.5. Mean activities of N- and P-degrading extracellular enzymes (LAP (a), NAG (b), and PHOS (c) by Mitomycin C induction treatment (MMC), drought length (Weeksdry), and rewetting (Rewet).

Panels are separated by drought length treatment (Weeksdry), with Dry samples in gray and Rewetted samples in blue; darker colors indicate application of pre-incubation MMC induction treatment. Error bars represent standard error of $n = 4$ replications per treatment combination.

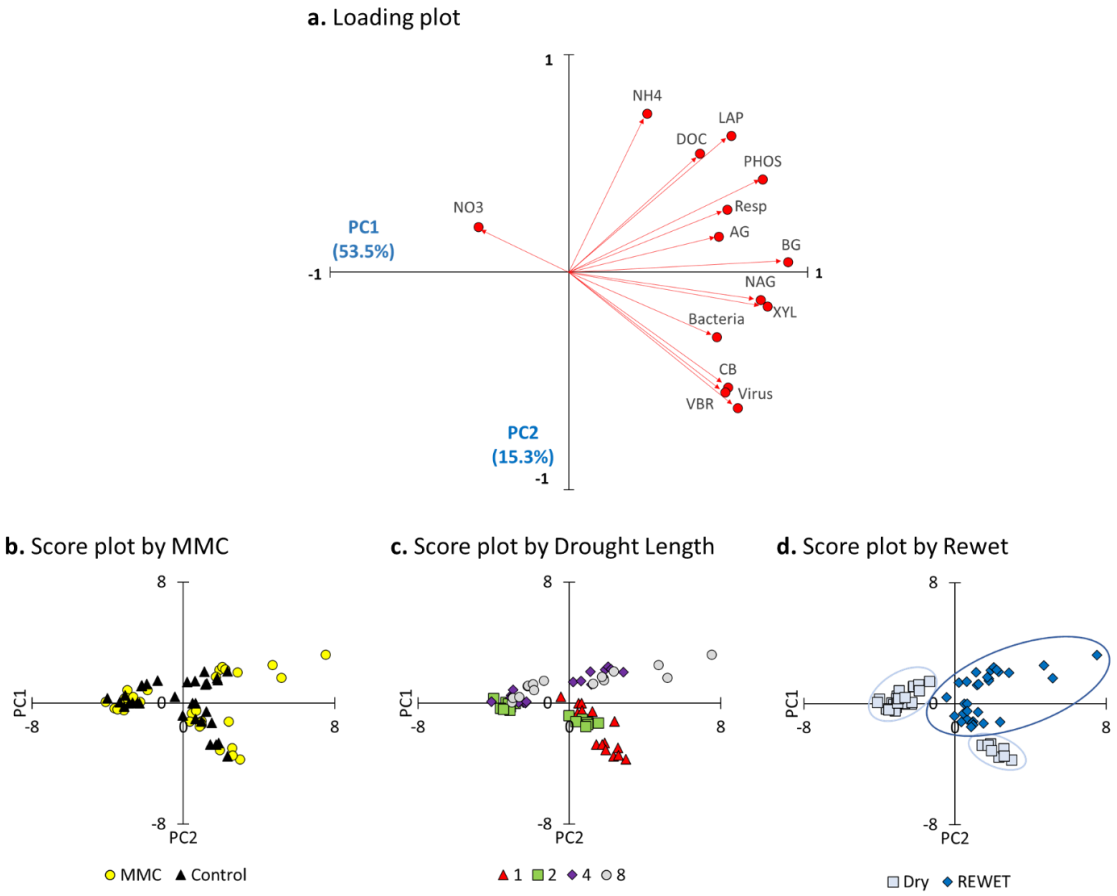

Figure 4.6. Loading plot (a) and Score plot with individual observations coded by Rewet treatment (b) from Principal Components Analysis (PCA) (*n* = 64).

Clustering of components in PC space was observed for Rewet but not MMC induction and drought length treatments.

CHAPTER FIVE
CONCLUSIONS

5.1 Research Summary

The overall aim of this dissertation research was to advance knowledge of interactions between soil physical structure and wetting dynamics as controls on microbial activity, virus-microbe interactions, and free viral abundance in soils. The controlled, extended incubation experiments conducted for this research have shed light on soil-specific mechanisms affecting major microbial functional activities directly related to C and nutrient cycling. Notably, this work also addresses long standing knowledge gaps in the fields of soil microbial and viral ecology regarding the influence of dynamic soil properties and water availability on viral production and destruction processes over time. The following specific findings are reported from this dissertation research:

1. Soil aggregation and water availability constrain microbial activity. Microbes are dependent upon soil water as a metabolic resource but also for accessibility of microbe-enzyme-substrate systems within the soil physicochemical matrix. Soil water dynamics (i.e., drought, flooding/saturation, drying-rewetting cycles) directly affect soil physical structure but also feedbacks between aggregation and microbial activity over time (*Chapters 2, 3, and 4*).
2. Free viral abundance and lytic production rates in soils varied significantly across aggregate size fractions, supporting the original hypothesis that virus-microbe

interactions exhibit variability within a bulk soil at the scale of soil aggregate fractions (*Chapter 3*).

3. Drying of soil beyond ~20% gravimetric water content declines viral abundance, likely resulting from the disintegration of viral particles within fine pore spaces under high water potential. Under extended drought conditions, stress responses and resource inaccessibility limit microbial growth which constrains lytic viral production (*Chapter 4*).
4. Rewetting of dry soil is associated with a burst of C and N mineralization referred to as the Birch effect which plays a key role in soil biogeochemical fluxes. This research provides supporting evidence for the original hypothesis that soil rewetting is also associated with the burst of free viral abundance reflecting increased lytic activity (*Chapter 4*).

Furthermore, results of multivariate statistical analyses across experiments indicate the following: i) widespread occurrence of two- and three-way interactions among treatment combinations is indicative of the highly complex nature of soil wetting as a control on microbial and viral processes in bulk soil and aggregate size fractions, ii) soil water and time have overarching control on microbial responses to viral lysis induction and aggregate size treatments, and iii) extracellular enzyme activities were found to contribute substantially to variability across all experiments but with high correlation between enzyme activities suggesting analytical redundancy. The suite of enzymes measured in this study has become standard in the past decade in soil biogeochemistry research but is largely targeted to assess microbially-mediated decomposition of plant

residues (i.e., cellulose, hemicellulose). Expanding or modifying the categories of enzymes assayed to include, for example, viral lytic enzymes and microbial cell wall/lipid degrading enzymes, could be valuable for studying virus-microbe interactions.

Finally, while the final experiment (Chapter 4) was performed on bulk soil rather than aggregate fractions, results from Chapters 2 and 3 indicate significant aggregate-scale variability in microbial responses to rewetting of dry soil and to induction of viral lysis via Mitomycin C under slurry conditions. From a mechanistic perspective, soil drying would likely lead to viral particle disintegration but within the context of soil pore-scale water potential that is dependent upon pore-size distribution and therefore varies across aggregate fractions. The observed burst of net viral particle production upon rewetting of dry soil is expected from all aggregates but with different magnitude arising from variability in microbial community composition, substrate availability, host infection status, and dynamic virus-soil interactions.

5.2 Broader impacts and closing remarks

Soils are unique microbial habitats characterized by low and fluctuating levels of available water and the presence of a complex, chemically reactive aggregated physical structure that directly impede resource accessibility. While these characteristics have been demonstrated to influence microbial growth and functional activity in bulk soil, knowledge of their interactions at the scale of aggregate size fractions and across time remains limited but critical for understanding the susceptibility of terrestrial ecosystems to climate change. This dissertation has contributed mechanistic information regarding

the interactive controls on soil microbial functional activities at lesser-studied spatial and temporal scales.

Work from this dissertation has also provided valuable insight into the dynamic nature of free viral abundance in soil. Despite rapidly growing availability of data on free viral particle abundance and community-scale diversity patterns, soil viral ecologists lack a soil-specific mechanistic framework that places these observations within the context of microbially-mediated processes that vary across space and time. Development of such a framework will require understanding of the fate of viruses released to soil but also the influence of interrelated hydrological and physicochemical conditions that directly influence the likelihood of an actively infective virus contacting a susceptible microbial host. Such understanding is key for quantifying the ecological roles of free viruses as drivers of microbial community functions within soils but also across ecosystem types.

VITA

Aubrey K. Fine was born in Dayton, Ohio in July 1985 and spent most of her childhood in Columbia, Missouri. Aubrey earned her Bachelor of Science from the University of Missouri in 2012 majoring in Soil, Environmental, and Atmospheric Sciences and minors in Geology and Biology. In 2015 she completed a Master of Science in Soil Science from The Pennsylvania State University advised by Dr. Enid Martinez at Cornell University. Aubrey joined the Cornell Soil Health Laboratory from 2015-2016 before coming to Knoxville to pursue a Ph.D. at the University of Tennessee advised by Dr. Sean Schaeffer. In her doctoral program, Aubrey has participated in multiple field- and laboratory-scale experiments that assess soil microbial responses to land management and climate change factors. Aubrey earned her Doctor of Philosophy in Plant, Soil, and Environmental Sciences with a focus on soil biogeochemistry and microbial ecology in December 2022.